Air Quality and Environmental Impact Assessment of Industrial Activities in East Java, Indonesia

Diah Dwiana Lestiani

2024

SUMMARY

A comprehensive study on air quality and the environmental impact assessment of industrial activities in Indonesia is still lacking. This dissertation aims to comprehensively assess the air quality across various regions of Indonesia, encompassing both urban and industrial areas, and environmental impact of industrial activities with a particular emphasis on East Java. The primary objectives of this research are to identify potentially toxic elements in airborne particulate matter using nuclear analytical techniques, determine the major sources contributing to these elements, and evaluate the environmental impact associated with health and ecological risks. Assessing the impact of industrial activities on air quality and the surrounding environment will be a key factor in better understanding and monitoring environmental challenges, especially considering the increasing number of industrial activities in the country. By achieving these objectives, this dissertation contributes to a better understanding of the environmental challenges posed by industrial activities in Indonesia. It provides crucial data on airborne particulate matter concentrations, chemical compositions, and major pollutant sources, providing a scientific basis for the development and improvement of various air quality policies.

This dissertation consist of 7 chapters and the details are described as follows:

Chapter 1 provides detailed information on the relevant background, a literature review of the increasing industrial activities, air quality monitoring status in Indonesia, the health impact of air pollution, the sources of air pollution, and the objectives of this research.

Chapter 2 presents urban air quality data from 17 sampling sites across 16 cities on the islands of Java, Sumatra, Kalimantan, Sulawesi, Maluku, and Papua, from 2010 to 2017. Over 6000 of samples of airborne particulate matter (APM) were collected in two size fractions: fine particulate matter ($PM_{2.5}$, particles with an aerodynamic diameter less than 2.5 μm) and coarse particulate matter ($PM_{2.5-10}$, particles with an aerodynamic diameter of 2.5–10 μm). These samples were collected 24 hours a week using a Gent stacked filter unit sampler and analyzed for mass concentrations, black carbon (BC) content, and elemental compositions. Surabaya, located in East Java, exhibited significantly higher concentrations of heavy metals, including Fe, Zn, and Pb, while Tangerang in Banten, Java, showed elevated levels of Pb compared to other cities. The average lead concentrations in Surabaya and Tangerang during this study period were 0.33 $\mu g/m^3$, and 0.22 $\mu g/m^3$, respectively. These

values were significantly higher when compared to other cities in Asian countries and exceeded the U.S. ambient air quality standard of 0.15 μg/m^3. It is assumed that there may be a similar source of Pb pollution in Surabaya, as was identified in the Tangerang study, which was associated with a lead battery recycling and bar production facility. Further investigation related to the heavy metal pollution in Surabaya needs to be conducted, given the adverse health effects of this element, and appropriate actions must be taken to reduce exposure in these areas.

Chapter 3 focuses on the vicinity of a lead smelter located in Lamongan, East Java. This lead smelting activity is suspected to have a correlation as a source causing the high Pb pollution in Surabaya, East Java. The research includes the characterization of $PM_{2.5}$ collected in the surrounding area of the lead smelter industry to identify the degree of Pb pollutant in the air, major pollutant sources and conduct potential risk assessments to the surrounding population. The average concentration of Pb in Lamongan was 0.46 μg/m^3, which violated the annual lead standard of US EPA (0.15 μg/m^3), and almost reached the limit of WHO (0.5 μg/m^3).

Chapter 4 describes the investigation of the characteristics of potentially toxic elements in soils collected from the vicinity of a lead smelter in Lamongan, East Java, with the objective of assessing the lead smelter's impact on the surrounding soil ecosystem. Following the discovery of elevated Pb levels in $PM_{2.5}$, it became crucial to assess the environmental impact on the soil, especially considering its location surrounded by the rice field and one of the rice-producing regions in East Java. The research involves chemical composition analysis in soil, spatial distribution mapping, and the evaluation of potential ecological and health risks assessment through several pathways including ingestion, inhalation and dermal.

Chapter 5 describes the utilization of particle-induced X-ray emission (PIXE) in characterizing fine and coarse particulate matter. The samples collected from two years period in Surabaya East Java were analyzed using particle-induced X-ray emission (PIXE) with a 4-MV Van de Graaff accelerator at Kyoto University. In this study, both helium and protons were employed to achieve optimal results. Both combinations provide optimal results, especially in the detection of light elements using helium and heavier elements using a proton beam, resulting in the detection of a total of 21 elements. This elemental analysis

revealed major, minor, and trace elements in $PM_{2.5}$ and $PM_{2.5-10,}$ providing significant and crucial information on chemical composition.

Chapter 6 utilizes the database of chemical composition in APM collected in Surabaya, which was obtained through PIXE analysis. This chapter employs various approaches for data analysis and health impact assessment. The results revealed that $PM_{2.5}$ concentrations exceeding the World Health Organization (WHO) annual standard of 5 $\mu g/m^3$. The positive matrix factorization (PMF) method was employed for the source apportionment of $PM_{2.5}$. It revealed eight factors for $PM_{2.5}$ sources: galvanizing industry, ammonium chloride, secondary sulfate, biomass burning emission, soil, steel industry, traffic emissions, and lead smelting industry. Metal industries such as galvanizing, steel industry and lead smelting were found to be a significant contributor to $PM_{2.5}$ with a total of 37.3%. Conditional bivariate probability function was carried out to identify the location/direction of the possible sources.

Chapter 7 is a conclusion briefly summarizes the main finding of the study in each chapter and what can be concluded. The long-term research has shown the benefits of nuclear analytical techniques such as XRF and PIXE in the characterization of airborne particulate samples and other environmental samples. These methods are still reliable and suitable methods for APM research. This research demonstrates that industrial activities, particularly those related to lead smelting and metal industries, have a substantial impact on Indonesia's air quality, resulting in elevated levels of potentially toxic elements in the atmosphere and soil. Recommendations include enhanced monitoring, source identification, community awareness, ecological impact assessment, international collaboration, and policy development, all aimed at addressing the challenges posed by industrial pollution while promoting sustainable development.

TABLE OF CONTENTS

LIST OF TABLES

LIST OF FIGURES

LIST OF ABBREVIATIONS

ABS	ABsorption factor of Skin
ACGIH	American Conference of Governmental Industrial Hygienists
ADD	Average Daily Dose
AES	Atomic Emission Spectrometry
AF	Adhesiveness degree of skin Factor
APM	Airborne Particulate Matter
AQMS	Air Quality Management System
ASCII	American Standard Code for Information Interchange
AT	Averaging Time
BAPPENAS	National Development Planning Agency
BATAN	National Nuclear Energy Agency
BC	Black Carbon
BLL	Blood Lead Level
BRIN	National Research and Innovation Agency
BW	Body Weight
CBPF	Conditional Bivariate Probability Function
CDC	Centers for Disease Control
Cf	Contamination factor
CO	Carbon Monoxide
CPF	Conditional Probability Function
CR	Cancer/carcinogenic Risk
DNA	Deoxyribo Nucleic Acid
EC	Elemental Carbon
ECPSSR	Energy loss, Coulomb deflection, Perturbed Stationary State and Relativistic
ED	Exposure Duration (year)
EDXRF	Energy Dispersion X-Ray Fluorescence
EF	Exposure Frequency
FAAS	Furnace Atomic Absorption Spectrometry
FWHM	Full Width at Half Maximum
GBD	Global Burden Disease
GDP	Gross Domestic Product
HI	Hazard Index
HQ	Hazard Quotient
IAEA	International Atomic Energy Agency
IARC	International Agency for Research on Cancer
ICP	Inductively Coupled Plasma
INAA	Instrumental Neutron Activation Analysis
IPCC	Intergovernmental Panel on Climate Change
IR	Inhalation Rate (m3/day)
IRIS	Integrated Risk Information System
ISO	International Standards Organization

IUR	Increased Unit Risk
LADD	Lifetime Average Daily Dose
LA-ICPMS	laser ablation inductively coupled plasma mass spectrometry
LULC	Land-Use and Land-Cover
MCA	Multi-Channel Analyzer
MoEF	Ministry of Environment and Forestry
MOFA	Ministry of Foreign Affairs
MS	Mass Spectrometry
NAAQS	National Air Ambient Quality Standard
NATs	Nuclear Analytical Techniques
NH3	Ammonia
NIST	National Institute of Standards and Technology
NOx	Nitrogen Oxide
O3	Ozone
OC	Organic Carbon
OES	Optical Emission Spectrometry
OM	Organic Matter
PCA	Principal Component Analysis
PEF	Particle Emission Factor
PI	Pollution Index
PIGE	Particle Induced Gamma Emission
PIXE	Particle-induced X-ray emission
PM	Particulate Matter
PM10	Particulate matter with aerodynamic with less than 10 um
PM2.5	Particulate matter with aerodynamic with less than 2.5 um
PMF	Positive Matrix Factorization
PWBA	Plane-Wave Born Approximation
R	Reflectance after sampling
R0	Reflectance before sampling
RCARO	Regional Cooperative Agreement for Research Organizations
RCM	ReConstructed Mass
RfD	Reference Dose
SA	Surface Area
SDD	Silicon Drift Detector
SF	Slope Factor
SFU	Stacked Filter Unit
SO_2	Sulfur dioxide
SRM	Standard Reference Material
SRXRF	Synchrotron Radiation X-Ray Fluorescence
TSP	Total Suspended Particle
UAQi	Urban Air Quality improvement
US EPA	United States Environmental Protection Agency
VOC	Volatile Organic Compounds
WHO	World Health Organization

CHAPTER 1 Introduction

1.1 Background

Indonesia, officially the Republic of Indonesia, is a vast island nation located in Southeast Asia and Oceania, situated between the Indian and Pacific Oceans. Comprising over 17,000 islands, including Sumatra, Java, Sulawesi, parts of Kalimantan, and Papua. With a population of approximately 278 million, Indonesia stands as the fourth most populous country globally [MOFA 2018]. Java, the world's most densely populated island, is home to over half of Indonesia's population [BPS Statistics Indonesia 2013; MOFA 2018]. In Indonesia, air pollution is one of many serious environmental problems facing major cities due to the population growth, increasing economic activity, and associated transportation and industrial activities [Haryanto 2018; Susanto 2020]. The country's rapid industrialization and urbanization have led to an increase in industrial activities, transportation, and the burning of fossil fuels, resulting in high levels of air pollution.

As shown in Figure 1. 1 the increasing of Indonesian gross domestic product (GDP) from industrial sector in every year in US$ million [Bashir et al. 2019]. The manufacturing industrial sector continues to be the largest contributor to supporting national economic growth in the quarter of 2023 [Ministry of Industry 2023]. Despite government efforts to decentralize, Indonesia’s manufacturing is concentrated in Java. Manufacturing firms are concentrated in Java, with 70% of the manufacturing sector’s value added created there, particularly in greater Jakarta (including Jakarta, West Java, and Banten) and East Java [Brodjonegoro 2019].

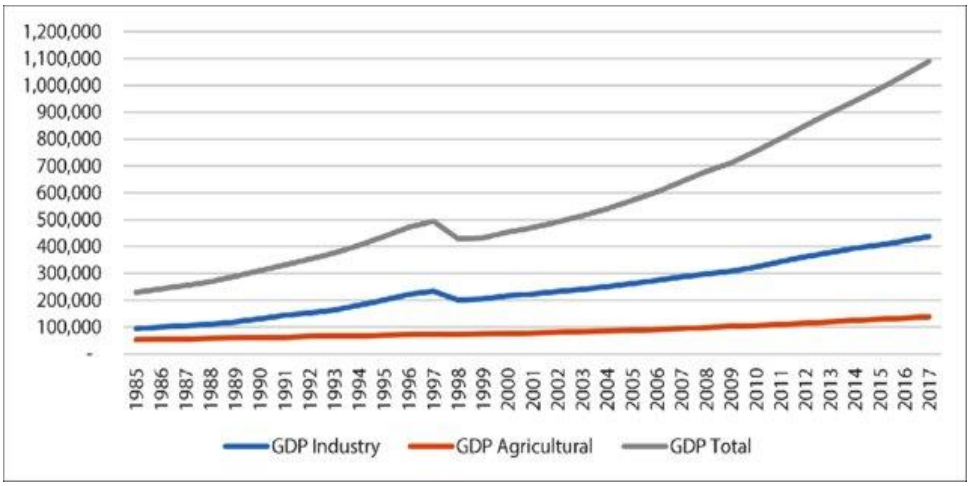

Figure 1. 1 Industrial sector contribution to the GDP [Bashir et al. 2019]

1.2 Airborne particulate matter (APM)

The United States Environmental Protection Agency (EPA) has designated six common air pollutants as criteria pollutants. These pollutants include particulate matter ($PM_{2.5}$ and PM_{10}), ozone, nitrogen dioxide, sulfur dioxide and carbon monoxide [US EPA 2006]. While the Act has undergone subsequent amendments that have introduced additional components, the six criteria pollutants remain the primary standards. The Clean Air Act directs U.S. EPA to identify and set national standards for pollutants with adverse public health and environmental effects [US EPA 2023].

Aerosols are defined as dispersed phases containing solid or liquid particulate matter (PM) within a colloidal system where the dispersing medium is a gas [Watson, 2002; Yadav & Devi, 2019]. They collectively constitute what we refer to as atmospheric aerosols, forming a collection of particles suspended in the air. The wide-ranging origins contribute to a diverse array of chemical compositions within PM. Furthermore, atmospheric aerosols encompass a heterogeneous mix of particles, varying in size, which gives rise to distinct classifications based on particle size ranges [Watson, 2002]. $PM_{2.5}$ or fine particulate matter is one of these classifications, defined as a collection of particles with an aerodynamic diameter of 2.5 µm or less [US EPA 2006]. There are additional classifications defined according to particle size, PM_{10}, encompassing particles with an aerodynamic diameter of 10 µm or less, and total suspended particulates (TSP), which encompasses all particles, typically below 100 µm, as indicated in Figure 1. 2 [US EPA 2023]. It illustrates a visual representation of the sizes of PM_{10} and $PM_{2.5}$ by comparing them to the thickness of a human hair and the dimensions of a grain of beach sand. The diameter of $PM_{2.5}$ particles is ~3-5% of those for human hair and beach sand.

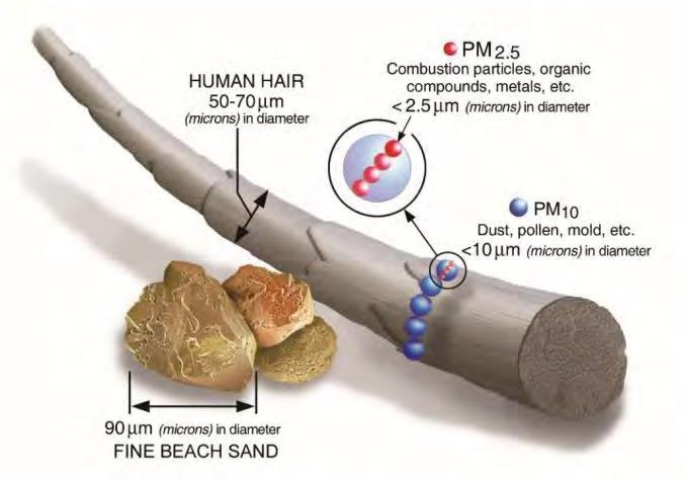

Figure 1. 2 Illustration of particles size of $PM_{2.5}$ and PM_{10} [US EPA 2023]

The airborne particles commonly occur in two distinct sizes- ‘fine fraction” denoted as $PM_{2.5}$ and ‘coarse fraction’ with diameter 2.5–10 μm $PM_{2.5\text{-}10}$ [US EPA 2006]. The PM_{10} consists of both fine and coarse fractions. The coarse particles primarily result from mechanical actions like crushing, abrasion, and the effects of wind. Anthropogenic origins encompass the dust suspended in the air due to activities like road construction and industrial processes. In contrast, natural sources, such as marine aerosols and wind-blown soils, frequently constitute a significant portion of the coarse particle fraction [Kelly & Fussell, 2012; Saksakulkrai et al., 2023; Watson, 2002]. It's worth noting that coarse fraction tends to settle out of the atmosphere more rapidly after formation or emission compared to finer $PM_{2.5}$ particles.

Figure 1. 3 depicts a section of a particle size distribution within the ambient environment, each originating from distinct particle formation mechanisms patterned after Chow and Watson [Watson, 2002; Wyzga, 1997]. These mechanisms can be natural or anthropogenic (human-made) and include nucleation, ultrafine, and accumulation modes. Nucleation is the process where gas molecules or other particles come together to form small clusters, which can then grow into larger particles [Watson, 2002]. It's a fundamental step in the formation of atmospheric aerosols. Nucleation and ultrafine modes denote particles less than 0.01 and 0.1 μm, respectively. Particles within the nucleation and ultrafine modes exhibit a brief stay in the atmosphere due to their rapid coagulation with one another or with larger particles [Watson 2002]. The accumulation-mode particles (~0.08 to ~2 μm) contain most of the fine particles from ~0.1 to ~2 μm, and primarily composed of secondary aerosols is mostly occupied by secondary aerosol. These secondary aerosols form in the atmosphere from emissions such as SO_2, NOx, ammonia (NH_3), and certain volatile organic compounds (VOCs), particularly those derived from internal combustion engines and vegetation [Watson, 2002]. The condensation mode, typically around 0.2 μm in size, results from chemical reactions in the gas phase, while the droplet mode, ~0.7 μm in size, originates from gas absorption and reactions in water droplets [Cao et al. 2013].

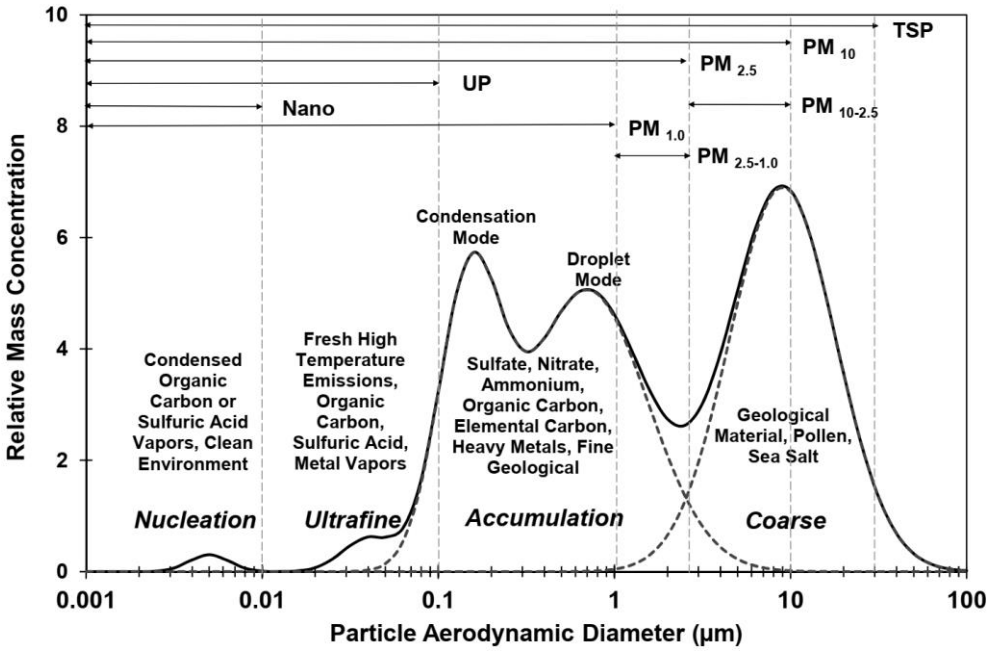

Figure 1. 3 Particle size distribution based on formation processes [Watson, 2002]

1.3 Impact on Human Health

In 2019, 99% of the world's population was exposed to air pollution levels exceeding the WHO air quality guidelines [WHO 2022]. While various toxins pose health risks, certain pollutants have substantial evidence concerning public health. These include particulate matter (PM), carbon monoxide (CO), ozone (O_3), nitrogen dioxide (NO_2) and sulfur dioxide (SO_2). Among these, fine particulate matter is an especially important source of health risks, due to its micro size, which allows it to deeply penetrate lung tissues, enter the bloodstream, and systematically affect organs, resulting in damage to cells and tissues [WHO 2018]. In 2013, the WHO's International Agency for Research on Cancer (IARC) designated PM as a substance linked to cancer development. The morbidity and mortality rates related to air pollution-induced lung cancer are closely correlated with increased levels of $PM_{2.5}$, driven by the epigenetic factors and micro environmental changes [WHO 2018].

Several epidemiological studies have consistently demonstrated a strong correlation between elevated levels of particulate matter in the air and an increased risk of mortality from various causes, particularly cardiovascular and respiratory diseases [Dockery et al., 1993; Samet et al., 2000; Wang et al., 2020; WHO, 2018]. Numerous studies have substantiated the adverse effects of PM_{10} on human health, encompassing a range of health issues such as congenital heart defects, ischemic heart disease, mortality related to respiratory and heightened risk of preterm birth, mutagenicity and DNA damage, influences

on fetal growth and adverse birth outcomes, cancer risk, and inflammatory responses [Mukherjee and Agrawal 2017].

Figure 1. 4 illustrates the characteristics of inhalation and deposition within the human respiratory system, based on adaptations from Chow with data sourced from Phalen et al. [Phalen et al. 1991; Chow 1995; Cao et al. 2013]. It shows that the lung deposition peaks at 40–60% for 30 nm size of particles and in tracheal deposition is 20–40% for <10 nm of particles. Most particles larger than 10 µm are filtered out in the mouth or nose before entering the body. Between 10% and 60% of particles with aerodynamic diameters smaller than 10 µm that pass through the trachea have the potential to settle in the lungs, where they could potentially cause harm. The lung deposition curve exhibits a bimodal distribution, with peaks at 20% for particles around ~3 µm in size and 60% for particles around ~0.03 µm. Additionally, it includes the standards set by the International Standards Organization (ISO) for mouth breathing, as referenced by the American Conference of Governmental Industrial Hygienists ACGIH [Cao et al., 2013]. The ISO curve closely resembles the "ideal inlet" sampling effectiveness, a component of the performance standard for PM_{10} samplers in the United States. These curves illustrate that a significantly higher number of particles larger than 2 or 3 µm can pass through when breathing occurs through the mouth compared to when breathing takes place through the nose.

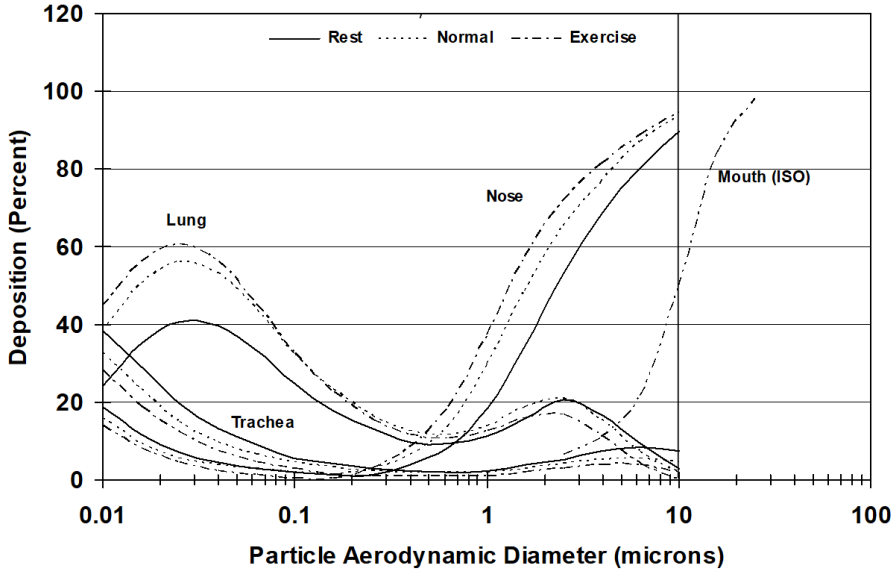

Figure 1. 4 The inhalation and deposition properties for the human respiratory system [Chow 1995]

Ambient air pollution, prevalent in both urban and rural settings, was responsible for an estimated 4.2 million premature deaths worldwide in 2019 [WHO 2022]. This mortality primarily resulted from exposure to fine particulate matter, contributing to cardiovascular and respiratory diseases, as well as various cancers. According to the World Health Organization (WHO), in 2019, approximately 37% of premature deaths attributed to outdoor air pollution were linked to ischemic heart disease and stroke [WHO 2022]. Additionally, 18% and 23% of fatalities were associated with chronic obstructive pulmonary disease and acute lower respiratory infections, respectively, while 11% were attributed to respiratory tract cancers. It's worth noting that individuals residing in low- and middle-income countries bear a disproportionate burden of outdoor air pollution, accounting for 89% of the 4.2 million premature deaths [WHO 2018]. The WHO South-East Asia and Western Pacific Regions experience the greatest share of this burden. These latest estimates underscore the significant role that air pollution plays in the prevalence of cardiovascular diseases and related fatalities.

Figure 1. 5 shows global attributable deaths for females and males in 2019 for the twenty risk factors at level 2 of the risk factor. The study published in the Lancet estimates mortality for 87 risk factors in 204 countries and territories using the Global Burden of Diseases, Injuries, and Risk Factors Study (GBD) 2019 [Murray et al. 2020]. The article examines risk factors from 1990 to 2019, as well as from 2010 to 2019, and shows that air pollution is the 4th leading cause of death. Air pollution is one of the top threats to global health, surpassed only by high blood pressure, tobacco use, and poor diet [Murray et al. 2020]. While in Indonesia, the leading risk factors for disability-adjusted life years in Indonesia in 2019 were high systolic blood pressure, tobacco use, dietary risks, high fasting plasma glucose, high BMI, and child and maternal malnutrition, and air pollution [Mboi et al. 2022].

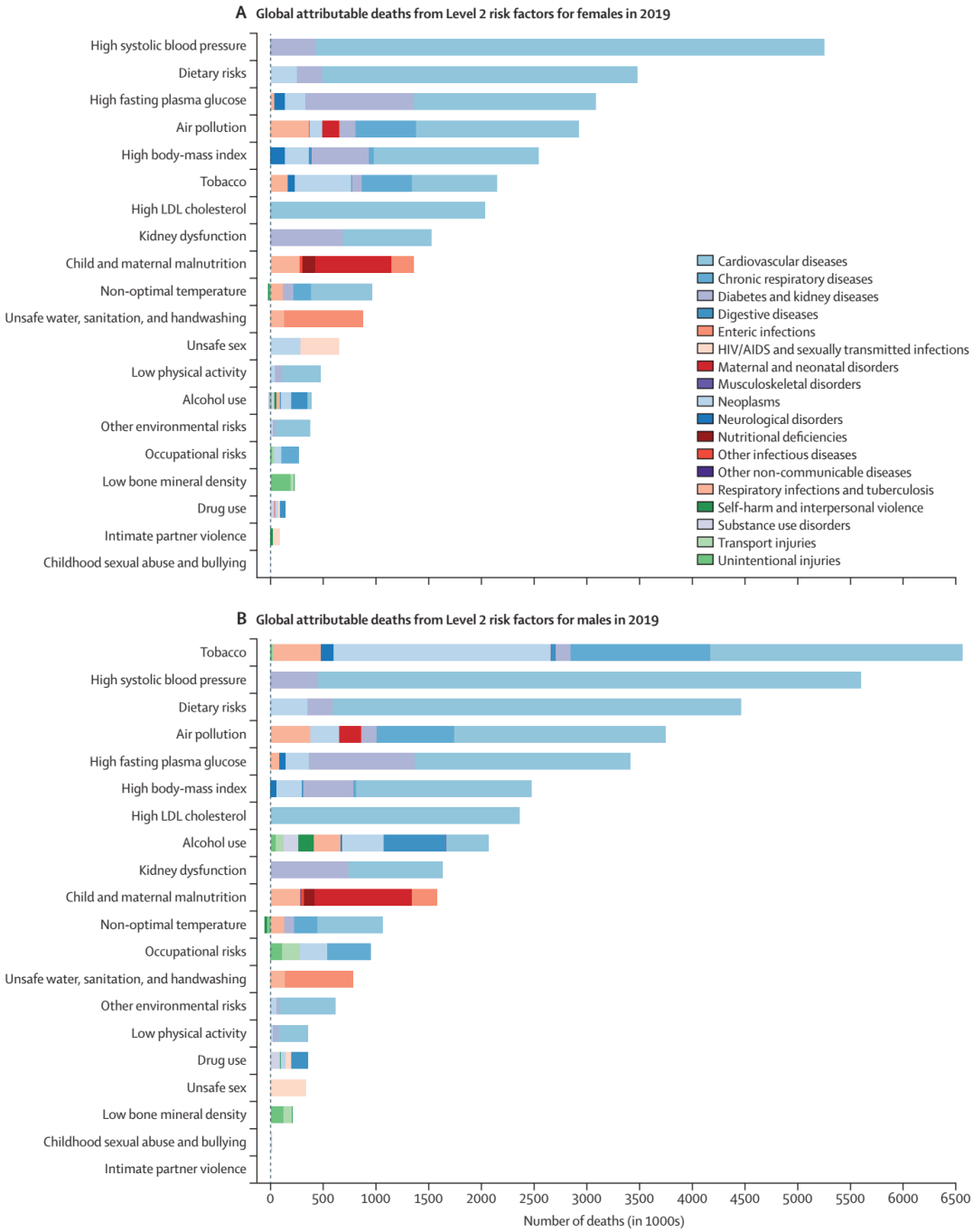

Figure 1. 5 The global attributable risk for females and males based on Global Burden of Diseases, Injuries and Risk factor study [Murray et al. 2020]

Furthermore, the presence of potentially toxic elements such as Cr, Cu, Mn, Fe, Pb, and Zn in $PM_{2.5}$ was found to be associated with PM toxicity and their co-exposure led to damage to biological cells and high mortality of human cells [Yuan et al. 2019]. The existence of potentially toxic elements in particulate matter potentially poses a diverse impact on human health, can cause both short- and long-term medical problems [Zhai et al.

2014; Soleimani et al. 2018]. The presence of potentially toxic elements in particulate matter underscores the complexity of health challenges posed by air pollution, with short-term and long-term implications that demand an attention and efforts to mitigate its impact on human well-being.

1.4 Sources of Particulate Matter

Particulate matter consists of components originating from both natural sources and human-made anthropogenic activities [Pey et al. 2009; WHO 2021; Saksakulkrai et al. 2023; US EPA 2023]. PM can be either primary or secondary. Primary PM is emitted directly into the air from sources such as combustion of fuels, such as from power plants, vehicles, and industrial facilities, windblown dust from soil, burning of wood, agricultural waste, and other materials, and volcanic eruptions [Mukherjee and Agrawal 2017]. While the secondary PM is formed in the atmosphere through chemical reactions of pollutants, such as sulfur dioxide and nitrogen oxides, that are emitted from primary sources [Hopke, 1999; Hopke et al., 2008; Saksakulkrai et al., 2023].

The primary sources of PM_{10} include natural sources such as road dust, which constitutes the most prominent contributor in many urban areas, arising from the wear and tear of vehicles on roads and tires [Mukherjee and Agrawal 2017]. Construction and demolition activities also release substantial amounts of dust into the atmosphere, contributing to PM_{10} levels. Additionally, agriculture plays a significant role, with windblown dust from agricultural fields and the burning of crop residues serving as significant sources of PM_{10} [Santoso et al. 2008; Kelly and Fussell 2012; Mukherjee and Agrawal 2017; Saksakulkrai et al. 2023]. Furthermore, residential wood burning, whether for heating or cooking, can release PM_{10} into the air. On the other hand, $PM_{2.5}$ is primarily sourced from traffic emissions, particularly notable in numerous urban areas, originating from the combustion of gasoline and diesel fuel in vehicles. Other sources encompass power plants burning coal or oil, releasing $PM_{2.5}$ as a combustion byproduct, as well as industrial processes such as metalworking and mining [Hopke et al., 2008; Pey et al., 2009; Sun et al., 2004]. Residential wood burning, similar to PM_{10}, can also release $PM_{2.5}$ into the air [Hopke 1999]. Potentially toxic elements in the atmosphere are mostly emitted from industrial emissions (mining, smelters, coal combustion), vehicular emissions, and secondary aerosols as the major sources [Pacyna et al. 2009; Li et al. 2012; Suvarapu and Baek 2017; Engel-Di Mauro 2021].

Understanding the sources of particulate matter is crucial for air quality management and public health. Research studies and references help scientists and policymakers assess the impact of different sources on air quality and human well-being and develop strategies to mitigate their effects. While natural sources are beyond our control, anthropogenic aerosol sources, while challenging to manage, are indeed controllable. Both human activities and industrial development play a role in influencing emissions from both anthropogenic and natural sources. Consequently, when evaluating the impact of air pollutants on public health, particularly in densely populated urban areas, the focus often shifts towards anthropogenic sources, which are of great significance and are the primary target for regulatory measures.

1.5 Air Quality Monitoring in Indonesia

Since 2006, Indonesia has been conducting an urban air quality improvement (UAQi) project with the vision of "Clean and Healthy Urban Air in Indonesia 2020". The project developed various strategies for each issue related to urban air quality improvement on the national and local levels in several large cities [BAPPENAS 2006]. However, this program was not fully implemented due to the lack of financial resources and air quality expertise. There is limited research focused on particulate matter, particularly concerning potentially toxic elements and associated health risks. This gap persists despite urgent needs and increasing awareness of environmental challenges. Comprehensive investigations into air quality within Indonesian industrial regions remain understudied.

Up to 2015, Indonesian authorities operated an air quality monitoring network that utilized a variety of techniques, such as the Air Quality Management System (AQMS), a network for continuous automated monitors for CO, SO_2, NO_x, O_3, and PM_{10} in 10 cities combined with passive monitors to measure NO_2 and SO_2 concentrations in 33 provinces [Santoso, et al., 2020]. Due to the limited resources, the AQMS does not operate effectively in all 10 cities since the equipment maintenance and calibrations require more support than were available. Additionally, at the beginning, the AQMS did not monitor $PM_{2.5}$ that is an important parameter because of its negative impacts on public health and urban visibility. The Indonesian Ministry of Environment and Forestry (MoEF) started to implement a new AQMS network in major cities to monitor 7 parameters (SO_2, O_3, CO, NO_2, HC, PM_{10}, and $PM_{2.5}$), and by 2023, AQMS stations have already established in 70 cities in operation and the data can be retrieved online on the website (https://ispu.menlhk.go.id/internal/web/site/ and https://ispu.menlhk.go.id/webv4/#/stasiun). AQMS is one of the air quality

measurements to determine the compliance with air quality standards. However, it cannot be used to identify and quantify the source contribution which is an important information to design the proper policy to improve the air quality, by identifying and regulating the major sources of air pollution.

1.6 Research Collaboration in National and Regional Scale

Starting in 1996, the International Atomic Energy Agency, through its Regional Cooperation Agreement with states in the Asian regions, initiated an air pollution project aimed at assisting Member States in collecting and analyzing particulate matter samples using nuclear analytical techniques [Hopke et al., 2008]. The fifteen participating countries, including Indonesia represented by the nuclear analytical techniques NATs laboratory at the National Nuclear Energy Agency of Indonesia (BATAN). I am as one of the research members of the nuclear analytical laboratory, and has been involved in this project as a project member. All the member countries have developed the capability to sample, analyze, and utilize the resulting data to assess particulate air pollution in various locations across the region [Hopke et al. 2008]. Our NATs laboratory in BATAN had received support to conduct research activities in Bandung and Lembang, West Java, representing both urban and rural areas. From the project, we carried out research on the composition and source apportionment of fine and coarse particle samples collected in Bandung and Lembang, Indonesia, between 2002 and 2004 [Santoso et al. 2008]. This regional technical cooperation under IAEA project was carried out over several four years cycles and accomplished in 2018 when we began to expand the sampling activities to other 16 cities in Indonesia [Santoso et al. 2020b]. For the sustainability of the project on a national scale, we also proposed a national project under IAEA technical cooperation to continue monitoring air quality, covering most of the major cities in Indonesia. This proposal was based on the memorandum of understanding between BATAN and the Ministry of Environment and Forestry of Indonesia (MoEF). The project's objective was to contribute to the improvement of air quality in Indonesia by applying advanced nuclear analytical techniques (NATs) to assess airborne particulate matter pollution. It commenced in 2013 and concluded in 2020 [Santoso et al. 2020b].

After concluding our cooperation with the IAEA, the Regional Cooperative Agreement for Research Organizations (RCARO) offered our laboratory a regional research project involving countries in the Asia-Pacific region to conduct air quality research. RCARO is a regional organization that fosters cooperation among member states in the Asia-

Figure 1. 6 Framework of international and national collaboration

Pacific region for the development and peaceful use of nuclear science and technology. Our laboratory was designated as the lead country coordinator for the project, tasked with executing collaborative, continuous, and long-term efforts to examine the impact of industrial activities on air quality. The project was conducted in two cycles and was completed in 2023. Figure 1.6 illustrates the framework of the research and development conducted under the IAEA project in collaboration with BATAN and Indonesia's national counterparts. BATAN involved several local environmental protection agencies in each city and province to participate in the project in cooperation with the MoEF.

1.7 Research Objectives

Based on the international and national collaboration as displayed in Figure 1. 6, with our capability to characterize APM samples using NATs and utilize the resulting data to assess air pollution, we started to focus our research on the air quality impact of industrial activities. Characterization of potentially toxic element concentrations to understand the impact of industrial activities is a very important step, especially in locations where these activities are close to agricultural ecosystems and the human living environment. Therefore, more data on chemical composition of size fractionated particulate matters are needed. The measurement of the elemental composition of the particulate matter is a key factor in utilization the data for the determination of possible sources, which the process of identification and apportionment of pollutants to their sources is an important step in air quality management. The application of source receptor models requires chemical characterization of these particles to apportion ambient concentration to their sources for development of emissions reduction strategies, and health risk assessment which is essential for understanding the potential health hazards associated with air pollution and guiding efforts to mitigate these risks and protect public health.

This study involves analysing airborne particulate matter samples collected in Indonesia, using nuclear analytical techniques such as X-ray fluorescence and particle-induced X-ray emission. The objective of the study is to provide a comprehensive understanding of air quality, pollutant sources, and associated ecological risks as an impact from industrial activities especially in East Java Indonesia, contributing valuable insights to environmental science and policymaking. Additionally, the study aims to assess the health risks associated with particulate-bound potentially toxic elements, considering both children and adults.

CHAPTER 2 Assessment of Urban Air Quality in Indonesia

2. 1. Introduction

Air pollution has become an important global problem that requires serious attention because of its impact on human health and environmental quality [Brauer et al. 2016; Yin et al. 2017; Lelieveld et al. 2019]. The degradation of ambient air quality, especially in major cities, needs major improvements. In Indonesia, air pollution is one of many serious environmental problems facing major cities due to the population growth, increasing economic activity, and associated transportation and industrial activities. Since 2006, Indonesia has been conducting an urban air quality improvement (UAQi) project with the vision of "Clean and Healthy Urban Air in Indonesia in 2020." The project developed various strategies for each issue related to urban air quality improvement on the national and local levels in several large cities [BAPPENAS 2006]. However, this program was not fully implemented due to the lack of financial resources and air quality expertise.

Several studies have reported on the identification of sources of air pollution in urban areas, such as Jakarta [Lestari and Mauliadi, 2009; Santoso et al., 2013], and Bandung West Java [Kim Oanh et al. 2006; Santoso et al. 2008]. Other research has focused on biomass burning related to forest fires in Riau, Sumatra [Siregar et al. 2022], and Palangka Raya Borneo [Lestiani et al. 2019]. Santoso et al. (2008) reported the mean $PM_{2.5}$ concentrations in Bandung and Lembang between 2002 and 2004 were 14.03 ± 6.86 and 11.88 ± 6.60 μg/m^3, respectively [Santoso et al., 2008]. The mean $PM_{2.5-10}$ concentrations in Bandung and Lembang were 17.64 ± 9.42 and 7.10 ± 7.04 μg/m^3, respectively. Santoso et al. (2013) reported that $PM_{2.5}$ concentrations measured in Jakarta at an arterial roadside were higher than the $PM_{2.5}$ at the urban site in Bandung. The mean concentrations of $PM_{2.5}$ and PM_{10} in Jakarta were 25.76 and 75.20 μg/m^3, respectively. Most $PM_{2.5}$ values measured in Jakarta exceeded the Indonesian annual ambient air quality standard of 15 μg/m^3 [Santoso et al. 2013]. The determination of chemical element concentrations in airborne particulate matter collected in suburban area of Lembang, Indonesia, was reported by Lestiani et al [Lestiani et al. 2013b]. Chemical elements including Mg, V, Cr, Mn, Fe, Co, Ni, Cu, Zn, As, Hg, and Pb were determined. In the fine fraction, principal component analysis (PCA) studies found sources such as vehicular emissions and biomass burning.

Although previous studies have presented the chemical composition of $PM_{2.5}$ and source identification results, there has not been a comprehensive study conducted for multiple cities across Indonesia covering more than 3 years that provides fine and coarse particle mass concentration and composition. The objective of the study was to provide an initial assessment of particulate air pollution including $PM_{2.5}$ and PM_{10} total mass concentrations, BC, and elemental concentration in 16 cities across Indonesia in the period 2010–2017.

2. 2. Methodology

2.2.1 Sampling

Sampling was conducted at 17 sites in 16 large cities in Indonesia. The sampling locations for these 16 cities are shown in Figure 2. 1. There are 7 sites on the island of Java (Jakarta, Tangerang, Bandung, Yogyakarta, Semarang, and 2 sites in Surabaya), 2 sites on Sumatra (Pekanbaru and Medan), 2 sites on Kalimantan (Palangka Raya and Balikpapan), 2 sites on Sulawesi (Makassar and Manado), 1 site on Maluku (Ambon), 1 site on Papua (Jayapura), 1 site on Bali (Denpasar), and 1 site on West Nusa Tenggara (Mataram). Jakarta is the capital and the mega-city of Indonesia with a 2017 population of 10,177,924 [BPS, 2018]. Many buildings, highways, and small- to large-scale factories are situated in and

Figure 2. 1 Locations of 17 sampling sites in Indonesia from 2010-2017

around the city. Tangerang is an independent city in Banten province near Jakarta and categorized as an industrial city. Bandung is located about 150 km southeast of Jakarta. It is the provincial capital of West Java and is categorized as an industrial city. Many small-scale factories are located around the city. Commercial activities are mostly concentrated in the center of the city, while industrial activities are concentrated on the west and east sides of Bandung. Yogyakarta is the capital city of special region of Yogyakarta, with an area of 32.5 km^2. It is the only royal city in Indonesia still ruled by a monarchy. Near the city is Mount Merapi, the most active volcano in Indonesia. Semarang is the provincial capital of Central Java and the sixth-largest Indonesian city. Surabaya is the second-largest city with a population of over 2.8 million and industrial activities such as cement factories, smelters, and other metal industries. Pekanbaru is the capital of Riau province that is growing rapidly with the development of industries especially those related to petroleum and is a major economic center on the island of Sumatra. Medan is the capital of the Indonesian province of North Sumatra. It is a multicultural metropolitan area and a busy trading center. Palangka Raya is the capital of Central Kalimantan province with an area of 2400 km^2 and part of its territory is still forest, including protected forest, nature conservation and Tangkiling Forest. Palangka Raya has the largest area in Indonesia, equivalent to 3.6 times the area of Jakarta. Balikpapan is a city in East Kalimantan province serving as largest in Kalimantan, which is based on an industrial sector dominated by oil and gas, trade and service industries. Makassar is the largest metropolitan city in Eastern Indonesia, having an area of 175.77 km^2 and a population of more than 1.5 million people, the fifth-largest city in Indonesia. Manado is the capital of the province of North Sulawesi with a land area of 157 km^2, a coastline of 18.7 km, and a population of 1.2 million. The city is surrounded by hills and mountain ranges. The economy of Manado consists of the trade, hotels and restaurants, transportation and communications, and other aspects of the service sector. Ambon is the center of the port, tourism and education for the Maluku Islands region. Ambon has a total area of 377 km^2 or two-fifths of Ambon Island that consists of land area of 359.45 km^2 and waters of 17.55 km^2 with a coastline of 98 km. Jayapura is the capital of Papua province, with an area of 940 km^2. The topography of this area is quite varied, from the plains to the slopes and hills or mountains ranging to 700 meters above sea level. Denpasar is the capital of Bali province, famous for its tourism industry giving it a high income per capita in Bali. The city of Mataram, the capital of West Nusa Tenggara province, has a topographic area at an altitude

of less than 50 meters above sea level and is close to Mount Rinjani. Information regarding the description of sampling sites and the measurement periods are provided in Table 2. 1.

Table 2. 1 Sampling sites description for air quality assessment in Indonesia

No	Site	Latitude	Longitude	Period	Site Description
1	Ambon	S 03°41′54.68″	E 128°10′25.22″	14 Mar 2013–22 Dec 2017	Urban
2	Balikpapan	S 01°16′37.4″	E 116°48′35.6″	24 Aug 2013–24 Nov 2017	Urban
3	Bandung	S 06°55′10.9″	E 107°36′39.1″	8 May 2012–26 Dec 2017	Urban
4	Denpasar	S 08°40′09.09″	E 115°14′09.31″	19 Sep 2012–17 Oct 2017	Urban
5	Jakarta	S 06°13′34.08″	E 106°50′04.42″	5 Mar 2010–28 Dec 2017	Mega city
6	Jayapura	S 02°33′43.42″	E 140°41′30.69″	10 Apr 2013–15 Aug 2017	Suburban
7	Makassar	S 05°05′08.72″	E 119°31′04.75″	8 Oct 2012–21 Dec 2017	Urban
8	Manado	N 01°28′04.9″	E 124°50′42.1″	10 Oct 2013–26 Dec 2017	Urban
9	Mataram	S 08°35′26.45″	E 116°05′39.71″	10 Dec 2013–31 Dec 2017	Urban
10	Medan	N 03°34′54.82″	E 98°40′28.46″	30 Mar 2014–27 Dec 2017	Urban
11	Palangka	S 02°10′30.72″	E 113° 52′49.26″	6 Oct 2011–22 Dec 2017	Suburban
12	Pekanbaru	N 00°30′38.54″	E 101°26′50.14″	12 Mar 2012–31 Dec 2017	Urban
13	Semarang	S 07°03′27.38″	E 110°24′40.50″	5 Mar 2012–13 Dec 2017	Urban
14	Surabaya_1	S 07°20′46.43″	E 112°44′03.12″	1 Jun 2015–28 Dec 2017	Urban
	Surabaya_2	S 07°18′44.68″	E 112°47′20.55″	6 Mar 2012–31 Dec 2017	Urban
15	Tangerang	S 06°21′02.5″	E 106°40′03.5′	15 Oct 2010–28 Dec 2017	Urban
16	Yogyakarta	S 07°46′39.6″	E 110°24′51.7″	8 Nov 2010–27 Dec 2017	Urban

Sampling at these 17 sites was conducted using Gent stacked filter unit (SFU) particle samplers to collect $PM_{2.5\text{-}10}$ and $PM_{2.5}$ size fractions [Hopke et al., 1997]. The samples were collected at least once per week for 24 h at urban residential sites on 8-µm pore coated Nuclepore filters for the coarse fraction sample and on 0.4-µm pore Nuclepore filters for the fine fraction sample. Most samples were collected on weekdays. The schematic of Gent stacked filter unit sampler is shown in Figure 2. 2.

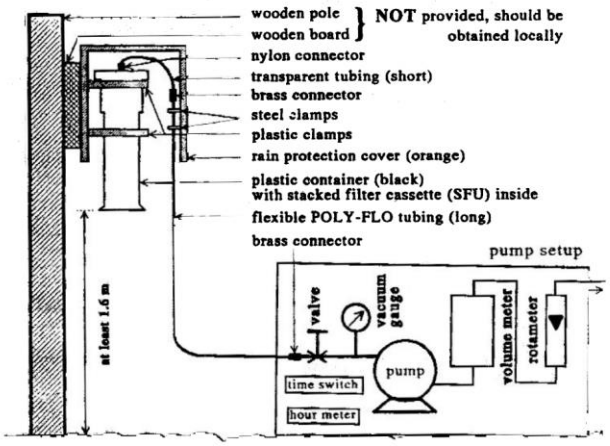

Figure 2. 2 Schematic of sampling system in Gent stacked filter unit sampler [Hopke et al. 1997]

2.2.2 Gravimetric method for mass concentration

The mass concentrations of $PM_{2.5}$ and $PM_{2.5-10}$ were determined by gravimetric analysis in environmentally controlled room. Moisture content can affect filter weight, therefor the filters were equilibrated for a minimum of 24 hours in prior to pre- and post-weighing. During the equilibration period, relative humidity was maintained at 45±5%, and air temperature at 20±2°C. The filters were weighing before and after sampling using microbalance with ± 0.001 mg precision (MX5 Mettler Toledo), then divided by the volume of air passing through the filter to obtain the concentration of $PM_{2.5}$ ($\mu g/m^3$). The PM_{10} concentrations were obtained by summing these two values of $PM_{2.5-10}$ and $PM_{2.5}$. More than 3300 pairs of samples were collected from the 16 cities across Indonesia.

2.2.3 Black carbon measurement

Black carbon (BC) is the primary agent responsible for light absorption within particles [Horvath 1997]. Black carbon (BC) found in airborne particulate matter results from the incomplete burning of carbon-based fuels. Black carbon (BC) or soot, also referred to as elemental carbon (EC) [Taha et al. 2007]. These terms BC and EC are operationally defined based on the measurement methods applied, and while they are often used interchangeably [Watson et al. 2005]. BC is defined based on its light-absorbing properties and includes both pure carbon and carbon with organic coatings, while EC specifically quantifies the pure carbon fraction. BC is a form of impurity resulting from incomplete combustion of fossil fuels, forest fires or biomass [Salako et al. 2012]. BC also constitutes a significant proportion of fine particulate matter in the atmosphere. Horvath states that over 90% of sunlight absorption in the atmosphere is dominated by BC [Horvath 1997]. BC has a rather complex effect on climate change. It induces atmospheric warming (positive radiative forcing) because of its ability to absorb solar radiation in the atmosphere. However, it also has a cooling effect on the Earth's surface (negative radiative forcing) as it prevents this radiation from reaching the Earth's surface. The Intergovernmental Panel on Climate Change (IPCC) in 2001 estimated that the impact of anthropogenic sources, including BC, on climate change would continuously increase from 2000 to 2100. BC is often considered the second most potent climate forcer after carbon dioxide (CO_2) because of its strong radiative forcing effect. BC is a short-lived climate pollutant, which means its atmospheric lifetime is relatively short compared to CO_2. However, its rapid removal from the atmosphere does not diminish its significant contribution to near-term climate warming.

In addition to its climate impacts, BC has adverse effects on air quality and human health [Ni et al. 2014]. It causes serious health problems by carrying carcinogenic compounds [Koelmans et al. 2006]. Many air quality standards and regulations do not explicitly include black carbon (BC) as a specific parameter for monitoring and compliance. Instead, they typically focus on broader measures of $PM_{2.5}$ and PM_{10}. However, organizations like the World Health Organization (WHO) have expressed concerns about the health impacts of BC and its contribution to air pollution. While BC may not be explicitly included in air quality standards, it is recognized as a significant component of $PM_{2.5}$, which is a common parameter used to assess air quality. $PM_{2.5}$ includes a mixture of particles, and BC is one of the components that contribute to its mass. Notably, in regions like Indonesia, biomass burning emerges as the dominant source of BC, contributing approximately 40% of $PM_{2.5}$ mass in suburban areas like Lembang and around 20% in urban settings like Bandung [Santoso et al., 2008]. In contrast, in European urban centre, BC is closely linked to vehicular traffic and represents a significant contributor to $PM_{2.5}$ [Almeida et al. 2020]

The primary sources of BC are anthropogenic, including biomass burning, motor vehicles (gasoline and diesel), and industrial sources such as coal combustion [Ramanathan and Carmichael 2008]. Reducing BC pollution sources is believed to be a beneficial strategy for mitigating and minimizing global warming [Ramanathan and Carmichael 2008]. Light absorbing carbon or BC in the samples was determined by reflectance measurement using an EEL Model 43D smoke stain reflectometer that measures the reduction in reflected white light as shown in Figure 2. 3 [Cohen et al. 2000; Taha et al. 2007; Salako et al. 2012]. Secondary standards of known black carbon concentrations are used to calibrate the reflectometer [Biswas et al. 2003]. A linear correlation of absorption (BC) by this method and elemental carbon (EC) measured by a thermo-optical analyzer has been demonstrated even for high concentrations (Salako et al., 2012). BC on the filters was estimated using the following equations [Cohen et al. 2000; Salako et al. 2012]:

$$BC\ (\mu g/cm^2) = \left\lceil 1000x \log \frac{R_0}{R} + 2.39 \right\rceil / 4.58 \qquad \text{Eq. (2. 1)}$$

$$BC\ (\mu g/cm^2) = \{100/2\varepsilon\} \ln \frac{R_0}{R} \qquad \text{Eq. (2. 2)}$$

$$BC\ (\mu g/m^3) = \frac{BC\ (\mu g/cm^2) \text{ x Filter area } (cm^2)}{\text{Volume of samples } (m^3)} \qquad \text{Eq. (2. 3)}$$

Eq 2. 1 is used using the constant of 2.39 and 45.8 derived by a series of 100 nucleopore polycarbonate filter samples which served as secondary standards, relative to standards, which was prepared by collecting burning acetylene soot on filters and determining the mass concentration gravimetrically the BC loading (in $\mu g/cm^2$) for these samples had been determined by Andreae from Max Planck Institute of Chemistry, Mainz, Germany. Similar results were obtained using Eq 2. 2, where R0 and R are the pre- and post-reflection intensity measurements at a given wavelength, respectively. It is common practice to set the pre-reflection intensity R0=100%. The BC concentrations were defined based on the amount of light that is absorbed by the filter sample and an assumed mass absorption coefficient (7 m^2/g, with an exposed area of 12.57 cm^2) to convert reflectance measurement to mass that can be divided by sample volume to give micrograms per cubic meter. Typically values of mass absorption coefficient for submicron aerosols range from 5–10 m^2/g [Taha et al. 2007].

Figure 2. 3 Smoke stain reflectometer

2.2.4 Elemental concentration

XRF analysis was conducted at the National Research and Innovation Agency of Indonesia (BRIN) laboratory, Indonesia. The spectrometer is equipped with 9 secondary targets (Fe, CaF_2, Ge, Zr, CeO2, Mo, Ag, Al and Barkla polarizing target (Al_2O_3), which are excited using an Sc-W tube. The characteristic X-ray radiation emitted by the sample is then detected by a Ge detector, which exhibited a measured energy resolution of approximately 150 eV FWHM at Mn-Kα (5.89 keV). To optimize analytical sensitivity and precision for the determination of specific groups of elements in aerosol particles on filters, each different measuring conditions were carefully selected as resumed in Annex Table A. 1. The live time for all measurements with secondary targets was set to 400–600 seconds. The entire analysis

was carried out under vacuum conditions. The quantification was applied based on calibration which was carried out by measuring thin-film single-element and compound reference materials provided by Micromatter. These materials were prepared on a polycarbonate filter. For method validation, National Institute of Standards and Technology (NIST) Standard Reference Material (SRM) 2783 air particulate on filter media were periodically analyzed. Several elements in $PM_{2.5,}$ including S, Fe, Zn, and Pb will be discussed. The detection limits of these elements were 5.9, 10.4, 1.9, 3.8, 2.9, and 6.2 ng/m^3, respectively.

2.3 Results and Discussion

2.3.1 $PM_{2.5}$ and $PM_{2.5-10}$ concentrations

The study involved the collection and analysis of a total of 6672 samples obtained from 17 distinct sites situated in 16 different cities throughout Indonesia. These samples were subjected to assessments for both mass and chemical composition, including the presence of black carbon. The data pertaining to the concentrations of $PM_{2.5}$, $PM_{2.5-10}$, and BC for each of the 17 sites, consisting of 7 sites located on Java Island and 10 sites situated outside of Java are summarized in Table 2. 2. Figure 2. 4 and 2. 5 show the site-by-site $PM_{2.5}$ and PM_{10} data distribution, respectively, including special event data, such as the Kelud volcanic eruption in Java and forest fires that occurred in Sumatra and Kalimantan. The whisker plot represents 25^{th} and 75^{th} percentile values, outliers, median (solid black line in the box), and mean (red line). Error bars represent the 5^{th} and 95^{th} percentile values.

Table 2. 2 Statistical values of $PM_{2.5}$, $PM_{2.5-10}$ and BC concentrations (μg/m^3) of the 17 sites in Indonesia

No	Island	City	n	$PM_{2.5}$ Concentration				$PM_{2.5-10}$ Concentration				BC	BC /$PM_{2.5}$
				Mean	Median	Min	Max	Mean	Media	Min	Max	Mea	%
1		Bandung	215	18 ± 8	18	2	56	24 ± 9	23	4	61	3.5	22
2		Jakarta	249	17 ± 8	17	1	70	28 ± 12	27	2	70	3.3	21
3		Semarang	235	16 ± 8	16	2	45	13 ± 9	11	2	84	3.1	22
4	Java	Surabaya_1	62	15 ± 5	15	6	27	7 ± 2	6	22	4	3.2	22
		Surabaya_2	208	16 ± 5	16	5	44	20 ± 10	19	6	99	3.6	23
5		Tangerang	328	14 ± 7	15	1	38	14 ± 8	12	2	44	2.5	20
6		Yogyakarta	340	11 ± 8	10	1	35	13 ± 8	11	2	74	2.4	23
7		Ambon	119	8 ± 4	7	3	31	7 ± 4	7	1	24	1.4	20
8		Balikpapan	141	10 ± 6	8	1	37	11 ± 8	10	1	46	1.5	16
9		Denpasar	178	13 ± 5	13	1	32	16 ± 7	16	3	44	2.8	24
10		Jayapura	144	5 ± 3	4	1	15	6 ± 3	5	1	24	0.7	16
11	Outside	Makassar	184	12 ± 7	10	2	49	8 ± 7	5	1	47	2.8	26
12	Java	Manado	172	7 ± 5	6	1	32	9 ± 5	7	2	40	1.1	18
13		Mataram	144	10 ± 5	10	1	23	14 ± 7	13	1	41	1.8	18
14		Medan	115	10 ± 6	9	1	30	20 ± 7	19	8	47	1.9	18
15		Palangka	272	8 ± 7	5	1	41	10 ± 8	9	1	74	1.1	15
16		Pekanbaru	230	16 ±	15	2	96	26 ± 21	2	1	157	2.7	19

[a]Sample collected on 14 Feb 2014 during the eruption of Mt. Kelud is not counted.

[b]Samples collected on 22-27 Oct 2015 when there was a large forest fire are not counted.

In Figure 2. 4, the Indonesian annual standard of 15 μg/m^3 (spanned horizontal line) and 24-h standard of 65 μg/m^3 (dashed line) is shown, while in Figure 2. 5, the U.S. annual standard of 50 μg/m^3 (spanned horizontal line) and 24-h of standard 150 μg/m^3 (dashed line) are shown. The majority of the average annual $PM_{2.5}$ concentrations measured at the Java sites (Bandung, Jakarta, Semarang, and Surabaya) exceeded the Indonesian annual ambient air quality standard (15 μg/m^3), although the other studied locations, excluding Pekanbaru and Palangka Raya, exhibited values below the standard. During the forest fire episodes of 2015, the average daily $PM_{2.5}$ concentrations in Pekanbaru and Palangka Raya exceeded the national daily ambient standard (65 μg/m^3).

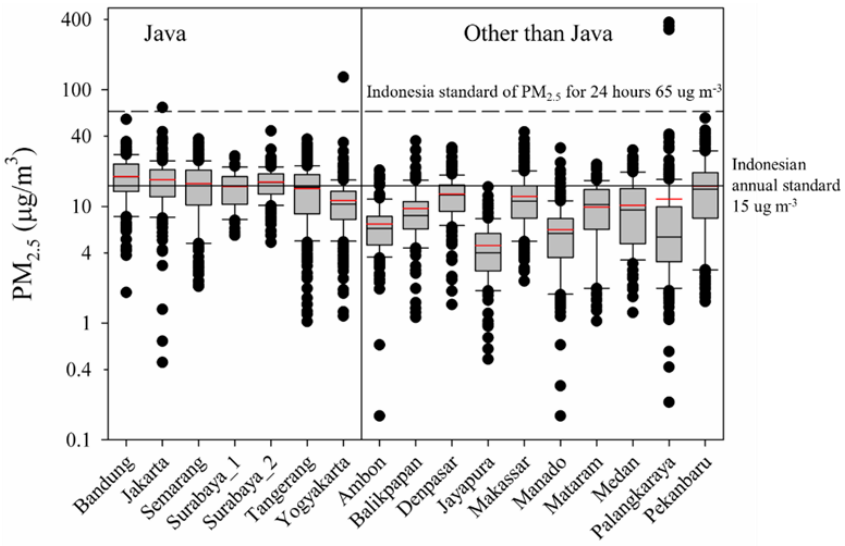

Figure 2. 4 Box-and-whisker plots of the $PM_{2.5}$ distributions across Indonesia

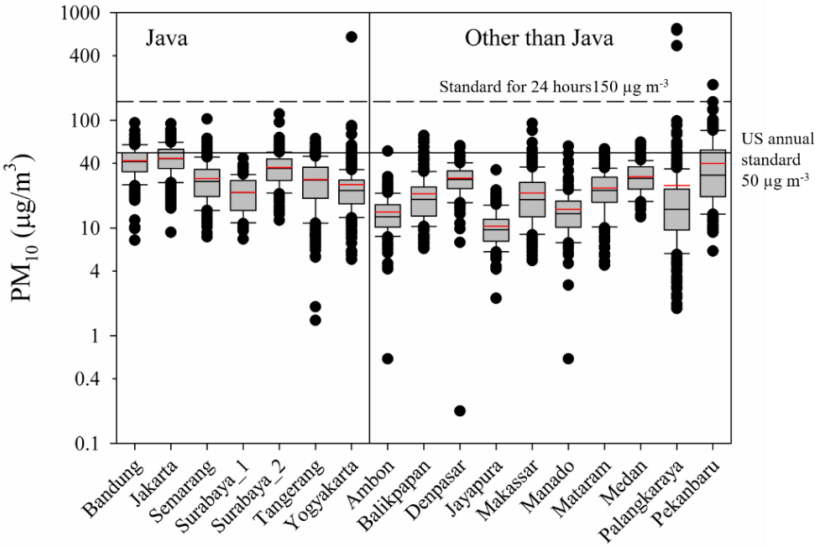

Figure 2. 5 Box-and-whisker plots of the PM_{10} distributions across Indonesia

The 2014 volcanic event significantly influenced air quality especially in Yogyakarta because volcanic ash was dispersed across an area of more than 500 km from the source [Lestiani et al. 2018]. The mass concentrations of $PM_{2.5}$ and PM_{10} in Yogyakarta during the eruption episode reached 128 and 592 µg/m^3, respectively, 10 times higher than $PM_{2.5}$ under normal conditions, and even higher for PM_{10}. The city of Yogyakarta is situated approximately 283 kilometers to the west of the volcano, whereas Semarang and Surabaya are positioned at distances of 318 kilometers to the northwest and 131 kilometers to the northeast of the volcano, respectively. Yogyakarta experienced the most significant impact compared to the other locations due to the eruption dynamics. During the eruption event, the volcano discharged materials as high as 17 kilometers into the atmosphere, and prevailing

winds carried these materials predominantly westward [Kristiansen et al. 2015]. Palangka Raya experienced elevated levels of $PM_{2.5}$ and PM_{10} concentrations during the forest fires that occurred in October 2015. This event has been represented in Figure 2. 4 and 2. 5. During this period, the observed concentrations of $PM_{2.5}$ and PM_{10} reached to 377 and 710 $\mu g/m^3$, respectively. The impact of the 2015 forest fires episode on the city's air quality was substantial, with PM concentrations reaching levels 10 to 100 times higher than usual. This heightened effect can be attributed to an exceptionally dry period from July to October 2015, driven by the strong El Niño conditions that year, which resulted in more intense fires. Thus, efforts to reduce the occurrence of large fires are enforced by the government and their resulting consequences need to be continued.

The annual average $PM_{2.5}$ values for all sites are provided in Table 2. 3. It shows that $PM_{2.5}$ concentrations in Bandung had a slight upward trend from 2012 to 2017 likely due to an increase in population and heavy traffic in the urban. The annual average $PM_{2.5}$ has exceeded

Table 2. 3 Annual average for $PM_{2.5}$ mass concentrations in the 16 Indonesian cities

No	Island	City	$PM_{2.5}$ Concentration ($\mu g\ m^{-3}$)							
			2010	2011	2012	2013	2014	2015	2016	2017
1	Java	Bandung			17 ± 7	14 ± 5	20 ± 8	21 ± 6	18 ± 7	19 ± 10
2		Jakarta	15 ± 7	17 ± 7	19 ± 8	17 ± 7	18 ± 6	16 ± 5	15 ± 5	19 ± 12
3		Semarang				15 ± 6	16 ± 9	19 ± 8	18 ± 6	15 ± 5
4		Surabaya 1						17 ± 5	13 ± 6	15 ± 5
		Surabaya 2			20 ± 5	15 ± 5	17 ± 4	16 ± 8	15 ± 4	17 ± 4
5		Tangerang	14 ± 7	16 ± 6	12 ± 5	14 ± 4	19 ± 7	13 ± 6	13 ± 6	13 ± 8
6		Yogyakarta[a]	9 ± 5	10 ± 3	10 ± 3	11 ± 4	14 ± 5[a]	12 ± 7	10 ± 5	10 ± 4
7	Outside Java	Ambon				7 ± 2	9 ± 4	9 ± 4	6 ± 3	7 ± 4
8		Balikpapan[e]				9 ± 6	6 ± 3[e]	17 ± 9[e]	9 ± 3	9 ± 3
9		Denpasar			15 ± 3	10 ± 4	14 ± 5		13 ± 6	12 ± 5
10		Jayapura				3 ± 2	5 ± 3	5 ± 2	4 ± 1	6 ± 3
11		Makassar			9 ± 4	7 ± 3	20 ± 10	14 ± 7	10 ± 4	10 ± 4
12		Manado				6 ± 3	7 ± 6	6 ± 5	8 ± 2	6 ± 2
13		Mataram[c]				7 ± 1	14 ± 4	11 ± 4	11 ± 5	7 ± 5[c]
14		Medan					7 ± 7		10 ± 6	11 ± 6
15		Palangka		9 ± 5	12 ± 10	7 ± 7	4 ± 4	8 ± 9[b]	5 ± 2	7 ± 2
16		Pekanbaru[d]			19 ± 9	18 ± 9	29 ± 11[d]	18 ± 9	8 ± 6	13 ± 5

[a] Without sample collected on 14 February 2014 during the eruption of Mt. Kelud, average PM2.5 in 2014 with volcanic eruption episodes was 16 ± 18 μg m–3.

[b] Without samples collected on 22–27 October 2015 when there was a large forest fire in Kalimantan, average PM2.5 in 2015 with forest fire episodes was 46 ± 111 μg m–3.

[c] In 2017, samples were collected on weekends (70%) and workdays (30%).

[d] In 2014, samples were only collected for 3 months (January–March).

[e] In the 2014–2015 period, samples were only collected January–June 2014 and August–December 2015.

the Indonesian standard. Based on data from the Central Statistics Agency of West Java, the 2017 population in the city of Bandung reached 2.497 million. Between 2012 to 2017, there was a significant increase in the number of motor vehicles, cars, and motorbikes. The various programs undertaken to improve air quality in Bandung, especially for $PM_{2.5}$, have succeeded in compensating for its dense population and increasing use of motorized vehicles.

The 8 years of monitoring in Jakarta (2010–2017) revealed that the annual average levels of $PM_{2.5}$, a hazardous air pollutant, consistently exceeded the Indonesian standard. Several programs have been implemented such as increasing the number and quality of mass transportation, requiring a minimum number of passengers in one car (three in one), implementing car-free days, and various other programs, but these efforts have not been able to reach the goal of bringing the annual average concentration of $PM_{2.5}$ below the Indonesian standard. High use of motor vehicles and dense population that in 2017 reached 10.37 million are major contributors to pollution in Jakarta. As the capital city of Indonesia, it is the center of government and business. Motorized vehicles in Jakarta are not only from local Jakarta but also from several cities around it. The commuters contribute significantly to the traffic density in Jakarta. Motor vehicles are the dominant sources that contributes 31.5% to the fine particulate matter in Jakarta. Other emission sources like industrial sources and biomass burning seem to contribute to the air quality in Jakarta [Santoso et al. 2013].

The annual average $PM_{2.5}$ values at Eat Java sites, Surabaya_1 and Surabaya_2 sites exceed Indonesian standards (Table 2. 3), except for the 2013 annual average at Surabaya_1. Surabaya_1 is located nearer to the urban centers, while Surabaya_2 is located on the border of Surabaya and Sidoarjo that has major industrial activity in the surrounding. Surabaya_2 sampling sites were surrounded by several industrial activities such as steel industries, galvanizing, electronic and metal industries. Therefore, in general, the $PM_{2.5}$ concentrations at Surabaya_2 tend to be higher than those at Surabaya_1. For Semarang, the annual average $PM_{2.5}$ concentration over the 5 years of monitoring (2013–2017) failed to achieve the Indonesian standard. As the capital city of Central Java province, Semarang has an industrial area with various industries including electronics assembly, motor vehicles industry, and garment industry. Comprehensive research needs to be carried out to confirm whether these industrial activities contribute significantly to the air quality in Semarang.

Monitoring over 8 years in Tangerang and Yogyakarta (Table 2. 3) shows that the annual average $PM_{2.5}$ meets the Indonesian standard except for Tangerang in 2011 and 2014. Although the annual average met the Indonesian standards, the 8-year annual average for both sites exceeds the World Health Organization (WHO) annual standard for $PM_{2.5}$ (10 $\mu g/m^3$). For the sites in Java, the results obtained from this study indicated that most cities failed to meet the Indonesian annual ambient air quality standard for $PM_{2.5}$. Several mitigation programs have been implemented, but these efforts have not been able to significantly reduce the PM concentration in these cities likely due to a rapid growth of industry, population, and motor vehicle usage.

2.3.2 BC concentration

The average BC concentrations at the Java sites varied between 2.38 and 3.55 $\mu g/m^3$, with BC accounting for 19.6% to 22.6% of $PM_{2.5}$ at these locations. While for the sites located outside of Java, the average BC concentrations ranged from 0.66 to 2.78 $\mu g/m^3$, with BC comprising 15.1% to 26.0% of $PM_{2.5}$, as indicated in Table 2. 2. The average BC of $PM_{2.5}$ levels ranged from 15% to 26%, showing the BC's significance as a major constituent of $PM_{2.5}$. This substantial presence of BC is likely linked to both traffic emissions and biomass burning. It is evident that BC concentrations in the Java Island sites (including Bandung, Jakarta, Semarang, and Surabaya) exhibited higher BC levels than sites located outside of Java. In the case of Denpasar, when compared with other outside-Java sites, the elevated BC concentrations were probably attributed to activities such as the burning of incense and other forms of biomass combustion. Conversely, in the case of Makassar, the highest BC concentrations were likely the result of biomass burning, as reported by another study in Makassar [Sattar et al. 2014].

Previous research conducted by Santoso et al. (2008) in Bandung identified biomass burning as the primary source of BC [Santoso et al., 2008]. In Tangerang, as reported by Santoso et al. (2011), BC sources were linked to a combination of diesel vehicles and biomass burning, often mixed with road dust [Santoso et al. 2011]. In Jakarta, BC sources were predominantly associated with motor vehicles due to the proximity of the sampling site to one of the busiest arterial roads [Santoso et al. 2013]. For Yogyakarta, Semarang, and Surabaya, the sources of BC concentrations remain relatively unclear.

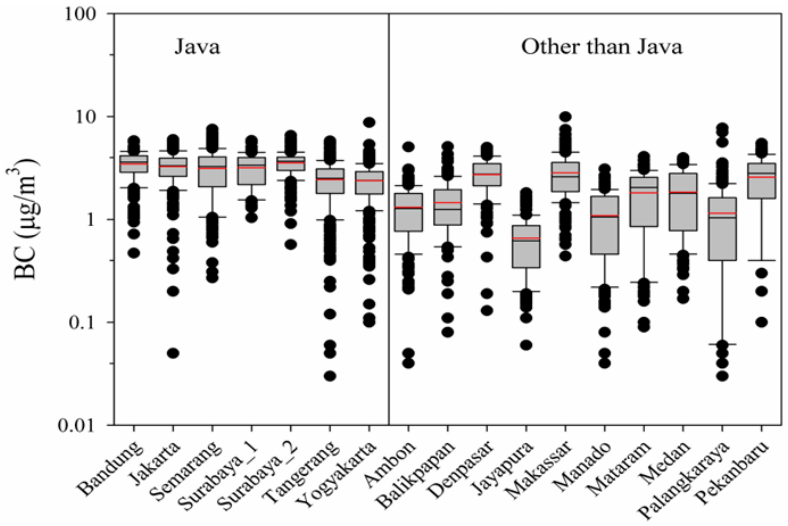

Figure 2. 6 The box-and-whisker plot for BC concentrations measured in the 16 cities in Indonesia.

However, it is generally believed that BC in these areas may be attributed to a combination of biomass burning and motor vehicle emissions. Additionally, there may be a contribution from open burning practices still used by farmers in Indonesia [Permadi and Kim Oanh 2013]. Figure 2. 6 displays the box-and-whisker plot illustrating BC concentrations at these various sites. Notably, the average BC levels depicted in Figure 2. 6 are lower when compared to findings reported in the Philippines, Bangladesh, and Sri Lanka [Atanacio et al. 2016; Pabroa et al. 2022].

2.3.3 Elemental S, Pb, Zn and Fe concentrations

The distributions for the elemental concentrations of S, Pb, Zn, and Fe in $PM_{2.5}$ measured at the 17 sites are shown in Figure 2. 7. The average sulfur concentrations in the 17 sites varied, as depicted in Figure 2. 7, reached a peak in Bandung at 1061 ng/m^3, lower than the average sulfur levels reported for Petaling Jaya (1935 ng/m^3) [Rahman et al. 2011] and Dhaka (1591 ng/m^3) [Begum and Hopke 2019]. In the case of Bandung, this high sulfur content may be partially attributed to contributions from the nearby volcano, Tangkuban Perahu volcano, situated approximately 30 km to the north of the city, where sulfur gas emissions are relatively continuous [Santoso et al. 2008]. The high S concentrations in Palangka Raya and Pekanbaru were likely from the peat forest fires that occurred in Kalimantan and Sumatra during the study period. Peat serves as the initial stage in the geological process of coal formation. Consequently, when a peat fire occurs, it leads to the emission of various elements, including sulfur and certain heavy metals. Forest fires,

primarily prevalent during the dry season from June to September, pose a recurring challenge in Indonesia, particularly in regions like Sumatra and Kalimantan, which boast extensive peatlands. The notably high sulfur concentrations observed in Palangka Raya can be attributed to samples collected during the forest fire events in October 2015. During this period, $PM_{2.5}$ values surged to levels as high as 400 µg/m^3.

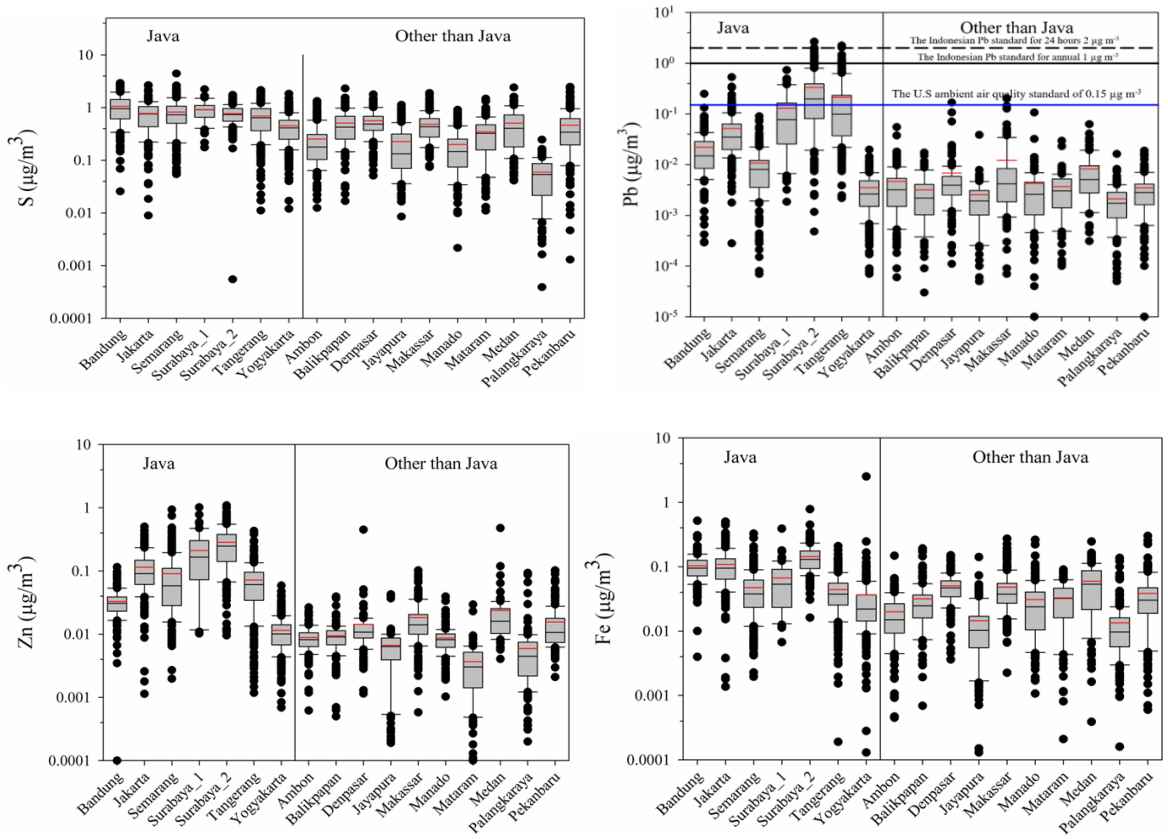

Figure 2. 7 Whisker plot of S, Pb, Zn and Fe concentrations in the studied area

Figure 2. 7 reveals that Pb concentrations in Surabaya and Tangerang were significantly higher in comparison to the other cities. Surabaya exhibited the highest lead concentrations among all the monitored cities. The maximum measured Pb concentrations at Surabaya_1, Surabaya_2, and Tangerang sites were 0.73, 2.7, and 2.3 µg/m^3, respectively. Both Surabaya_2 and Tangerang sites exceeded Indonesia's 24-hour National Ambient Air Quality Standard for lead in total suspended particulate matter, which is set at 2 µg/m^3. During the study period, the average lead concentrations in Surabaya_1, Surabaya_2, and Tangerang were measured at 0.13, 0.33, and 0.22 µg/m^3, respectively. These values significantly surpassed those reported in other cities across Asian countries [Hopke et al. 2008]. Notably, both Surabaya_2 and Tangerang sites exceeded the U.S. ambient air quality

standard of 0.15 μg/m^3. Additionally, similar condition with Bangladesh, where Begum showed that in Bangladesh, the yearly average Pb levels in the air have exhibited a gradual increase, possibly stemming from activities such as battery recycling and industrial processes [Begum and Hopke 2019]. Studies of the high Pb concentrations in Tangerang were conducted previously in 2008. The source of lead in $PM_{2.5}$ was identified to be associated with a lead battery recycling and bar production facility [Santoso et al. 2011]. The high level of Pb in airborne particulate matter in Tangerang has also affected the lead concentrations in the soil around the Tangerang lead smelting area. The highest lead concentrations were 1784 mg/kg and 2125 mg/kg resulting from the formal lead smelter and informal lead smelter, respectively [Adventini et al. 2017]. These findings underscore the pressing need for immediate action to mitigate potential adverse effects on human health and the associated economic outcomes resulting from emissions originating from this facility. Lead pollution poses significant environmental and health risks, particularly for children, as it has been linked to the potential for mental retardation and effects on intelligence quotient (IQ) [Sullivan 2015]. There is some evidence that long-term occupational exposure to lead may contribute to the development of cancer [WHO 2010; Sullivan 2015]. Effective measures must be set in motion, requiring the proactive involvement of local government authorities and the Ministry of Environment and Forestry to address this critical issue.

Figure 2. 7 also shows that high concentrations of Zn were found in several cities. Zn was likely emitted by motor vehicles and industrial activities. Two-stroke motor vehicles use oil containing additives that include zinc compounds to increase their lubricating capability. Zn is then released when the oil is burnt along with the gasoline. Zinc is also emitted from industrial activities such as non-ferrous metal smelting, galvanizing operations, and municipal solid waste incineration [Hopke et al. 2008]. The high concentrations of Zn in Surabaya, Semarang, and Jakarta with average concentrations of 285, 91 and 114 ng/m^3, respectively. The concentration of Zn in Surabaya was similar with Dhaka (335 ng/m^3) which has the main sources of Zn from diesel emission and coal power plant [Begum et al. 2010]. The high concentrations of Zn in Surabaya, Semarang, and Jakarta are estimated to be the result of contributions from multiple industrial activities in these cities including the galvanizing process in the industrial area around the sampling location. Source identification needs to be done to better estimate the impacts of these sources.

Figure 2. 7 also shows the Fe concentration distributions. The results showed high concentrations of Fe in Surabaya and Jakarta. Sources likely include industrial activities,

extensive infrastructure construction across the city including highways and mass transit lines. Yogyakarta showed its highest values in the samples collected during the eruption of Kelud in February 2014. Further investigation related to the elevated Fe in Surabaya and Jakarta is needed.

2.4 Conclusions

The National Ambient Air Quality Standards of Indonesia, which were last evaluated in 1999, are presently being reviewed for potential revision. This study, which provides current data about air quality in the nation, offers valuable input for the new regulatory standards. The average annual $PM_{2.5}$ concentrations at most of the urban sites on Java exceeded the national standard. The cities outside of Java, however, except for Pekanbaru and Palangka Raya, were in compliance with the standard. The percentage of BC in the $PM_{2.5}$ averaged between 15% and 26% (a significant fraction), and higher concentrations of BC, which is associated with traffic emission and biomass burning, were found in Java as well as in Denpasar and Makassar. Additionally, the concentrations of the major elements in the $PM_{2.5}$, S, Fe, Zn, and Pb, varied between the sites. Owing to forest and peat fires, Palangka Raya displayed the maximum concentrations of sulfur, and high values for this element were also observed in Bandung, where relatively continual gaseous emission from Mount Tangkuban Perahu and the combustion of high sulfur vehicular fuel were contributing factors. Finally, higher concentrations of heavy metals, Fe, Zn, and Pb, were measured in Surabaya than in the other cities. The concentration of Pb was 10–100 times higher in Surabaya and Tangerang. Considering the adverse health effects of this element, appropriate actions must be taken to reduce exposure in these areas. Further investigations related to the source identification and possible sources are needed to be carried out.

CHAPTER 3 Heavy Metals, Sources, and Potential Risk Assessment of $PM_{2.5}$ in the Vicinity of a Lead Smelter in Indonesia

3. 1. Introduction

The existence of heavy metals in particulate matter (PM) especially fine particles of $PM_{2.5}$ potentially poses a diverse impact on human health [Zhai et al. 2014; Soleimani et al. 2018]. Heavy metals such as Cr, Cu, Mn, Fe, Pb, and Zn in $PM_{2.5}$ were found to be associated with PM toxicity and their co-exposure led to damage to biological cells and high mortality of human cells [Yuan et al. 2019]. Heavy metals in the atmosphere are mostly emitted from industrial emissions (mining, smelters, coal combustion), vehicular emissions, and secondary aerosols as the major sources [Pacyna et al. 2009; Li et al. 2012; Suvarapu and Baek 2017; Engel-Di Mauro 2021]. Characterization of heavy metal concentrations to understand the impact of industrial activities is a very important step, especially in locations where these activities are close to agricultural ecosystems and the human living environment.

Lead or battery recycling smelters have the potential to emit lead and other heavy metal particulates into the air which can be carried by the wind and deposited on the ground [Gao et al. 2016; Qiu et al. 2016]. It may expose and pose a hazard to the people surrounded through inhalation, dust ingestion, and food chain [Jallad 2015; Gao et al. 2016; Engel-Di Mauro 2021]. Lead exposure and poisoning in children living near lead smelters continue to occur in developed and developing countries [Mohammed et al. 1996; Ji et al. 2011; Cohen and Amon 2012; Haryanto 2016; Taylor et al. 2019]. Lead is considered hazardous due to its persistent, highly toxic, and bio accumulative. The effects of lead exposure in children who are the most susceptible groups can cause hearing, behavior, and learning problems, anemia, slower growth, lower IQ, and hyperactivity [Cohen and Amon 2012; Sullivan 2015; Suvarapu and Baek 2017; Prihartono et al. 2019]. There are more than 200 used lead acid battery lead smelters which are located in several areas in Java, mostly in Tangerang, Tegal (Central Java), and East Java [Haryanto 2016; Hindratmo et al. 2018; Prihartono et al. 2019]. However, only a limited numbers of information is available on the characteristics and levels of lead in ambient particulate emissions from industrial areas, especially lead smelters in Indonesia [Santoso et al. 2011]. Our previous study has presented the results related to heavy metal pollution in air particulate matter in Serpong district, Tangerang city [Santoso et al. 2011]. We found that the concentrations of atmospheric lead were higher in Serpong, Tangerang than in Jakarta, and the lead concentration in ambient air in Serpong was mainly

from a lead industry that recycles lead-acid batteries and produces lead bar/ingots. A study by Haryanto found that very high blood lead levels (BLLs) have been identified in children living near used lead acid batteries recycling smelters [Haryanto 2016; Prihartono et al. 2019]. It was found that many children in the area had learning difficulties and poor grades in school, and some had physical development problems such as stunting or other problems. Another study by Hindratmo also reported that the BLL in elementary school children collected from Tangerang (60 children) and Lamongan (69 children) who lived near the lead smelter industries, all the values of BLL were found above the CDC standard for BLL (5 μg/dL), and some children's BLL were out of the measurement range (above 65 ug/dL) [Hindratmo et al. 2018]. Because $PM_{2.5}$ has a major impact on human health, especially in children, it really needs to understand the associated pollutants, particularly heavy metals in $PM_{2.5}$ to identify the impact of these industrial activities to the surrounding air quality. It is important to establish the data for baselines of air quality in industrial sites to evaluate the effectiveness of a strategic plan for improving the air quality over time. By identifying the heavy metals contamination in the air ambient and its potential risk assessment to the environment, it could be used as an evidence and reference for the government and related stake holders to design the policy and take proper action to reduce the pollution and minimize the impact.

Studies of heavy metals in fine particulate matter $PM_{2.5}$ in industrial areas have been reported from several countries in Asia, the US, Australia, and Europe [Alias et al. 2020; De Vleeschouwer et al. 2010; Jallad 2015; Li et al. 2012; Li et al. 2020; Pönkä 1998; Sullivan 2015; Suvarapu and Baek 2017; Taylor et al. 2019; Vega et al. 2021]. In the case of industrial sites in Indonesia, several studies have presented their findings, including those conducted in Serpong, Banten [Santoso et al. 2011], Cilegon Banten [Damayanti and Lestari 2020], Surabaya East Java [Humairoh et al. 2020]. Santoso reported that in the industrial site of Serpong for short-term study in August–November 2008, and diesel vehicles were identified as the primary source of $PM_{2.5}$, with the other sources included power plants, road dust, biomass burning, and a combination of the lead industry with a small portion of road dust. Diesel vehicles, categorized as traffic-related sources, were identified as contributing 30% to $PM_{2.5}$ levels, characterized by elevated concentrations of Zn and S due to the high sulfur content in diesel fuel [Santoso et al. 2011], while the Pb industry mixed with road dust was found to contribute 12% of $PM_{2.5}$. Another short-term research study, conducted on industrial sites in Cilegon in August – November 2015, was reported by Damayanti et al

[Damayanti and Lestari 2020]. However, this research primarily focused on the total suspended particulate TSP and identified the major contributor of crustal elements, accounting for 40.1%. Other industry-related sources were revealed, including iron and steel production (22.2%), coal combustion (16.5%), biomass burning (11.8%), and smelting (8.6%). It is worth noting that due to its particle size, TSP is mostly composed from the dominance of natural sources, especially crustal elements.

Furthermore, research on APM in East Java has indicated concerning levels of air particulate matter, especially regarding potentially toxic elements. Our study on air quality in several cities in Indonesia 2010–2017 revealed that concentrations of $PM_{2.5}$ in the industrial areas of Surabaya exceeded the Indonesian annual ambient air quality standard (15 $\mu g/m^3$). Additionally, significantly higher concentrations of potentially toxic elements such as Fe, Zn, and Pb were identified [Santoso et al. 2020b]. These findings highlight a similar air quality condition to that in the Serpong area, which is contaminated with high levels of Pb in the air. Another investigation conducted by Humairoh, part of our continuous research efforts in monitoring air quality in East Java, showed the elevated of potentially toxic elements, including Pb, in air particulate matter samples collected from industrial zones in Waru, East Java [Humairoh et al. 2020].

There is a lack of available information on the levels of lead in the ambient air in the vicinity of lead smelters in East Java, specifically in Lamongan. While some studies have been conducted on heavy metals in the ambient air in industrial areas in other cities in Java, such as Tangerang and Jakarta, there is a gap in research on this issue in Lamongan. Given the potential health and environmental impacts of lead smelter emissions, it is important to conduct studies on the levels of lead in the ambient air in the vicinity of lead smelters in East Java, especially in Lamongan which several lead smelters are operating in this area. This research can help to identify potential health risks to residents and inform the development of policies and regulations to reduce exposure to lead and other pollutants. Therefore, in this study, the characterization of heavy metals in fine particulate matter $PM_{2.5}$ collected in the near lead smelter in Lamongan, East Java was carried out. The identification of sources of heavy metals in $PM_{2.5}$ was applied using Principal Component Analysis (PCA) and toxic heavy metals associated with non-carcinogenic and carcinogenic elements are used to estimate the potential health risk of the presence of heavy metals. This result will provide a basis for government/policymakers in designing the proper and suitable control strategies.

3. 2. Methodology

3.2.1 Sampling site

Sampling was conducted in Lamongan regency of East Java province in 07°05’5.71” S and 112°17’22.38” E (Figure 3. 1). Lamongan is a regency of the East Java province and is classified as an agricultural city with an inhabitant of more than 1.45 million in an area of approximately 1812.8 km^2 with a length of 47 km along the coastline. The sampling site is located 1.7 km northeast of the lead smelter (with coordinates 07°05’14.46” S and 112°16’28.13” E) and 2 km north of the main national coast highway, surrounded by the rice field where more than 43.8% of the land is used for agricultural purposes in the form of irrigated and rainfed rice fields.

Figure 3. 1 Sampling site and Pb smelter near the location in Lamongan, East Java

Additionally, the site is near a plumbing pipe factory and a wood industry. Sampling was conducted in April – May 2015 using a Gent stacked filter unit sampler [Hopke et al. 1997], 3–4 times a week for 24 hours, and a total of 21 samples were collected. The samples were then stored in a clean plastic petri dish and stored in a clean room at a temperature of 18–25°C and humidity below 60% for mass stabilization [Lestiani et al. 2015].

3.2.2 Samples characterization

The masses were determined by weighing the filters before and after sampling using a microbalance with 0.001 mg precision (MX5 Mettler Toledo), then they were divided by the volume of air passing through the filter to obtain the concentration of $PM_{2.5}$ ($\mu g/m^3$). The

black carbon (BC) concentrations of the samples were determined by reflectance measurement using a smoke stain reflectometer (Diffusion Systems Ltd. Model 43D). Elemental analysis of all samples was done by using EDXRF at a nuclear analytical laboratory in Bandung, Indonesia. Analysis was carried out using EDXRF Epsilon5 (PANalytical). It has equipped with an X-ray generator (Sc/W tube, 600 W with max 24 mA and voltage 100 kV), a high-resolution Germanium detector with Be window of 150 µm thickness and 30 mm2 surface area. EDXRF spectrometer 5 optimum conditions were used to characterize the samples (Table A. 1). The method validation was applied by analyzing the standard reference materials SRM NIST 2783 air particulate on filter media as routine and employed as quality control. The recovery of SRM analysis ranged from 0.92% to 1.09% except for Na and Mg which have low energy X-rays and low fluorescence yields leading to higher uncertainties [Santoso and Lestiani 2014]. The XRF analyses resulted in the concentrations of several elements such as Na, Mg, Al, Si, S, Cl, K, Ca, Ti, V, Cr, Mn, Fe, Ni, Cu, Zn, Br, and Pb.

3.2.3 Data Analysis

Principal Component Analysis (PCA)

The simplest form of factor analysis is principal components analysis. Statgraphics® software was used to do a multivariate principal component analysis of the $PM_{2.5}$ data set. By finding a new set of variables as a linear combination of the measured variables, it is assumed that the observed variations in the data can be reproduced by a reduced number of these causal factors. The PCA was applied to identify the key elements that are closely related to the sources. This method attempts to simplify the identification of the correlation between the measured components and possible sources [Suvarapu and Baek 2017; Alias et al. 2020; Vega et al. 2021]. The varimax rotation was used to obtain the best solution for factor loadings. Factors with one or more elements having factor loadings over 0.5 were considered for the association of the factor with the source. The varimax factor loadings represent a linear combination that shows the value of a correlation coefficient. Loading values over 0.50 are considered to provide significant insights into the origin of the sources.

Risk Assessment for Noncarcinogenic metals

The average daily dose (ADD) is the estimated value for exposure by considering several exposure factors. The evaluation of potential chronic (non-carcinogenic) effects was carried out by comparing the level of exposure over a specific time of ADD with a reference

dose (RfD) for the same period of exposure. This ratio value is a hazard quotient (HQ) [US EPA 1989, 2011]. The approach using a hazard index (HI) has been frequently used, to assess the overall potential for chronic effects caused by more than one type of substance/chemical or heavy metals. HI is equal to the sum of all HQs. The following equations determine the average daily dose (ADD), HQ, and HI [US EPA 1989, 2011]:

$$ADD = \frac{C\ x\ IR\ x\ ED\ x\ EF}{BW\ x\ AT}$$

Eq. (3. 1)

$$HQi = \frac{ADD}{RfD}$$

Eq. (3. 2)

$$HI = \sum_{i=1}^{n} HQi$$

Eq. (3. 3)

where C is the heavy metal's concentration (ng/m^3), IR is the inhalation rate (m^3/day), and ED is the exposure duration (years) which is 6 and 24 years for children and adults, respectively, EF is the exposure frequency (350 days), BW is the body weight (kg) 15 and 70 kg for children and adults, respectively and AT is the averaging time (ED x 365) [US EPA 1989, 2011].

Carcinogenic Metals Risk Assessment

An average risk of carcinogenic can be calculated through this following equation:

Cancer Risk CR (inhalation) =LADD × SF Eq. (3. 4)

$$SF = IUR \times \left[\frac{1}{IR}\right] \times BW$$

Eq. (3. 5)

where LADD is the metal's exposure concentrations, IR is the inhalation rate (m^3/day), and IUR is an estimate of the increased cancer unit risk value through inhalation (m^3/µg). LADD was calculated using equation 3.2 using AT averaging time for cancer risk 70 × 365 days. According to the EPA approach, the inhalation exposure estimate was derived from the daily

air intake in mg/kg per day. IUR value is provided by the Integrated Risk Information System (http://www.epa.gov/iris).

3.3 Results and Discussion

3.3.1 Mass and BC concentrations

Table 3. 1 provides a comprehensive overview of $PM_{2.5}$, BC, and Pb concentrations derived from various research efforts conducted within East Java's industrial regions in Indonesia. In Lamongan, the average 24-hour $PM_{2.5}$ concentration was 20.65 $\mu g/m^3$, with a range from 7.3 to 30.6 $\mu g/m^3$, as illustrated in Figure 3. 2. The data from a 6-week sampling period suggests that this duration is sufficient to estimate the long-term average $PM_{2.5}$ concentration, given its relatively low variability. If these 6 weeks of sampling data are extrapolated to represent the annual mean $PM_{2.5}$ levels, they have exceeded the Indonesia's national ambient air quality standard for an annual average of $PM_{2.5}$ (15 $\mu g/m^3$) in Government Regulation 22/2021.

Table 3. 1 includes a comparison of heavy metal concentrations between the present study and a prior study conducted in industrial areas of Banten Province and East Java, considering the limited scope of research on heavy metal concentrations in Indonesia. Due to the limited availability of studies on heavy metal concentrations in industrial areas of Indonesia, it is not possible to compare our results with those from similar sites from other studies. Instead, we focus our comparison on the results from Banten and East Java provinces. The average $PM_{2.5}$ concentration at our sampling site in Lamongan was marginally lower than that observed in other industrial sites within the Tangerang area (23.0 and 26.1 $\mu g/m^3$). Tangerang, similar to Lamongan, faces lead air pollution issues due to its proximity to a Pb smelter industry [Santoso et al. 2011]. However, compared to other cities in the same province in East Java, the $PM_{2.5}$ value collected in Lamongan was higher than the value reported by our study in the city of Surabaya site 1 and site 2 (15±5 and 16±5 $\mu g/m^3$) [Santoso et al. 2020b]. The Lamongan sampling site is near a lead smelter, surrounded by rice fields, and intersected by several small roads and highways. The elevated concentration of $PM_{2.5}$ in Lamongan is likely the result of diverse pollution sources, including the Pb smelter industry, rice husk burning activities, and vehicular emissions in the vicinity. Nonetheless, as shown in Figure 3. 2, none of the daily $PM_{2.5}$ measurements exceeded the Indonesian National Ambient Air Quality Standards (NAAQS) threshold value for a 24-hour $PM_{2.5}$ period (55 $\mu g/m^3$) or the US standard (35 $\mu g/m^3$). A comparison with another researcher's study in Waru reveals that there is no significant disparity in $PM_{2.5}$

concentrations. However, the Waru study revealed significant fluctuations in $PM_{2.5}$ concentrations, indicating that the levels of fine particulate matter can vary widely in different industrial areas [Humairoh et al. 2020].

Table 3. 1 Summary of $PM_{2.5}$ and BC concentrations from several studies (µg/m^3) in Indonesia

Sampling sites	n	$PM_{2.5}$		BC		Ref
		Mean	Range	Mean	Range	
Lamongan, East Java	21	20.65	7.33 - 30.63	3.1	2.1 - 4.5	This study
Tangerang, Industry 1, Banten	6	23	15 - 34	4.4	3.3 - 6.4	[Santoso et al. 2011]
Tangerang, Industry 2, Banten	8	26.1	21 - 42	4.5	2.9 - 10	[Santoso et al. 2011]
Surabaya site 1, East Java	62	15	6 - 27	3.2	-	[Santoso et al. 2020b]
Surabaya site 2, East Java	208	16	21 - 42	3.6	-	[Santoso et al. 2020b]
Waru, East Java	35	17.67	2.65 - 32.68	-	-	[Humairoh et al. 2020]

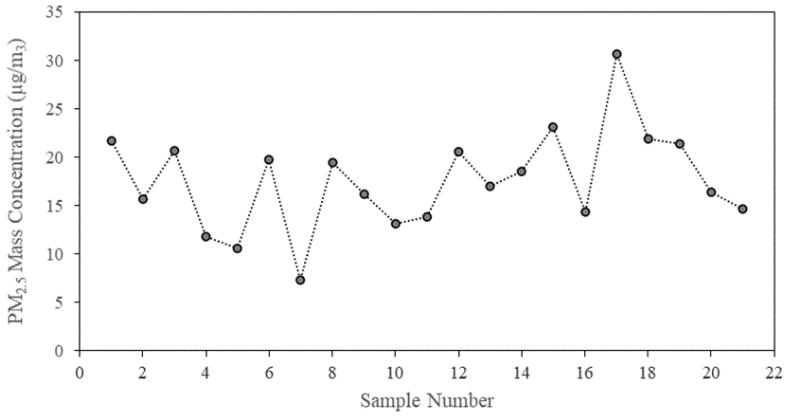

Figure 3. 2 $PM_{2.5}$ concentration collected at Lamongan, East Java

The average BC concentration was 3.1 µg/m3, a value consistent with the BC concentrations at Surabaya sites 1 and 2 (as presented in Table 3. 1). Notably, Figure 3. 3 reveals that BC concentrations during the sampling period exhibited minimal fluctuations, ranging from 2.1 to 4.5 µg/m^3. It's worth highlighting that BC represents a significant component of $PM_{2.5}$, with the BC to $PM_{2.5}$ ratio ranging from 11% to 30%, averaging 19%. In urban environments, BC sources are typically associated with incomplete combustion processes, including activities such as biomass burning and transportation [Alias et al. 2020; Ivošević et al. 2016; Pey et al. 2009; Santoso et al. 2008; Vega et al. 2021]. In these sampling sites, the activity of harvesting and rice husk burning were seen during the period of sampling. Additionally, the proximity of the sampling location to the north coast highway (approximately 2 km away) indicates that vehicle and transportation-related activities could also be a source of

BC. Specifically, in Lamongan, the emission from rice husk burning is a probable source of BC. This is consistent with findings from Tangerang, where Santoso's study identified BC sources as originating from biomass burning and diesel vehicle emissions mixed with road dust [Santoso et al. 2011]. For the Surabaya site in East Java, the major source of BC is not clearly and definitively known, but in general, BC is most likely to be emitted by motor vehicles and biomass combustion, as described by Permadi that there may be a contribution from open burning that still often seen in harvesting season used by Indonesian farmers [Permadi and Kim Oanh 2013].

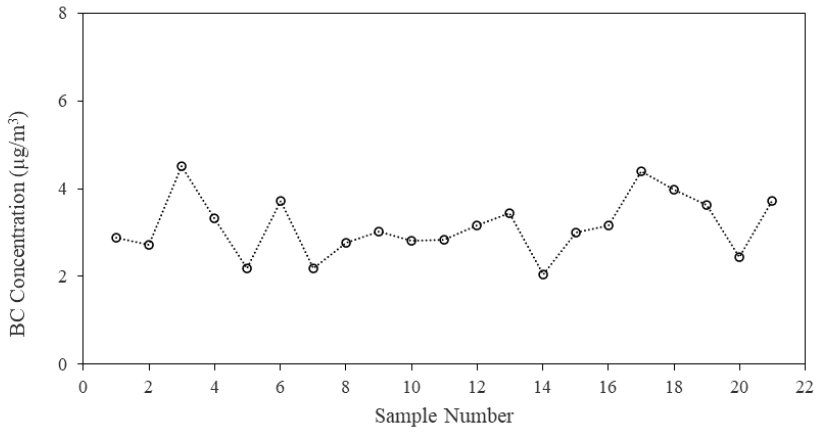

Figure 3. 3 Black carbon concentrations at Lamongan sampling site

3.3.2 Heavy metals concentrations

Table 3. 2 presents a comprehensive breakdown of the chemical composition within $PM_{2.5}$, while Figure 3. 4 illustrates the concentrations of various elements, including BC, Na, Mg, Al, Si, S, Cl, K, Ca, Ti, V, Cr, Mn, Fe, Ni, Cu, Zn, Br, and Pb. The findings highlight sulfur as the dominant element, with an average concentration of 796.6 ng/m^3 and a maximum of 1505 ng/m^3, followed by other elements Pb, K, Fe, and Zn. The high S concentrations could be due to the high S content fuel used in diesel vehicles [Davy et al. 2011; Lestiani et al. 2013; Santoso et al. 2011; Vega et al. 2021]. Additionally, the analysis identifies the presence of crustal elements like Al, Si, Ca, and Fe in substantial concentrations within $PM_{2.5}$.

Table 3. 2 Average and maximum chemical composition of $PM_{2.5}$ at Lamongan, East Java

Elemental (ng/m^3)	Average± SD	Max
Na	283.2±50.4	384.84
Mg	58.39±30.53	123.48
Al	29.32±15.51	73.13
Si	65.10±37.87	145.44
S	796.6±321.5	1505.1
Cl	25.11±5.59	36.94
K	215.4±117.3	539.8
Ca	55.06±23.77	135.3
Ti	1.80±1.19	5.00
V	0.51±0.40	1.73
Cr	1.95±0.58	3.36
Mn	0.97±1.04	4.06
Fe	29.83±15.06	72.40
Ni	0.30±0.25	0.83
Cu	1.38±1.51	7.28
Zn	27.88±28.68	112.3
Br	4.44±1.99	8.29
Pb	457.7±563.6	1974.3

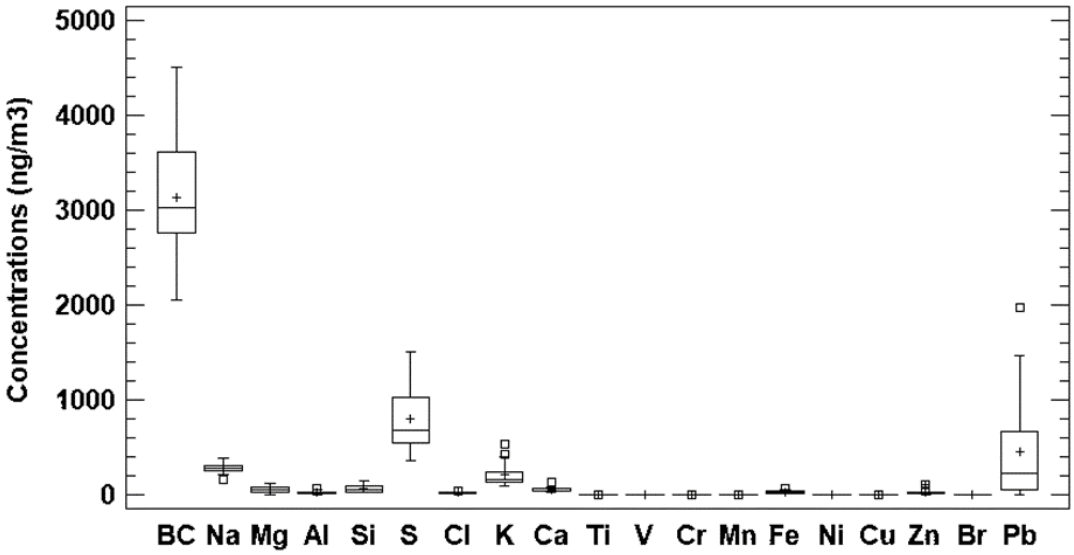

Figure 3. 4 Chemical composition of $PM_{2.5}$

Figure 3. 5 shows multiple correlation plots focusing on these crustal elements—Al, Si, Ca, and Fe. This correlation analysis is crucial because crustal elements are frequently found in soil and road dust, making them potential major contributors to $PM_{2.5}$ in industrial areas. By analysing the correlation between crustal elements, it showed that one of the pollutant sources of $PM_{2.5}$ in the study area may have originated from soil or road dust. The first column of the matrix contains plots of the first variable on the x-axis versus each of the other variables on the y-axis. The plots show good linear correlations for all crustal elements,

especially Al vs Si, Al vs Ca, etc. These correlations suggest that the pollution source of road dust near the sampling site is likely due to transportation, specifically from vehicles passing the main road since the sampling site is located near the highway.

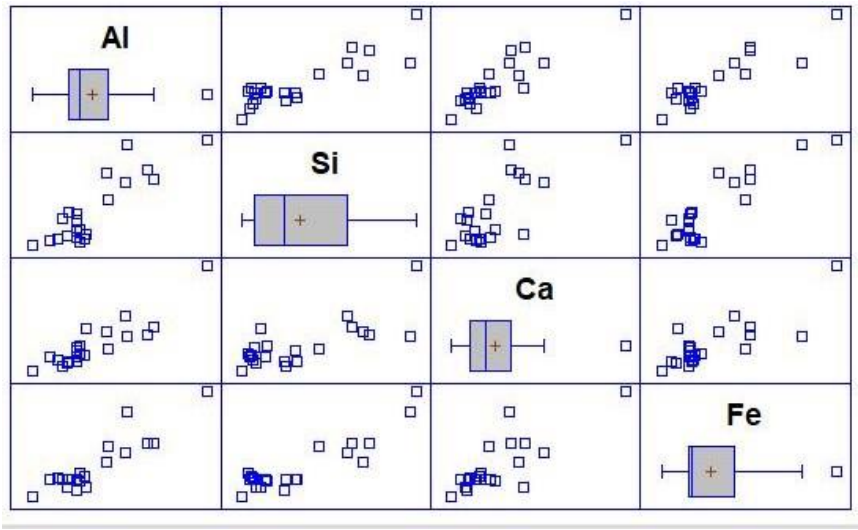

Figure 3. 5 Correlation of crustal elements Al, Si, Ca, and Fe

Due to the significant contribution of lead to the overall $PM_{2.5}$ concentration, the comparing the lead concentrations with those reported in previous studies in industrial sites in Indonesia especially in East Java and other sites in the world. The comparison of lead concentration in Lamongan with other sites in Indonesia and in the world was resumed in Table 3. 3. It showed that the average concentrations of Pb in Lamongan 0.46 µg/m^3 was a similar level to industrial sites 1 and 2 in Tangerang with average values were 0.17 and 0.63 µg/m^3, respectively [Santoso et al. 2011]. The average Pb concentrations in Tangerang violated the annual lead standard of WHO and the US EPA (0.5 and 0.15 µg/m^3), while Lamongan almost reached the limit of WHO and exceeded the US EPA standards. The maximum concentration of Pb in $PM_{2.5}$ 1.9 µg/m^3 was 3 to 13 times higher than the WHO and US EPA standard. Since there is no other study available that investigates lead concentration in the air of industrial areas in East Java. Therefore, we compared our findings only with the limited studies available that focused on heavy metal concentrations in the air of industrial sites in Indonesia.

Table 3. 3 Lead concentrations in $PM_{2.5}$ from several industrial sites in Indonesia and other countries in the world.

Sampling sites	Lead (μg/m^3)		Ref
	Mean	Max	
Lamongan, East Java	0.46	1.97	This study
Tangerang, Industry 1, Banten	0.63	4.25	[Santoso et al. 2011]
Tangerang, Industry 2, Banten	0.17	1.61	[Santoso et al. 2011]
Surabaya site 1, East Java	0.13	0.73	[Santoso et al. 2020b]
Surabaya site 2, East Java	0.33	2.70	[Santoso et al. 2020b]
Other countries in Asia			
Southern Malaysia	0.008		[Alias et al. 2020]
Gwangju, Korea	0.031		[Yu and Park 2021]
Seoul, Korea	0.058		[Park et al. 2008]
Singapore	0.03		[Zhang et al. 2017]
Dhaka, Bangladesh	0.131		[Rahman et al. 2021]
Kitakyushu, Japan	0.06		[Zhang et al. 2021]
Baoshan, China	0.149		[Chen et al. 2008]
Beijing, China	0.31		[Sun et al. 2004]
Taiwan	0.023		[Hsu et al. 2016]
Segzi Isfahan, Iran	0.062		[Soleimani et al. 2018]
Kolkata, India	0.37		[Matawle et al. 2014]
Karachi, Pakistan	0.473		[Mansha et al. 2012]

Comparison with other industrial sites in the world indicates that the average lead (Pb) concentrations in $PM_{2.5}$ in our study were notably elevated compared to findings in various Asian countries. Specifically, Pb levels in Lamongan surpassed those observed in industrial sites in several countries including Malaysia, Korea, Singapore, Bangladesh, Japan, China, Taiwan, Iran, and India. The Pb concentrations in $PM_{2.5}$ at Lamongan were at a similar level with Karachi, Pakistan (0.473 μg/m^3) which has several industrial activities in the area, and lead was estimated to be caused by the vehicular emissions and battery manufacturing [Mansha et al. 2012]. Compared with other countries in Europe, Pb concentration in Lamongan was much higher than industrial sites in South Wales, the UK, and Greece (0.0002 and 0.28 μg/m^3, respectively) [Thomaidis et al. 2003; Taiwo et al. 2014]. These findings underscore the considerable heavy metal contamination present in the ambient air of Lamongan, East Java, and needs special pre-caution as well as suitable countermeasure to minimize the impact on the surrounding environment. Regarding the source of lead (Pb), it's worth noting that Indonesia phased out leaded gasoline back in 2001.

Consequently, the elevated lead concentrations likely arise from alternative lead sources. The sampling site in Lamongan is located near the lead smelter, therefore the high lead concentration could be dominated from the smelter emissions that might play a significant role in elevated lead concentrations. This potential source of Pb emission would be clearly revealed by showing the correlation between each element using principal component analysis.

3.3.3 Source profile using PCA

Statistical analysis was carried out using principal component analysis (PCA). The analysis is focused on the elements that have factor loadings above 0.5 which are contained in each factor. This value is considered to provide significant insights into the origin of the sources [Zhai et al. 2014; Soleimani et al. 2018; Vega et al. 2021]. The loadings show the value of a correlation coefficient between the original variables and new factor variables that represent a linear combination. Table 3. 4 presents the varimax factor loadings after rotation and the five factors identified by PCA accounted for 82.1% of the total $PM_{2.5}$ variance. The first factor with 40.7% of variance associated with a crustal element and biomass burning indicated by black carbon and potassium which are strongly associated with biomass combustion. Biomass burning activities such as rice husk burning were often seen during the study period during the harvesting time. In this factor, the high loading of Cu was also observed, it was expected to be related to the plumbing valve factory located southeast of the sampling location.

Table 3. 4 Principal component analysis for $PM_{2.5}$

	Factor 1	**Factor 2**	**Factor 3**	**Factor 4**	**Factor 5**
BC	0.75				
Na		0.63			
Mg					
Al	0.79	0.53			
Si	0.59	0.65			
S		0.74			
Cl					
K	0.91				
Ca	0.78				
Ti	0.42	0.72			
V					
Cr				0.81	
Mn		0.75			
Fe	0.70	0.65			
Ni					0.85
Cu	0.73				
Zn		0.89			
Br					
Pb			0.86		

The second factor (14.2% of variance) has high loading of S and Zn and crustal elements Al, Si, Ca, Fe and Ti. This factor is related to vehicle emissions and road dust indicated by high S, Zn, and crustal elements. The presence of Zn was found in the compositions of brake lining and tire accumulated in road dust [Mansha et al. 2012; Alias et al. 2020; Vega et al. 2021; Yu and Park 2021]. Zn is used for lubricating oil, while S is related to the fuel combustion of diesel vehicles [Santoso et al. 2011; Zhang et al. 2017]. The sampling location is located near the main highway with a heavy number of vehicles. The third factor with an 11.9% variance is clearly indicated the lead smelter. This result clarified the emission source from the Pb smelting industry. The fourth and fifth factors were mainly associated with a high loading only for Cr and Ni, respectively. Cr may originate from industrial emissions. Vega reported that Cr with Pb and Sb can be emitted from the processes in cement plants and metal manufacturing [Vega et al. 2021]. Because there are several metal industries on the site, Cr is probably emitted from industrial sources. A large amount of Ni could be emitted from shipping emissions. Ni along with V are considered the most abundant trace metals in ship exhaust burning heavy fuel oils [Zhao et al., 2021]. The emission from oil refinery and thermoelectric plants had been reported to be sources of Ni [Vega et al. 2021]. Zhong found that Ni was from various industrial processes [Zhong et al. 2016]. There are shipping activities at the port of Surabaya within a radius of 50 km from the sampling location. Thus, Ni in Lamongan can be related as a signature emission from shipping activities. Using the PCA, it explained the possible sources from biomass burning, road dust, vehicles, lead smelter, metal industry, and shipping emissions. Separation of mixture pollutant sources was a challenge in this method, and it was seen in the profile of the factors. It allows the identification of the major sources and reveals the correlation between each element, but not a quantitative apportionment.

3.3.4 Risk assessment

The average daily dose ADD for Pb, Ni, and Cr for children and adults is summarized in Table 3. 5. Since the Cr concentration in this study is total Cr, therefore the ratio of 1:6 proportion in ambient air for the concentration of carcinogenic Cr(VI) to non-carcinogenic Cr(III) is used for calculation [Vega et al. 2021]. Table 3. 6 summarized the excess lifetime cancer risk with the assumption of 70 years of lifetime. Generally, the acceptable CR for a

regulatory range is between 1×10^{-6} and 1×10^{-4}. The CR was calculated only for heavy metals representing carcinogenic elements in $PM_{2.5}$ (Pb, Cr, and Ni).

Table 3. 5 Summary of ADD, HQ, and HI

	ADD (ng/kg/day)		HQ		HI	
Element	Children	Adults	Children	Adults	Children	Adults
Pb	39.37	33.75	0.0112	0.0096		
Cr	0.024	0.021	0.0001	0.0001	0.0115	0.0098
Ni	0.026	0.022	0.0001	0.0001		

Table 3. 6 The cancer risk CR of Pb, Cr, and Ni for Children and Adults

	SF		CR	
Element	Children	Adults	Children	Adults
Pb	1.15×10^{-5}	5.35×10^{-5}	4.51×10^{-7}	1.81×10^{-6}
Cr	2.29×10^{-3}	1.07×10^{-2}	5.51×10^{-8}	2.20×10^{-7}
Ni	2.29×10^{-4}	1.07×10^{-3}	5.89×10^{-9}	5.89×10^{-9}

The hazard quotient for Pb is the highest value (0.0112 for children and 0.0096 for adults). Although this value is less than 1 since this HQ was calculated using the average concentration of Pb (4 times lower compared to the maximum value). By HQ and HI less than 1, there is little possibility for non-cancerous health risks, but still, Pb remained to pose a threat to children's health. Hence, Pb was more potentially hazardous as compared to Cr and Ni. For the CR value, Pb is also significantly higher than other metals Cr and Ni. The adults were more affected than the children in cancer risk assessment since the exposure time was longer than children. However, this CR value of Pb in adults was slightly higher than the minimum acceptable risk value 1×10^{-6}. The total CR value was 1.81×10^{-6} indicating that ~2 cases of cancer can occur per 1000,000 adult population at the Lamongan site. This result suggests that in order to reduce the risk of health impact, exposure to the heavy metals in $PM_{2.5}$ should be avoided as minimally as possible. The government should take appropriate measures to control heavy metal emissions and minimize the health risk of the exposed people living near the industrial sites.

3.4 Conclusions

This study focused on the characterization of $PM_{2.5}$ collected in the vicinity of a lead smelter industry, aiming to identify pollutant sources and assess potential risks. The unique and valuable nature of this research lies in its examination of lead concentrations in $PM_{2.5}$, their sources, and potential risks within an industrial area in East Java—a region with limited prior research in this domain. This study successfully identified five key factors with significant loadings, including biomass burning, road dust, vehicle emissions, the lead smelter, metal industries, and shipping activities. The findings strongly indicate that the lead smelter and metal industry exert a predominant influence on the environmental conditions in the study area. Furthermore, health risk assessment, as indicated by the Hazard Quotient (HQ) and Cancer Risk (CR) values for lead (Pb), revealed values slightly surpassing acceptable levels. The CR value of 1.81×10^{-6} implies that approximately two cases of cancer per 1000,000 adults in Lamongan could arise due to the lead contamination. These findings emphasize the need to minimize exposure to heavy metals in $PM_{2.5}$ to mitigate health risks and underscore the importance of government awareness and action. It is evident that these heavy metals in $PM_{2.5}$ pose significant health risks and the potential for cancer. Continuous air quality monitoring is essential, along with comprehensive studies evaluating the impact on the surrounding environment, including soil, water, and vegetation. In conclusion, this study fills a critical information gap regarding lead in ambient air in East Java. Its findings can serve as a valuable foundation for future management and control strategies, guiding efforts to safeguard both public health and the environment.

CHAPTER 4 Impact of Lead Smelter in Soil Collected in East Java, Indonesia

4.1 Introduction

Potentially toxic elements are environmental constituents that have the potential to cause harm to human health or the ecosystem. They are often associated with industrial activities such as mining, smelting, manufacturing, as well as agricultural practices and urbanization. Lead, arsenic, cadmium, mercury, selenium, and antimony are some examples of potentially toxic elements known for their potential toxicity, persistence, and ability to bioaccumulate in the food chain [Bowen 1979; Valko et al. 2005; Tchounwou et al. 2012]. The damaging effects of potentially toxic elements are attributed to their non-biodegradability, long biological half-lives, and potential for accumulation [Jaishankar et al. 2014; Hu et al. 2017]. The excessive accumulation of these elements in the soil can be highly harmful to humans and other animals. For instance, the metalloid arsenic (As) is considered a toxic element that can cause skin damage, bladder cancer, kidney cancer, and major abnormalities in the circulatory system [Smith et al. 1998]. Chromium (Cr) is carcinogenic, leading to lung inflammation, fibrosis, emphysema, and tumors. Copper (Cu) can cause health complications such as liver and kidney damage [Hasan et al. 2023]. Chronic exposure to lead (Pb) may lead to plumbism, disrupting children's cognitive development and cognitive function [Hasan et al. 2023]. Additionally, these potentially toxic elements (PTEs) have been associated with various health disorders, including bone fractures, kidney dysfunction, and hypertension [Li et al. 2014]. When PTEs accumulate in critical organs like the liver, kidneys, and bones, they pose a direct threat to human health, potentially resulting in numerous serious health disorders [Duruibe et al. 2007; Jolly et al. 2013]. Considering these health risks is essential when assessing the impact of potentially toxic elements on the environment and their potential effects on human populations. Exposure to potentially toxic elements can occur through various pathways, including inhalation, dermal contact, and ingestion, involving air, dust, water, soil, and food sources [Nagajyoti et al. 2010; Wuana and Okieimen 2011; Bermudez et al. 2012; Qu et al. 2012; Tchounwou et al. 2012; Kim et al. 2015; Tóth et al. 2016]. The exposure can result from metal discharges during mining, milling, and smelting processes [Bowen 1979; Loska et al. 2004; WHO 2010; Ettler 2015]. Additionally, they are discharged from activities associated with metal use and processes designed to recover metals, such as battery recycling and secondary smelting [WHO 2010; Wuana and Okieimen 2011;

Tchounwou et al. 2012; Ettler 2015]. Mining, manufacturing, and other industrial activities, as well as the use of synthetic products (paints, batteries, etc.) and smelting of nonferrous metals, are among the significant sources of potentially toxic elements contamination in urban and agricultural soils [Douay et al. 2008; Wang et al. 2015; Qiu et al. 2016; Hu et al. 2017]

Characterizing potentially toxic elements and understanding their spatial concentrations is crucial for assessing environmental impacts and identifying responsible contributors. Li et al. found significantly high concentrations of As, Pb, and Cd in the soil surrounding a lead smelter in Jiyuan, China, compared to background sites [Li et al. 2015]. In Veles, a study by Stafilov showed high Pb, Cd, and Zn contamination in topsoil due to 30 years of smelter plant activities [Stafilov et al. 2010]. One thing to be concerned about is that the soil contaminated with potentially toxic elements is still used for horticulture, thus it poses potential risk for food safety and security [Lockitch 1993; Markus and McBratney 2001; Douay et al. 2008; WHO 2010; Kim et al. 2015; Ebong et al. 2018]. However, limited information is available regarding potentially toxic elements pollution in the soil near lead smelters in Indonesia. Studies have investigated potentially toxic elements pollution in air particulate matter in Serpong [Santoso et al. 2011], near the lead smelter, while separate research has focused on the levels of blood lead in children living near lead smelters in Tegal [Haryanto 2016]. Atmospheric pollution of potentially toxic elements from the lead industrial complex in Serpong district, suburban area located 25 km southwest of Jakarta has been reported by Santoso et al., with the finding that atmospheric lead concentrations were higher in Serpong district than in Jakarta [Santoso et al. 2011]. The lead concentration in ambient air was mainly from the lead industry that recycles lead-acid batteries and produces lead ingots. The study by Haryanto claimed that very high blood lead levels (BLLs) had been found in children living near used lead acid batteries recycling smelters in Tegal Regency [Haryanto 2016]. A similar study was conducted by Budiyono, which found a correlation between blood lead levels and intelligence levels among elementary children living around used lead battery smelters in Tangerang and Lamongan [Budiyono et al. 2016]. Many children in the contaminated areas near lead industries were observed to face challenges in achieving high grades in school and experienced stunting or other physical development problems [Haryanto, 2016].

Agricultural soils contaminated with potentially toxic elements can result in elevated metal levels in crops [Douay et al., 2008; Li et al., 2020; Xing et al., 2016]. Therefore, assessing potentially toxic element concentration in soils is important for evaluating the impact from the lead smelter to the surrounding agricultural and other areas. The findings can serve as an early warning to avoid greater disadvantages and mitigate risks to human life and ecology. By knowing the level of potentially toxic element contamination in soil, a proper action and strategy for reducing pollution or environmental remediation could be designed. This study investigates the potentially toxic element contamination in soils collected from an area in the vicinity of lead smelter in East Java, Indonesia, as a preliminary step in assessing the impact of a lead smelter on the neighboring agricultural and other areas. The study aims to identify the spatial distribution of selected potentially toxic elements, conduct a health risk assessment, and provide valuable scientific information for designing effective actions and policies to reduce pollution, implement soil remediation, and introduce health interventions. The results of this study will contribute to recommendations for industrial regulations, restrictions, and interventions to minimize exposure and protect the health of local residents.

4.2 Methodology

4.2.1 Study area and sampling

Soil samples were collected near a lead smelter in Lamongan city located in the northwestern of East Java Province, Indonesia (6°51'54"–7°23'6"S and 112°4'41"–112°33'12"E). Lamongan city covers a total area of 1812.8 km^2, with approximately 79.20% (1435.1 km^2) of the area dedicated to agricultural fields, of which 61.15% (877.62 km2) is utilized for rice cultivation [BPS Statistics Indonesia 2015]. The lead smelter is situated in the immediate vicinity of a small town, approximately 1.5 km away, and only 100 meters away from the rice-cultivated fields. The lead smelter primarily focuses on producing lead alloys by recycling used lead-acid batteries. Although the smelter was legally closed by the local government in 2014, it continues to operate illegally during nighttime activities [Asnawi 2022]. The solid waste or slag from the smelter is disposed of in the surrounding open spaces, commonly used for landfills or as a covering material for pathways near the rice fields and in the mixture of building materials. The sampling locations are depicted in Figure 4. 1. Soil samples were all collected within the same period in a week during the dry season from various locations within a radius of 1.5 km, 3 km, and 5 km from the center of the lead smelter. These sampling locations were chosen

randomly from all directions surrounding the lead smelter to ensure representation and to assess the extent of its impact on the surrounding environment. A total of 36 samples were collected within the selected regions, encompassing both the topsoil (0–15 cm) and subsurface (15–30 cm) layers at each site. Additionally, two background samples were collected in a residential area located 15 km away from the smelter, chosen due to its significant distance from the industrial site, ensuring minimal exposure to potential contaminants. The majority of the sampling points were situated in rice fields. To assess the influence of selected potentially toxic elements over the region, three consecutive buffers of 1.5 km, 3 km, and 5 km were created around the industrial sites (Figure 4. 1).

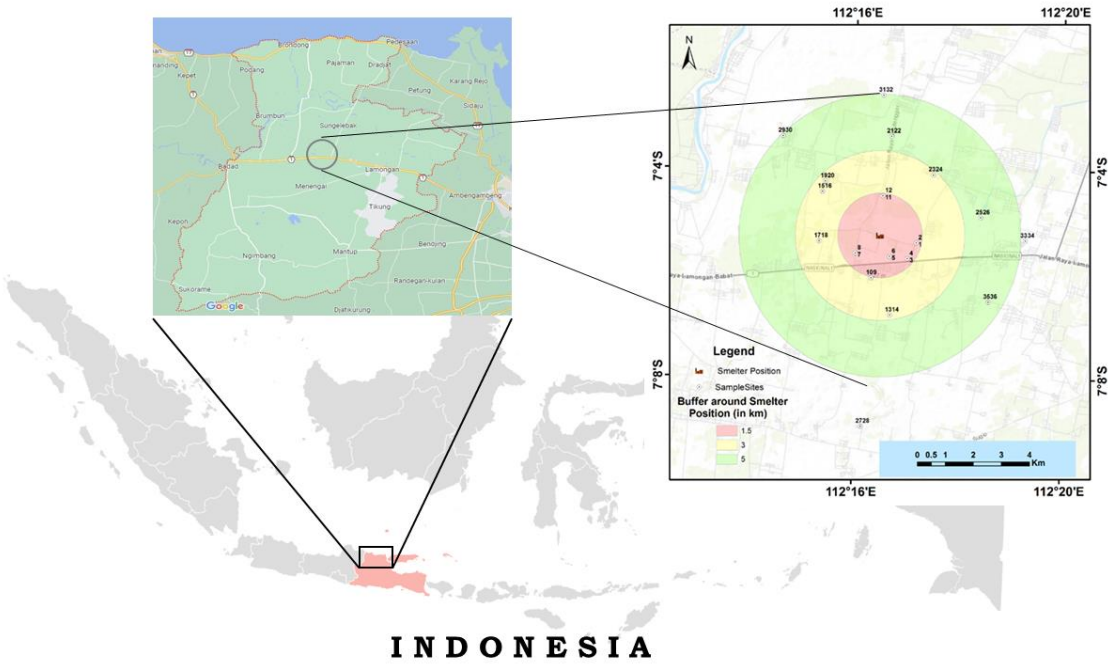

Figure 4. 1 Map of Indonesia, study site and sampling points

Furthermore, a 7 km buffer (Figure 4. 2) was established around the smelter to analyze the land-use and land-cover (LULC) patterns in the region. The sampling points encompassed approximately 80.11% of the area dedicated to crops or agricultural land, while built areas accounted for 15.04% of the total area. Other LULC units, such as water bodies, natural vegetation (trees), and flooded vegetation, comprised a minimal percentage of the land, amounting to 2.97%, 0.48%, and 0.59%, respectively, within the 7 km buffer around the smelter. The details of each sampling point are summarized in Table 4. 1.

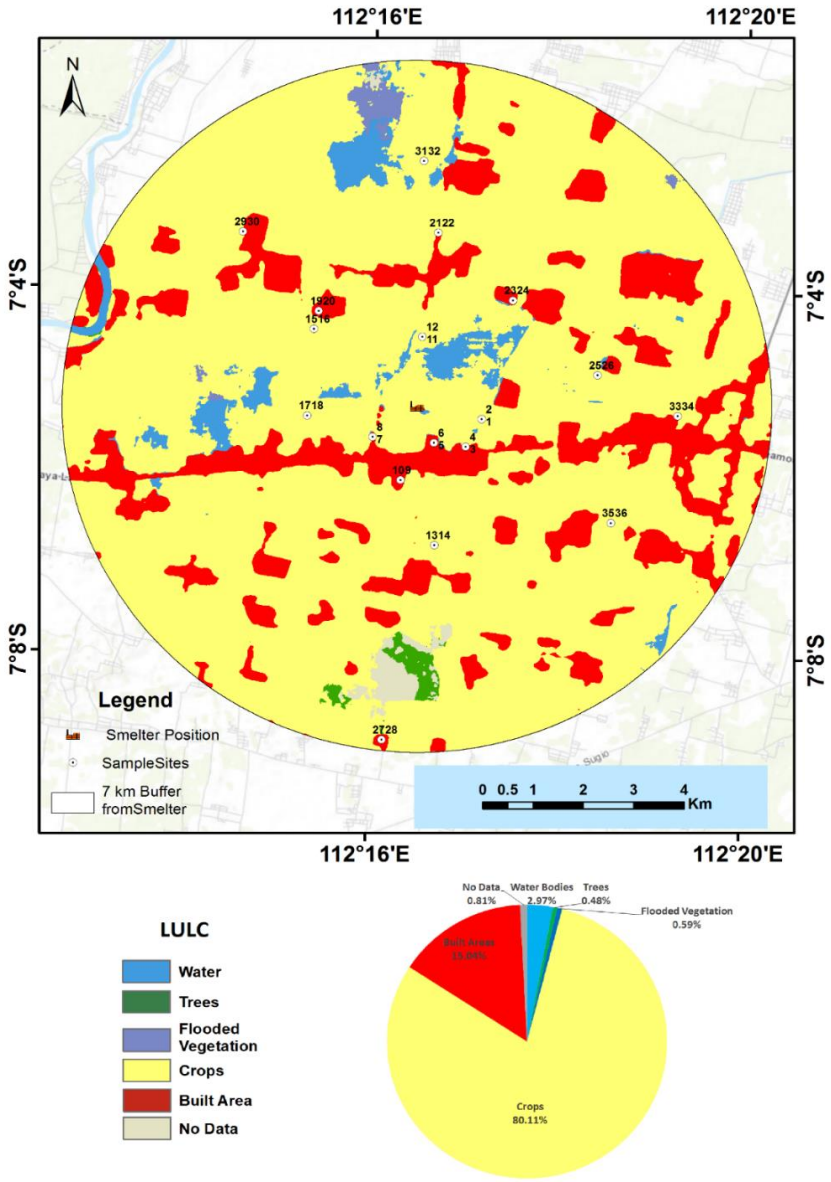

Figure 4. 2 Different Land Use Land Cover (LULC) units have been mapped over the East Java province

Table 4. 1 Sampling site, direction, and characteristics of collected soils

Distance	Direction (n samples)	Sample ID	Sampling location	Latitute	Longitude	Characteristic
≤1.5 km	East (2)	1, 2	Desa Plososetro, Kec. Pucuk	07˚05'24.4"	112˚17'10.1"	On the edge of rice field
	Southeast (2)	3, 4	Desa Waru, Kec. Pucuk	07˚05'42.8"	112˚17'01.0"	On the edge of rice field
	South (2)	5, 6	Desa Waru Kulon, Kec. Pucuk	07˚05'40.4"	112˚16'39.6"	On the edge of rice field
	Southwest (2)	7, 8	Desa Waru Kulon, Kec. Pucuk	07˚05'37.1"	112˚16'01.0"	On the edge of rice field
	West (2)	9, 10	Desa Miru, Kec. Sekaran	07˚05'65.3"	112˚16'18.7"	On the edge of rice field
	North (2)	11, 12	Desa Miru, Kec. Sekaran	07˚04'30.8"	112˚16'31.1"	On the edge of swamp and rice field
1.5 -3 km	South (2)	13, 14	Desa Deplek, Kec. Sukodadi	07˚06'47.8"	112˚16'40.9"	Open ground near the rice field
	Southwest (2)	15, 16	Desa Menango, Kec. Sukodadi	07˚06'26.6"	112˚15'21.3"	Open ground near the rice field
	West (2)	17, 18	Desa Tritunggal, Kec. Babat	07˚05'23.7"	112˚15'18.0"	Open space near the rice field
	Northwest (2)	19, 20	Desa Trosono, Kec. Sekaran	07˚04'14.7"	112˚15'24.3"	On the edge of rice field
	Northeast (2)	23, 24	Desa Bugel, Kec. Sekaran	07˚04'05.9"	112˚17'29.0"	On the edge of swamp and rice field
≥3 km	South (2)	27, 28	Desa Teseh, Kec. Sugiyo	07˚08'56.4"	112˚16'09.0"	Open ground near the rice field
	Northwest (2)	29, 30	Desa Jugo, Kec. Sekaran	07˚03'23.2"	112˚14'34.9"	Open space near the rice field
	North (4)	21, 22	Desa Bulutengger, Kec. Sekaran	07˚03'22.1"	112˚16'40.3"	On the edge of swamp and rice field
		31, 32	Desa Karang, Kec. Sekaran	07˚02'35.0"	112˚16'30.4"	On the edge of rice field
	East (2)	25, 26	Desa Kuwanun, Kec Pucuk	07˚04'54.4"	112˚18'24.2"	On the edge of swamp
	East (2)	33, 34	Kec. Sukodadi	07˚05'20.5"	112˚19'16.1"	Open ground near the rice field
	Southeast (2)	35, 36	Kec. Sukodadi	07˚06'31.5"	112˚18'34.2"	Open ground near the rice field

4.2.2 Elemental analysis

All soil samples, each with a mass of 1 kg, were sun-dried for 5–6 hours per day over 3–7 days, with an average ambient temperature of 29.1°C. Subsequently, the dried samples were ground into a fine powder and 100 grams were sieved to a size of less than 100 µm for further analysis. Elemental analysis of the 1-gram dried soil powder samples was conducted in two replicates using the ED-XRF Minipal4 from Panalytical, Ltd. The suitability of ED-XRF Minipal4 for soil analysis has been discussed in other studies [Oreščanin et al. 2008; Kurniawati et al. 2012]. For the purpose of environmental risk assessment, the concentrations of six potentially toxic metals, namely As, Cr, Cu, Ni, Pb, and Zn, were determined in the soil samples. These metals were selected based on their prevalence as contaminants in soil. To ensure the accuracy and validity of the analysis method, the elements in the soil samples were also analyzed using a standard reference material from the National Institute of Standards and Technology (SRM NIST) 2711a Montana Soil. The average recovery rates of As, Cu, Cr, Ni, Pb, and Zn were 101.1%,

101.3%, 101.5%, 99.4%, 101.0%, and 96.5%, respectively. The limit of detection for these elements was determined to be 0.5, 0.7, 2.5, 1.7, 1.1, and 1.4 mg/kg, respectively, as reported by Kurniawati et al. (2012). This analysis method has also been successfully applied to characterize the elemental composition of soil samples collected in Nepal, demonstrating good accuracy and precision [Kafle et al. 2022].

4.2.3 Statistical analysis and assessment of soil pollution

The degree of contamination in soils was evaluated using the contamination factor (Cf). The contamination factor (Cf), also referred to as the single pollution index (PI) in other studies [Liu et al. 2014; Mitkova and Markoski 2015], was employed to assess the level of soil pollution. This index is determined by calculating the ratio of the potentially toxic element concentrations in the soil to the corresponding background values.

$$Cf = \frac{C_{heavymetal}}{C_{background}} \qquad \text{Eq. (4. 1)}$$

The contamination level was classified based on the intensity of the contamination factor (Cf). The classification criteria were as follows: $Cf < 1$ indicated low contamination, $1 \leq Cf \leq 3$ indicated moderate contamination, $3 \leq Cf \leq 6$ indicated considerable or high contamination, and $Cf > 6$ indicated very high contamination [Liu et al. 2014].

4.2.4 Health Risk Assessment

Health risk assessment is a crucial approach for identifying potential health risks associated with human activities and providing decision-makers with essential risk evidence [Hu et al. 2016]. In this study, the methodology for health risk assessment followed the guidelines and Exposure Factors Handbook issued by the United State Environmental Protection Agency [US EPA 1989, 2011]. To address behavioral and physiological differences, the assessment covered both children and adult populations, taking into consideration three exposure pathways: inhalation, dermal contact, and ingestion.

The average daily dose (ADD, mg/kg/day) served as the basis for assessing the exposure to potentially toxic elements in the soil. The estimation of direct soil exposure involved three pathways: (1) inhalation of particulates emitted from the soil, (2) dermal contact with the soil, and (3) incidental ingestion of the soil. To define the ADD for each of these pathways, the methodology recommended by the US EPA was utilized [US EPA

1989, 2011]. The three corresponding equations are presented as follows [Hu et al. 2016; Xiao et al. 2022]:

$$\mathrm{ADD}_{inhalation} = \frac{C_{soil} \times ET \times IR_{air} \times EF \times ED}{BW \times AT \times PEF} \quad \text{Eq (4. 2)}$$

$$\mathrm{ADD}_{dermal} = \frac{C_{soil} \times SA \times PE \times AF \times ABS \times ED}{BW \times AT} \quad \text{Eq (4. 3)}$$

$$\mathrm{ADD}_{Ingestion} = \frac{C_{soil} \times IR_{soil} \times EF \times ED}{BW \times AT} \quad \text{Eq (4. 4)}$$

The average daily exposure dose (ADD) is expressed in milligrams per kilogram of body weight per day (mg/kg-day). The pollutant's concentration in the soil (C_{soil}) is measured in milligrams per kilogram (mg/kg). For adults, the ingestion frequency (IR_{soil}) is set at 100 mg/day, while for children, it is 200 mg/day. The inhalation frequency of soil (IR_{air}) is 15.7 m^3/day for adults and 10.1 m^3/day for children [US EPA 1989, 2011]. The particle emission factor (PEF) is measured in cubic meters per kilogram (m^3/kg) [US EPA 2011]. The surface area of exposed skin (SA) is given in square centimeters (cm^2), and the adhesiveness degree of skin (AF) is measured in milligrams per square centimeter per day (mg/(cm^2/d)). The absorption factor of skin (ABS) is a dimensionless factor. Body weight (BW) is measured in kilograms (kg), and exposure duration (ED) is given in years. Exposure frequency (EF) represents the number of exposure days per year (day/year). The average exposure time (AT) is calculated as the product of exposure duration (ED) and 365 days for non-carcinogenic effects. For carcinogenic effects, AT is fixed at 25,550 days (70 years × 365 days/year) [US EPA 1989].

To assess the potential for chronic non-carcinogenic effects over a specified period, the Hazard Quotient (HQ) was calculated by comparing the exposure to a reference dose (RfD) for a similar exposure period. The HQ represents the ratio of exposure, as defined by the US EPA guidelines [US EPA 1989, 2011]. The overall potential for chronic effects due to multiple potentially toxic elements was determined by calculating the Hazard Index (HI), which is the sum of all HQ values. The definitions of HQ, and HI were based on the guidelines provided by the US EPA [US EPA 1989, 2011; Xiao et al. 2022] and are defined as follows:

$$HQ = \frac{ADD}{RfD} \quad \text{Eq. (4. 5)}$$

$$HI = \sum_{i=1}^{n} HQ_i = HQ_{inhalation} + HQ_{dermal} + HQ_{ingestion} \quad \text{Eq. (4. 6)}$$

The U.S. Environmental Protection Agency (USEPA) has provided the RfD values for the selected potentially toxic elements across various exposure pathways [Hu et al. 2017]. To assess the overall potential risk associated with multiple HMs, Hazard Quotients (HQs) are combined to calculate a Hazard Index (HI) using Equation (4. 6). If the HI exceeds 1.0, there is a possibility of non-carcinogenic effects occurring, with the probability increasing as the HI value rises. Conversely, if the HI is below 1.0, it is unlikely that non-carcinogenic effects will manifest. The Hazard Quotient (HQ) and Hazard Index (HI) results indicate that adverse health effects and potential chronic effects should be a concern when HQ or HI ≥ 1 [Leung et al. 2008; Li et al. 2011]. The variable 'i' represents the specific potentially toxic elements, and the corresponding Reference Doses (RfD) of ingestion for As, Cr, Cu, Ni, Pb, and Zn are 0.0003, 0.003, 0.04, 0.02, 0.0035, and 0.3 mg/kg, respectively, according to the US EPA guidelines [US EPA 1989, 2011].

In the context of carcinogens, risk is assessed based on the additional probability of an individual developing cancer throughout their lifetime due to exposure to potential carcinogenic agents. The evaluation of potential carcinogenic risk involves utilizing the following equations [US EPA 1989, 2011; Xiao et al. 2022]:

$$CR = LADD \times SF \quad \text{Eq. (4. 7)}$$

Where CR represents the dimensionless probability of carcinogenic risk, while SF stands for the carcinogenic slope factor of each metal, measured in (1/mg/kg/day). The total carcinogenic risk is calculated as the sum of risks from all exposure pathways and all individual metals. The specific values of SF for the chosen potentially toxic elements in various exposure pathways are provided by the US EPA [US EPA 1989, 2011]. For regulatory purposes, the acceptable range of total risk typically lies between 1×10^{-4} to 1×10^{-6}. LADD (Lifetime Average Daily Dose) represents the metal's exposure concentrations for carcinogenic risk, therefore it is calculated using Equation (4. 2), (4. 3) and (4. 4) with an averaging time (AT) for cancer risk of 70 years multiplied by 365

days. The IUR value is obtained from the Integrated Risk Information System (IRIS), a database provided by the US EPA that contains human health risk information. The IUR value is expressed in units of $m^3/\mu g$ and represents the increased risk of cancer per microgram of exposure. By integrating these parameters, analysts can evaluate the potential health risks associated with metal exposure through inhalation, taking into account factors such as LADD, IR, and IUR values. A Total CR equal to or less than 10^{-6} indicates a state of virtual safety in regulatory terms, while a total CR equal to or greater than 10^{-4} signifies a potentially significant risk [US EPA 1989, 2011].

4.3 Results and Discussion

4.3.1 Potentially toxic elements concentrations

The concentrations of six potentially toxic elements (As, Cr, Cu, Ni, Pb, and Zn) were measured in soil samples collected from Lamongan, located in East Java, Indonesia. The concentrations of these potentially toxic elements in Lamongan soils are shown in Figure 4. 3. The data presented in Figure 4. 3 reveals the highest accumulation of potentially toxic elements, specifically As, Pb, and Zn, in the soil surrounding the smelter. The range of minimum and maximum concentrations of the potentially toxic elements is presented in Table 4. 2. The maximum concentrations of potentially toxic elements in the soil were found to be as follows: As (330.8 mg/kg), Cr (74.6 mg/kg), Cu (71.1 mg/kg), Ni (35.1 mg/kg), Pb (5334 mg/kg), and Zn (146.3 mg/kg). The results revealed that the mean concentrations of As, Cu, Pb, and Zn were higher than those found in the background levels. The concentrations of potentially toxic elements in Lamongan soils were compared to those found in soils collected near lead smelters or lead-zinc smelters in other countries. The results of this study were also compared with regulatory standards from other countries as well as global standards due to the lack of standard for soils from Indonesia (Table 4. 2). When compared to other sites in Asia, the maximum concentrations of As and Pb in Lamongan exceeded the levels observed in soil samples from Yunnan and Zhuzhou, China, as well as South Korea [Li et al. 2015; Kang et al. 2019; Zhou et al. 2022]. These values surpassed the global soil standards and regulations. This indicates a significant accumulation of As and Pb in the soil samples collected around the smelter. The maximum concentrations of As and Pb were tens to hundreds of times higher than the global average and other standard limits. Furthermore, the maximum concentration of Zn exceeded the global average, and the mean concentration was slightly above the global average. However, both values still remained within the

acceptable range of China's standards. The average concentrations of Cu, Cr, and Ni were also within the range reported for industrial soils in other countries and were below the global average and China's standard values. Moreover, when compared to other countries, the values reported in this study were lower than Armenia [Akopyan et al. 2018], Bulgaria [Bacon and Dinev 2005], France [Sterckeman et al. 2000], and Macedonia [Stafilov et al. 2010]. To further interpret the data and assess the impact of the smelter activity, the distribution of potentially toxic elements within each radius was classified. The concentrations of potentially toxic elements at varying distances from the smelter are summarized in Table 4. 3, and their distribution across each radius is illustrated in Figure 4. 4.

Table 4. 2 Statistical parameters (n=36) of potentially toxic element concentrations and comparison with other sites in the worldwide and standards (value in mg/kg)

	As	Cr	Cu	Ni	Pb	Zn	Reference
Min.	11.5	47.2	18.1	17.9	36.2	80.1	This study
Max.	330.8	74.6	71.1	35.1	5334	146.3	
Mean	35.0	59.0	40.8	23.1	424.8	106.2	
S.D	70.3	7.1	11.9	3.8	1148	14.7	
Mean background	12.3	68.0	30.7	23.4	53.0	97.0	
Baoding, China	10-12	72.9-99.2	23.9-37.8	40-62.7	46-89	99.4-134.2	[Liu et al., 2014]
Yunnan, China	2.2-71.7	83-183	195-316	59.9-103	13-2485	144-8078	[Li et al., 2015]
Zhuzhou, China	1-58.3	7.9-177	10.5-105	2.8-55.9	16.7-782	26.4-1750	[Zhou et al., 2022]
Hunan, China	52-93	-	82-157	-	602-1197	1654-3349	[Li et al., 2011]
Seocheon, South Korea		-	0.0-2147	-	18.7-1079	132-5984	[Kang et al., 2019]
Alaverdi, Armenia	24-1064	-	-	-	9-3703	-	[Akopyan et al., 2018]
Akhtala, Armenia	9-276	-	-	-	15-30083	-	
France	-	-	16.8- 170.4	-	103-3215	287-6439	[Sterckeman et al., 2000]
Plovdiv, Bulgaria	-	16-193	11-432	11-303	46-4196	86-5231	[Bacon and Dinev 2005]
Veles, Macedonia	1.3-110	17-1800	11-1700	73-600	13-15000	22-27000	[Stafilov et al., 2010; Mitkova and Markoski 2015]
World average	6	70	30	50	35	90	[Bowen, 1979]
Standard China	30	250	100	50	300	250	[China EPA, 1995]
Standard Thailand	3.9	300	-	1600	400	-	[Inboonchuay, 2016]
Standard Dutch	4.5	3.8	3.5	2.6	55	16	[Vodyanitskii, 2016]

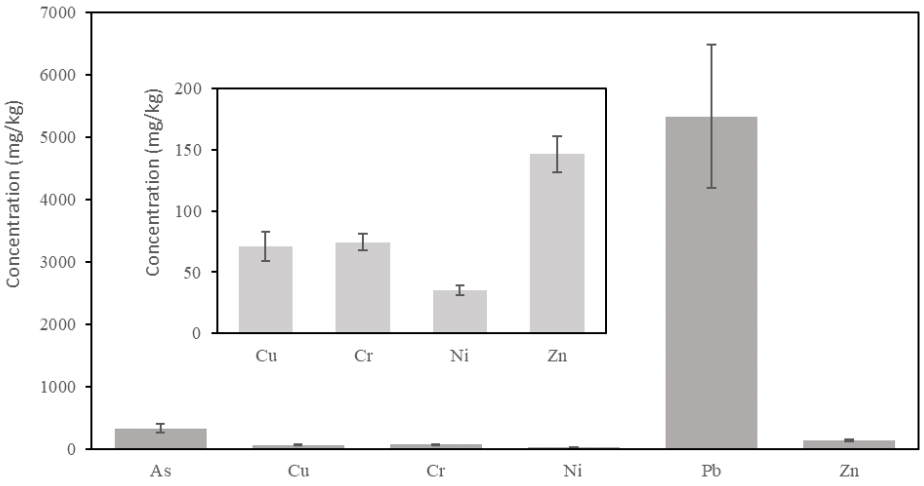

Figure 4. 3 The concentration of potentially toxic elements As, Cu, Cr, Ni, Pb and Zn in soil samples

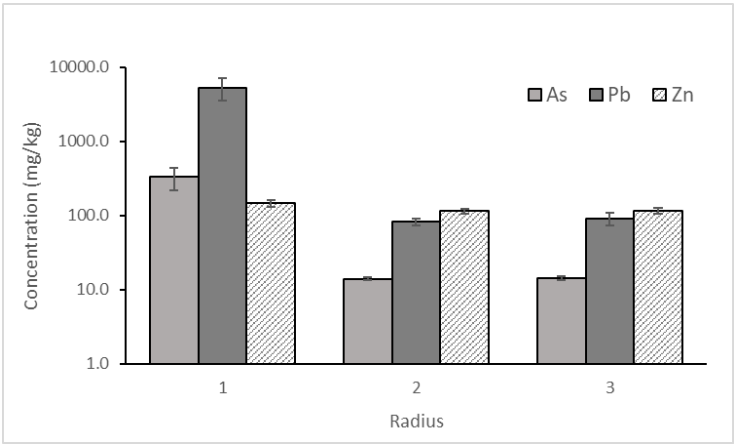

(a)

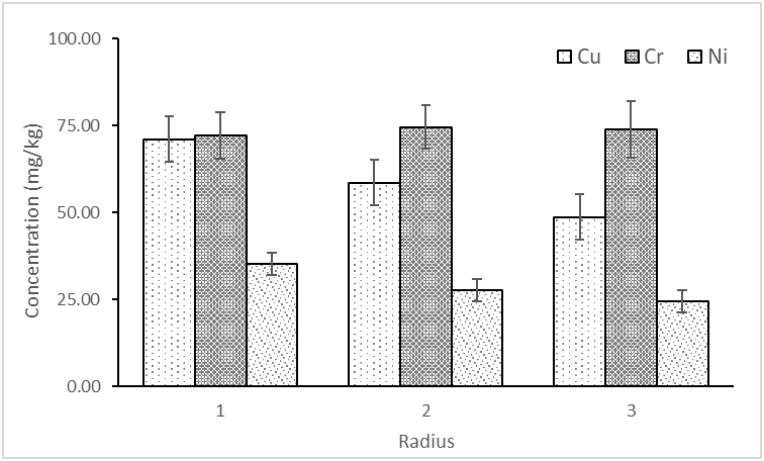

(b)

Figure 4. 4 The concentration on radius from smelter as the center point (a) As, Pb and Zn, and (b) Cu, Cr and Ni

Table 4. 3 The potentially toxic element (PTE) concentration of As, Pb, Zn, Cu, Cr, and Ni

Distance	Direction	Sample ID	As (mg/kg)		Pb (mg/kg)		Zn (mg/kg)		Cu (mg/kg)		Cr (mg/kg)		Ni (mg/kg)	
			Top	Subsurface	Top	Subsurface	Top	Subsurface	Top	Subsurface	Top	Subsurface	Top	Subsurface
Radius 1 (≤1.5 km)	East	1, 2	117.9	103.9	1,728	1,502	122.6	117.4	50.3	50.8	57.2	54.3	27.2	27.9
	Southeast	3, 4	17.0	16.8	131.0	127.5	110.6	107.0	47.4	44.7	54.2	55.7	22.4	19.9
	South	5, 6	277.5	330.8	4,331	5,334	145.3	146.3	67.3	71.1	54.8	54.7	35.1	34.1
	Southwest	7, 8	15.1	14.0	98.0	81.6	122.9	125.9	28.6	28.4	71.1	72.2	25.1	19.9
	West	9, 10	21.5	16.3	190.9	112.3	104.2	98.0	29.9	27.1	67.5	65.1	18.7	21.5
	North	11, 12	15.9	13.8	114.3	82.3	115.4	109.6	42.2	40.2	60.9	61.5	25.5	21.1
Radius 2 (1.5-3 km)	South	13, 14	12.8	12.0	67.0	48.7	102.1	111.8	44.1	22.8	50.2	74.6	21.1	22.6
	Southwest	15, 16	12.3	12.4	61.0	61.2	80.1	89.7	34.2	41.1	47.2	59.6	20.9	20.5
	West	17, 18	12.5	12.7	62.8	64.4	112.2	112.3	45.9	46.9	53.2	56.2	21.3	20.3
	Northwest	19, 20	12.0	12.2	52.3	55.7	103.4	99.0	58.6	41.8	60.9	57.9	25.2	20.9
	Northeast	23, 24	12.6	11.8	65.1	53.0	97.5	91.9	38.5	38.5	56.2	54.9	23.1	20.9
Radius 3 (≥3 km)	North	21, 22	14.0	12.6	82.9	63.6	114.4	97.3	43.7	40.5	55.6	56.8	26.4	27.7
	South	27, 28	12.8	12.4	61.3	56.4	89.1	90.5	23.7	25.3	66.5	73.9	21.5	19.6
	East	25, 26	13.2	12.4	73.9	60.1	107.9	102.0	49.1	47.0	54.7	53.3	23.8	25.1
	Northwest	29, 30	11.7	11.7	47.0	46.1	98.0	96.1	44.8	41.2	53.6	55.0	24.4	23.9
	North	31, 32	14.5	13.4	91.7	76.2	115.7	105.7	40.8	39.1	57.3	66.8	22.8	21.5
	East	33, 34	12.7	12.8	66.9	68.6	103.3	103.8	47.2	48.7	50.4	49.0	18.7	17.9
	Southeast	35, 36	11.5	11.7	36.2	38.7	86.1	87.4	18.1	19.6	65.7	63.7	22.6	22.0

Note the odd sample ID is topsoil samples

The results indicate that there are no significant differences in contamination levels for most of the elements. However, the concentrations of potentially toxic elements in the surface soils were slightly higher than in the subsurface soils. This suggests that potentially toxic elements have accumulated on the surface and undergone illuviation, moving downwards into the subsurface soil. Li et al. also observed a decrease in Pb concentrations with depth, with a notable drop occurring at approximately 50 cm [Li et al. 2015]. The distribution of potentially toxic elements in soil cores was also investigated by Liu et al., who reported a gradual decrease in the concentrations of Cd, Pb, and Zn with depth in the surface soil, reaching a constant level in the subsurface soil (20–50 cm) [Liu et al. 2014]. Figure 4. 4 illustrates the concentration of potentially toxic elements in each distance radius. It is evident that within a 1.5 km distance from the smelter, all potentially toxic elements, with the exception of Cr, exhibited the highest concentrations. Notably, the potentially toxic elements As, Pb, and Zn were significantly higher in soils collected in close proximity to the lead smelter industry. Furthermore, as the distance from the smelter increased, there were no discernible differences in the concentrations of potentially toxic elements between the soil samples collected within radius 2 (1.5–3 km) and radius 3 (3–5 km). The concentration of Pb in the soil exhibited a consistent decrease with increasing distance from the smelter. It followed a linear trend in the southern direction, with concentrations decreasing from the magnitudes of thousands (4331–5334 mg/kg) in the immediate vicinity of the smelter (within 1.5 km) to levels below a hundred (49–90 mg/kg) at distances exceeding 3 km from the smelter (Table 4. 3). The observed trend of decreasing concentrations with distance was also evident for As and Zn in the soils. It is presumed that the primary source of contamination for As, Pb, and Zn is the deposition of smelter dust. The preliminary findings suggest that smelting activity significantly influences the concentrations of As, Pb, and Zn. Similar studies conducted in China and Europe have reported higher soil concentrations of Cd, Pb, and Zn near lead-acid smelters compared to locations farther away from the smelters [Douay et al. 2009; Li et al. 2011, 2015; Liu et al. 2014]. These findings suggest that smelter dust emissions are generally the primary contributors to metal contamination in the nearby soils. On the other hand, the concentrations of Cu, Cr, and Ni in the soils were found to be comparable to background values. The concentration of Cr, as depicted in Figure 4. 3, exhibited no significant variations across the entire radius, indicating that it was not influenced by the smelting activity. Regarding Cu and Ni, slightly higher concentrations

were observed in radius 1 compared to radius 2 and 3, although the differences were not statistically significant.

4.3.2 Spatial distributions

To analyze the spatial distribution of the three most heavily polluted potentially toxic elements (As, Pb, and Zn), a spatial map was generated using ArcGIS software. This map provides valuable insights into the deposition patterns within the vicinity of the smelter. In the spatial map, the yellow asterisk represents the location of the smelter, serving as the central reference point, while each sampling point is assigned a unique sample code. The spatial distribution of Pb concentrations indicated that the highest levels were observed in the surface soils collected from the eastern and southern regions surrounding the smelter (Figure 4. 5). In these areas, the Pb concentrations ranged from 1502 to 1728 mg/kg in the east and 4331 to 5334 mg/kg in the south. These findings suggest a pronounced contamination gradient, with the highest Pb concentrations being detected in the immediate vicinity of the smelter, particularly towards the east and south directions.

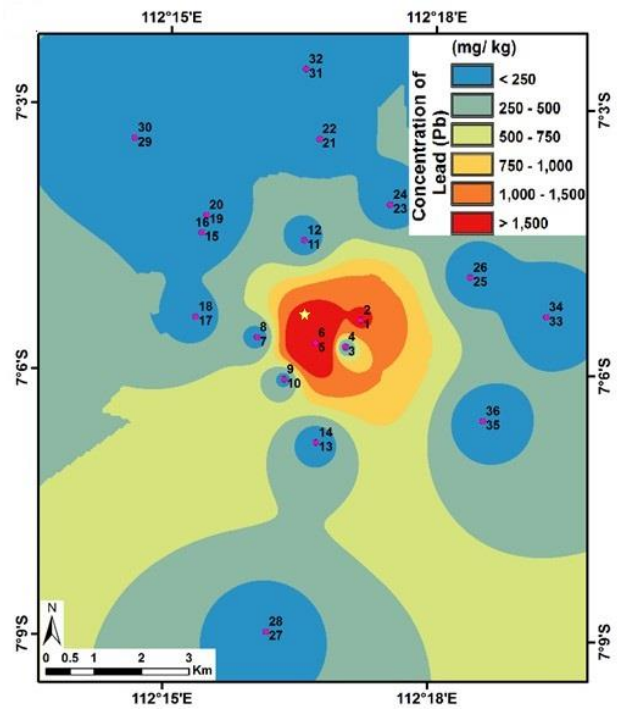

Figure 4. 5 Distribution of Pb concentrations at sampling sites nearby smelter

Similar patterns were observed for As and Zn, as depicted in Figure 4. 6 and Figure 4.7, respectively. Notably, the regions located to the south and east of the smelter exhibited higher concentrations of As, Pb, and Zn compared to other directions. Specifically, sampling

points 5 and 6, situated in the southern area, displayed the highest concentrations of these potentially toxic elements, indicating a substantial impact from the possible pollutants. These findings emphasize the significance of the south and east regions as major hotspots for As, Pb, and Zn contamination, likely influenced by the prevailing wind patterns and dispersion of pollutants. These specific areas are located within the smelter site, particularly around the wastewater runoff zone. The deposition of smelter dust onto the soil, along with the transport of contaminants by wind and water, has contributed to the contamination in these regions. An irrigation canal flows across the smelter site from west to east, passing through the southern side as well as shown in Figure 4. 8. The improper disposal of smelter waste into the canal has likely led to higher concentrations of lead on the south and east sides, primarily due to the runoff of wastewater. It is important to note that these contaminated soils in the east and south of the smelter area are still actively utilized for agricultural purposes, particularly for paddy crops. Consequently, the crops grown in these areas are at a higher risk of accumulating potentially toxic elements. While the eastern and southern sides of the smelter exhibit significant contamination with As, Pb, and Zn, it is crucial to highlight that within a radius of less than 1.5 km from the smelter, there is a higher potential risk of exposure to pollutants from potentially toxic elements compared to the other sides of the smelter in the same radius.

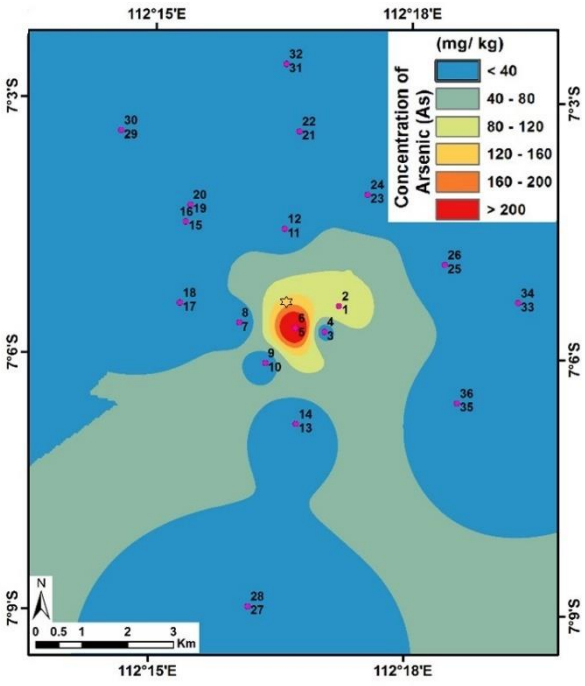

Figure 4. 6 Distribution of As concentration in surrounding soils nearby smelter

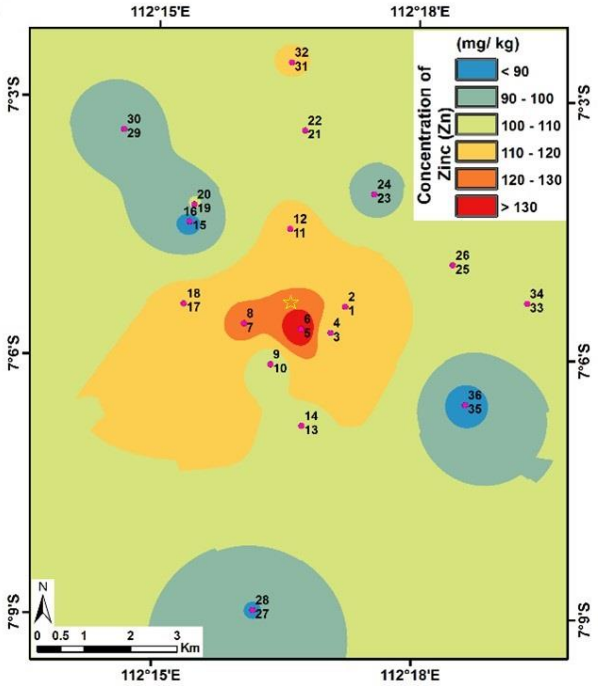

Figure 4. 7 Distribution of Zn concentration in surrounding soils nearby smelter

Figure 4. 8 The lead smelter and its surrounding area

Considering that Lamongan is one of the largest paddy production areas in East Java, it is imperative not to overlook the contamination of these metals, particularly lead. The spatial distribution of As, Pb, and Zn clearly indicates the direct influence of the smelter on their dispersion. Surface runoff and atmospheric deposition resulting from smelter emissions and waste play a significant role in transporting the pollution load to neighbouring regions. It is crucial to recognize that the impact of the smelter can extend beyond a distance of 6 km, primarily due to the dispersion of aerosols. Other studies [Cartwright et al. 1977; Douay et al. 2009; Li et al. 2015; Qiu et al. 2016] have also highlighted the potential long-range effects of smelter emissions. Consequently, further investigations are necessary to evaluate the impact on distant regions and assess the extent of contamination.

4.3.3 Source analysis of potentially toxic elements in the surface soils

Principal component analysis (PCA) was conducted to investigate the sources of potentially toxic elements in agricultural soils. PCA is widely recognized as an effective tool for identifying the sources of potentially toxic elements in soils [Douay et al. 2009; Li et al. 2015; Wang et al. 2015; Dimitrijević et al. 2016; Xiao et al. 2022]. The Varimax rotated PCA yielded two components that accounted for 87.5% of the total variance in the dataset (Figure 4. 9). The first component explained 66.2% of the total variance and comprised As,

Ni, Pb, and Zn. It represented the factor influenced by emissions from lead smelters and served as the primary source of soil contamination. The second component solely included Cu, explaining 21.3% of the total variance. This component may represent a geogenic source or soil mineral factor. It is worth noting that Cu also exhibited a high factor loading (0.6) in the first component, suggesting its possible contribution from smelter activities as well as other sources. Cu was presumed to be associated with the plumbing valve factory located southeast of the sampling area. Furthermore, Cr did not exhibit significant correlations with As, Pb, and Zn in the soils. Similar observations were made in other Pb/Zn smelting regions in northern France [Sterckeman et al. 2000]. This suggests that Cr originates from sources unrelated to the lead smelter. The consistent findings of the PCA analysis in the studied soils further confirm the sources of potentially toxic elements in the area. The PCA results indicate that As, Pb, and Zn primarily originate from the release of wastewater and smelter dust deposition, thus validating the spatial distribution map that highlights the concentration hotspots of these potentially toxic elements in the south and east areas surrounding the smelter. Other studies have demonstrated the potential long-range effects of smelter dust deposition, indicating that the influence of the smelter can reach more than 6 km by the dispersion of aerosols studies [Cartwright et al. 1977; Li et al. 2015; Qiu et al. 2016].

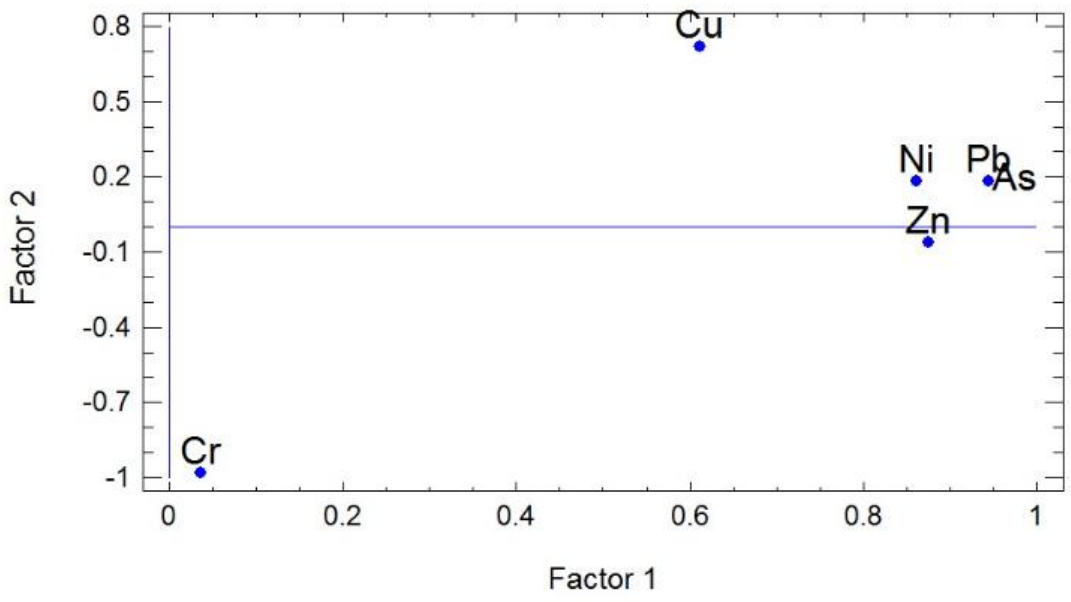

Figure 4. 9 The plot of factor loading from PCA results

Ecological risk assessment

Table 4. 4 summarizes the contamination factors of potentially toxic elements. It showed that the average of contamination factors for all heavy elements, except for As and Pb, ranged from 0.8 to 1.4. These values indicate that the pollution levels of Cu, Cr, Ni, and Zn were not extremely severe. However, the contamination factor for lead (Pb) in the sampling sites within a radius of less than 1.5 km from the smelter was 22.0, indicating a very high lead pollution. The elevated Cf values for Pb and As suggest significant pollution from these elements in the majority of the analyzed soils. The agricultural soils in close proximity to the lead acid battery smelter exhibited the highest Cf values, which gradually decreased with increasing distance from the smelter.

Table 4. 4 The average contamination factor in each radius for each potentially toxic elements

	As	Cu	Cr	Ni	Pb	Zn
Cf (≤1.5 km) (n=12)	6.5	1.4	0.9	1.1	22	1.2
Cf (1.5-3 km) (n=14)	1.1	1.2	0.9	1.0	1.1	1.0
Cf (3-5 km) (n=10)	1.0	1.4	0.8	0.9	1.3	1.1

Health risk assessment

All parameters used in this calculation are resumed in supplementary in Table 4. 5 and Table 4. 6. A comprehensive non carcinogenic risk assessment of potentially toxic elements contamination in soils and the associated potential health risks, specifically related to the lead acid used in battery smelters, was conducted using Health Quotients (HQs) and Hazard Index (HI) for children and adults from several pathways including ingestion, inhalation, and dermal contact (Table 4. 7).

Table 4. 5 Parameters used in health risk assessment [US EPA, 1989; 2009; 2011; Hu et al., 2016; Zeng et al.,2019]

Parameter	Definition	Units	Adults	Children
IR_{soil}	Ingestion rate	kg/day	1.00E-04	2.00E-04
IR_{air}	Inhalation rate	m^3/day	15.7	10.1
EF	Exposure Frequency	day/year	350	350
ED	Exposure Duration	year	24	6
BW	Body weight	kg	70	18.6
AT	AT carcinogenic (70x365)	day	25550	25550
	AT non carcinogenic (ED x 365)	day	8760	2190
SA	Exposed skin area	cm^2	5700	2800
AF	Adherence factor	kg/cm^2/day	7.00E-08	2.00E-07
ABS	Absorption factor of dermal	unit less	As 0.03, others 0.001	
PEF	Particle emission factor	m^3/kg	1.36E+09	

Table 4. 6 Reference dose and cancer slope factor for several potentially toxic elements (US EPA 1989; 1996; Hu et al., 2016)

PTE	RfD (mg/kg day)			SF (kg day/mg)		
	Ingestion	Dermal	Inhalation	Ingestion	Dermal	Inhalation
As	3.00E-04	1.23E-04	3.01E-04	**1.50**	1.50	12.00
Cr	3.00E-03	6.00E-05	2.86E-05	0.50	20.00	42.00
Cu	4.00E-02	1.20E-02	4.02E-02			
Ni	2.00E-02	5.40E-04	9.00E-05	1.70	20.00	84.00
Pb	3.50E-03	5.25E-04	3.52E-04	0.00850	0.00001	
Zn	3.00E-01	6.00E-02	3.00E-01			

Table 4. 7 HQs and HIs of individual potentially toxic elements for children and adults

Elements	Groups		Non carcinogenic risk			
			HQ ingestion	**HQ inhalation**	**HQ dermal**	**HI**
As	Children	Min	3.95E-01	1.46E-05	8.10E-02	4.76E-01
		Max	**11.4**	4.21E-04	2.33	13.7
		Mean	**1.2**	4.45E-05	2.46E-01	1.45
	Adults	Min	5.25E-02	6.04E-06	1.53E-02	6.78E-02
		Max	**1.51**	1.74E-04	4.41E-01	1.95
		Mean	1.60E-01	1.84E-05	4.67E-02	2.06E-01
Cr	Children	Min	1.62E-01	6.32E-04	2.27E-02	1.86E-01
		Max	2.56E-01	9.99E-04	3.59E-02	2.93E-01
		Mean	2.03E-01	7.90E-04	2.84E-02	2.32E-01
	Adults	Min	2.16E-02	2.61E-04	4.30E-03	2.61E-02
		Max	3.41E-02	4.12E-04	6.80E-03	4.13E-02
		Mean	2.69E-02	3.26E-04	5.37E-03	3.26E-02
Cu	Children	Min	4.67E-03	1.72E-07	4.35E-05	4.71E-03
		Max	1.83E-02	6.77E-07	1.71E-04	1.85E-02
		Mean	1.05E-02	3.89E-07	9.82E-05	1.06E-02
	Adults	Min	6.20E-04	7.12E-08	8.24E-06	6.28E-04
		Max	2.43E-03	2.80E-07	3.24E-05	2.47E-03
		Mean	1.40E-03	1.60E-07	1.86E-05	1.42E-03
Ni	Children	Min	9.23E-03	7.61E-05	9.57E-04	1.03E-02
		Max	1.81E-02	1.49E-04	1.88E-03	2.01E-02
		Mean	1.19E-02	9.83E-05	1.24E-03	1.32E-02
	Adults	Min	1.23E-03	3.15E-05	1.81E-04	1.44E-03
		Max	2.40E-03	6.17E-05	3.55E-04	2.82E-03
		Mean	1.58E-03	4.06E-05	2.34E-04	1.86E-03
Pb	Children	Min	1.07E-01	3.94E-05	1.99E-03	1.09E-01
		Max	**15.7**	5.80E-03	2.93E-01	16.0
		Mean	**1.25**	4.62E-04	2.34E-02	1.28
	Adults	Min	1.42E-02	1.63E-05	3.77E-04	1.46E-02
		Max	**2.09**	2.40E-03	5.55E-02	2.15
		Mean	1.66E-01	1.91E-04	4.42E-03	1.71E-01
Zn	Children	Min	2.75E-03	1.02E-07	3.85E-05	2.79E-03
		Max	5.03E-03	1.87E-07	7.04E-05	5.10E-03
		Mean	3.65E-03	1.36E-07	5.11E-05	3.70E-03
	Adults	Min	3.66E-04	4.22E-08	7.30E-06	3.73E-04
		Max	6.68E-04	7.71E-08	1.33E-05	6.81E-04
		Mean	4.85E-04	5.60E-08	9.67E-06	4.95E-04

Among the different potentially toxic elements analyzed, the maximum HQs followed the order of Pb>As>Cr>Cu>Ni>Zn. Maximum HQ values greater than 1 were observed for As and Pb, indicating potential health risks for children and adults. However, for the other elements, the HQ values were below 1, suggesting a lower level of concern. The HI caused by Pb was the largest for all children and adults as shown in Figure 4. 10 (a). It has been known that children are particularly vulnerable to lead (Pb) toxicity due to their

increased intestinal absorption, which is five times higher than that of adults [Liu et al. 2014]. In this study, the non-carcinogenic risk for children was seven times higher than that of adults, indicating their vulnerability to the adverse health effects of these potentially toxic elements, as shown in Figure 4. 10 (a). Considering the pathway of potentially toxic elements exposure, Figure 4. 10 (b) demonstrates that the highest contribution to the potentially health risk for both children and adults was from ingestion followed by dermal contact, as indicated by the hazard quotient (HQ).

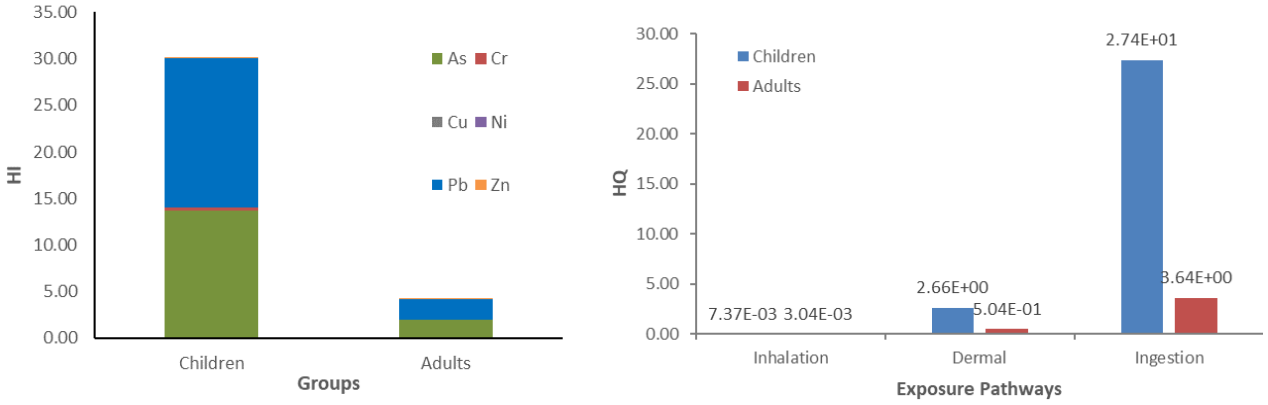

(a) (b)

Figure 4. 10 Hazard index (a) for children and adults, and (b) for different exposure pathways

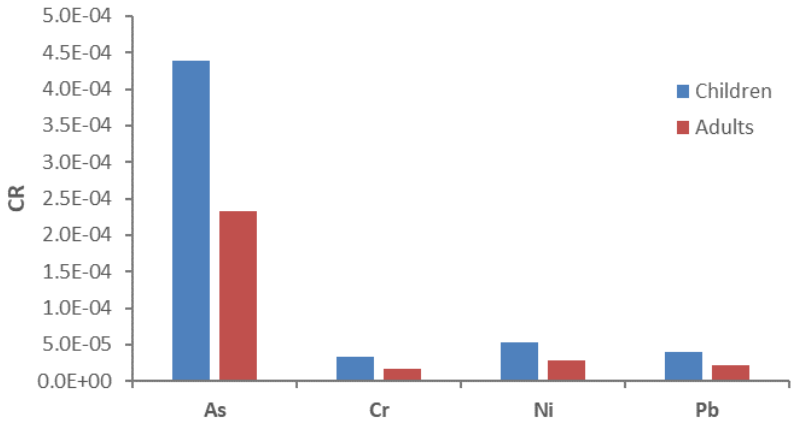

Figure 4. 11 Carcinogenic risk (CR) for different elements for children and adults

Carcinogenic risk (CR) was calculated for As, Cr, Ni, and Pb, representing the carcinogenic elements. The CR value for each element was illustrated in Figure 4. 11.

Notably, the CR value for As was significantly higher than that of the other potentially toxic elements. In the assessment of cancer risk, it was evident from the CR values that children were more susceptible than the adults' group. Specifically, the total CRs for children and adults were 5.65×10^{-4} and 3.00×10^{-4}, respectively. These results indicate that both children and adults exceeded the threshold limit of 10^{-4} set by the US EPA for potential carcinogenic risks resulting from exposure to these potentially toxic elements. Based on these CR values, it is estimated that approximately 6 cancer cases can occur per 10,000 children and 3 cases per 10,000 adults in Lamongan sites near the lead smelter areas. The findings highlight that the soil in the studied area may potentially pose a health risk to humans due to elevated levels of potentially toxic elements. Additionally, there is a concern that consuming crops grown in the affected area could also contribute to human health risks. Therefore, effective measures need to be carried out to prevent the exposure of potentially toxic elements, especially children in the vicinity of lead smelter.

4.4 Conclusions

In conclusion, the analysis of soil samples collected from the vicinity of a lead smelter industry in East Java, Indonesia revealed significant contamination with potentially toxic elements. Concentrations of As, Pb, and Zn exceeded the global average soil standards as well as standards in several countries in Europe and Asia. Ecological risk assessment based on the contamination factor (Cf) demonstrated that lead pollution was particularly severe within a radius of less than 1.5 km from the smelter, with a Cf value of 22. This indicates a very strong contamination of lead in the soil samples collected from this area. Moreover, high Cf values for Pb (22) and As (6.5) highlighted the extensive pollution of these metals throughout the studied area. Principal Component Analysis (PCA) results suggested that As, Pb, and Zn share similar sources, strongly associated with the lead smelting activity. Although potentially toxic elements concentrations in the soil samples beyond a radius of 1.5 km from the smelter were below the established standards, it is important to note that the surrounding region is predominantly used for agricultural purposes, particularly paddy production. Given this, there is a potential for accumulation in vegetation, posing risks to human health. Furthermore, the assessment of human health risk revealed that both children and adults were exposed to non-carcinogenic risks through As and Pb in soils. Carcinogenic risk from soil potentially toxic elements was found to exceed the acceptable level for children and adults in the study region. Oral ingestion was identified as the primary exposure route impacting health risk. This study provides significant

information related to exposure through soil contamination, and to obtain comprehensively evaluate the impact of lead pollutants on human health, it is recommended to conduct further investigations on potentially toxic element pollution in ambient air, water, and vegetation within the studied area. The findings emphasize the urgent need for measures to mitigate the environmental and health risks posed by potentially toxic elements contamination in the vicinity of the lead smelter industry.

CHAPTER 5 Particle-induced x-ray emission (PIXE) for characterization of $PM_{2.5}$ and $PM_{2.5-10}$

5.1 Introduction

Particle-induced X-ray emission (PIXE) is a nuclear analytical technique based on measuring the X-ray emission induced by charged particles [Johansson 1992a; Johansson 1992b; Johansson and Johansson 1976; Johansson et al. 1970]. Charged particles, usually protons from an accelerator enter an evacuated chamber containing the specimen to be analysed. The proton excites the electrons in the innermost shells of the atom in the specimen and X-rays are emitted. The X-ray energy spectrum consists of a continuous background together with the characteristic X-ray lines of the atoms present in the specimen. The X-rays are detected by means of a Si (Li) detector and the pulses from the detector are amplified and finally registered in a pulse height analyser. The number of pulses in each peak, which is a measure of the concentration of the corresponding element in the specimen, is calculated. If the current is measured as indicated, it is possible to calculate the absolute amounts of the various elements since all the parameters such as X-ray production cross sections, solid angle subtended by the detector, efficiency of the detector and so on are known. PIXE thus permits absolute determination of the concentration which is great advantage although it is often convenient and desirable to calibrate against standard specimens or reference materials [Johansson et al. 1970; Johansson and Johansson 1976; Gonsior and Roth 1983].

PIXE offers several advantages for analysis, such as high sensitivity (the detection limits are on the order of parts per billion), simple sample preparation, and non-destructive, rapid and multi-element analysis [Johansson 1992b; Johansson 1992a; Johansson et al. 1970]. Thus, PIXE is widely used in elemental analyses in archaeology, agriculture, biology, chemistry, environmental studies, earth science, forensics, cultural heritage, geology, health, fisheries, food and nutrition, medicine, petrology, materials science, criminal investigations, semiconductors, contamination monitoring, and other fields [Johansson 1992a; Vadrucci et al. 2019; Smith 2020; Ishii 2019; IAEA 2004; Chiari et al. 2018; Kasahara et al. 1993; Roumié et al. 2004].

Most PIXE studies use protons as incident projectiles due to their high ionization power and large penetration depth [Johansson 1992a; Johansson 1992b; Beck 2005]. Cohen et al. found that the ionization cross section of proton, in the plane-wave Born approximation (PWBA) with correction for energy loss, Coulomb deflection, perturbed stationary state and relativistic (ECPSSR) effects, was higher than that of helium in their calculations [Cohen

and Harrigan 1985]. However, utilizing heavier ions like helium can be advantageous, particularly for improving the sensitivity of light element analysis. Johansson reported the first use of 5-MeV helium ions, which improved the detection limit by 3-4 times compared to 1.8-MeV protons [Johansson 1992b]. Several other studies, including those by Watson, Flocchini, and Beck, have also demonstrated the use of helium in PIXE analysis to enhance the detection limits of light elements, especially in high-Z matrices [Beck 2005; Watson et al. 1971; Flocchini et al. 1972; Beck et al. 2002]. The main advantage of using helium ions is reducing the bremsstrahlung background, and helium seems more advantageous when ionization cross sections are 2–3 times greater than protons [Cohen and Harrigan 1985; Beck et al. 2002].

PIXE has emerged as a highly valuable method for studying air pollution in various regions worldwide. Numerous studies have identified PIXE as a suitable and useful technique for characterizing airborne particulate matter, making it a standard method for atmospheric research [Cohen 1999; Trompetter et al. 2005; Hopke et al. 2008; Lucarelli et al. 2011]. PIXE has outstanding performance characteristics, however, its very high initial cost makes it inaccessible to general environmental laboratories. Instrumental neutron activation analysis (INAA), due to its price and safety restrictions, is also unsuitable for regular use in monitoring agencies, however, due to its specific calibration requirements, it is ideal for developing certified reference materials [Ogrizek et al. 2022]. Inductively Coupled Plasma (ICP) is the most used technique for atomic spectrometry-based techniques. ICP is based on the ionization of a sample under intense argon plasma atmosphere and the principle of analysis and detection defines the terms Mass Spectrometry (MS) and Optical Emission Spectrometry (OES), sometimes referred by Atomic Emission Spectrometry (AES). High temperatures induced by the plasma excite electrons above a steady state. In the IPC-OES, when these electrons return to steady-state, a photon of light is emitted and then analysed by interaction with electromagnetic radiation (absorption and emission). ICP (OES and MS) have some attractive features for elemental analysis. They are a fast and multi-elemental technique that present high sensitivity and low detection limits, typically in the order of ppb, although ICP-MS can show the limit of detection in the order of ppt, an order of magnitude lower than other elemental techniques [Galvão et al. 2018]. On the other hand, laser ablation inductively coupled plasma mass spectrometry (LA-ICPMS) has the potential for becoming an alternative to the standardized method (as also EDXRF), with some shortcomings (e.g. calibration, autosampler) that still need to be overcome [Lucarelli

et al. 2011; Ogrizek et al. 2021]. Synchrotron radiation x-ray fluorescence (SRXRF), on the other hand, performs with a very high precision for heterogeneous and complex samples, but it requires synchrotron radiation as an excitation source, which makes its access very limited and not feasible for routine analysis. Among the compared techniques, energy dispersive x-ray fluorescence (EDXRF) was proven the simplest and most accessible, in the form of initial and operation costs, calibration options, and sample throughput. However, using XRF, the analysis time and sensitivity for several light elements such as Na, Mg, Al, and Si, as well as heavy metals, are limited. Compared to XRF, PIXE offers a better sensitivity and detection limit than the X-ray excitation used in XRF analysis [Ivošević et al. 2014; Vadrucci et al. 2019]. Comparison PIXE with other methods based on atomic spectrometry, X-ray and ion beam analysis are resumed in Table 5. 1.

In this study, we employed a combination of two particle-induced X-ray emission techniques: helium particles induced X-ray emission (He-PIXE) and proton particles induced X-ray emission (H-PIXE). This approach enables a more comprehensive understanding of the air quality in Surabaya's industrial sites, facilitating improved detection of both light elements and heavy metals. The datasets obtained will provide valuable information and can be utilized to identify the primary contributors to the pollution.

Table 5. 1 Comparison PIXE with other methods

Technical Principal	Method	Advantages	Disadvantages
X-ray	ED-XRF	Non-destructive; Non-destructive; Fast and multi-elemental analysis; Wide range of Z; No sample handling; Applied for liquid matrices; Equivalent LoD to ICP-AES in vacuum medium; inexpensive.	Matrix-effect interference; Low sensitivity for low-Z elements: applied for Z > 11; Loss of mass and semi-volatile compounds in vacuum medium; Homogeneous sample is mandatory.
	SR_XRF	Multi-elemental; Non-destructive, and fast analysis; High sensitivity: LoD in the order of pg; Minimum background; Small amounts of sample required.	High-cost operation Synchrotron access required
Atomic Spectrometry	ICP-MS/OES	High sensitivity; Low detection limits; Fast multi-element analysis; Low volume of sample (liquid)	Sample handling: Time-consuming and contamination risk; Destructive analysis; Relative large amounts of samples
	FAAS	Low cost; Easy operation; Complementary technique for Na and Mg.	Destructive High background; Individual analysis for each element; Sampling handling: risk of contamination and co-precipitate;
Ion Beam Analysis	PIXE	Multi-element analysis; Favors lighter elements quantification; Wide range of Z; No sample handling, Non-destructive; High sensitivity	Risk of loss of semi-volatile. Not for H, C, N, O; Only for solid samples. Accelerator access required
	PIGE	High sensitivity for light elements; Multi-elemental analysis; No sample handling; Non-destructive;	Only for solid samples. Accelerator access required
Reactor based	INAA	High sensitivity: Matrix independent Standard required	High analytical time and cost; Sample handling; Require nuclear reactor; Destructive technique

5.2 Methodology

5.2.1 Sample collections

Samples were collected from industrial sites in one sampling site (S 07°18′44.68″ and E 112°47′20.55) in Surabaya, East Java province, Indonesia. Surabaya is the capital city of East Java province, Indonesia which is the second-largest city in the country, with a population of over 2.8 million people. As a major industrial center, Surabaya has a diverse range of industries, including textiles, petrochemicals, food processing, and electronics, which are known to have a significant impact on the environment and public health [BPS Statistics Indonesia 2020]. Therefore, Surabaya is an important location for conducting environmental monitoring studies. Sampling was conducted on a nucleopore filter using a Gent stacked filter unit sampler; this sampler is capable of collecting particulate matter in two fractions: coarse fraction $PM_{2.5–10}$ and fine fraction $PM_{2.5}$ size [Hopke et al. 1997]. The sampler was positioned on the rooftop of a building, approximately 4–5 meters above ground level. The samples were collected on 47 mm diameter nucleopore filters with an 8 µm-pore coated filter (coarse fraction), and a 0.4-µm-pore filter (fine fraction). Sampling was conducted over a period of 24 hours once a week, Sampling was conducted over a period of 24 hours once a week. These samples were stored in clean plastic petri dishes and kept in a controlled environment to ensure mass stabilization After the mass measurements, for the preparation of PIXE analysis, samples were cut in 0.4×1.2 cm to be mounted into the sample's holder.

5.2.2 Comparison between helium- and proton-induced X-ray emission

The X-ray yield is primarily controlled via the ionization cross section, transmission of photons through the filter matrix, absorption of X-rays by the sample matrix, and geometry of the measurement. The geometry of the measurements for both methods was similar, whereas the absorption of X-rays by the sample matrix, which was dominant in the silicon matrix samples, was dependent on the mass thickness of the sample. Upon calculating the X-ray attenuation using the mass attenuation coefficient and sample thickness, the absorption of X-rays by the samples was found to be more severe in light elements, as depicted in Figure 5. 1 [Hubbell and Seltzer 2004]. As the thickness of the aerosol sample target used in this study is minute, i.e., less than 70 µg/cm^2, the absorption by the sample matrix is negligibly small [Johansson 1992a; Chiari et al. 2018; Kasahara et al. 1993]. For aerosol samples in the polycarbonate filter, thicknesses ranging from 10 to 100 µg/cm^2 are desirable for preventing the degradation of X-ray intensity and the absorption of X-rays

within the samples [Kasahara et al. 1993]. The aerosol samples collected in the Teflon filter were also considered as infinitely thin substrata for the PIXE analysis [Chiari et al. 2018].

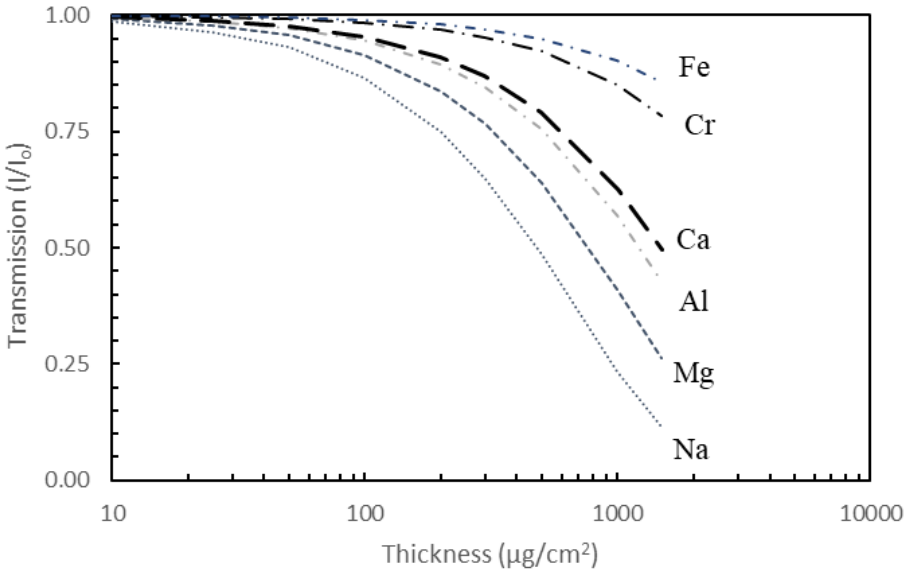

Figure 5. 1 Self-absorption effects as a function of the thickness of the sample matrix

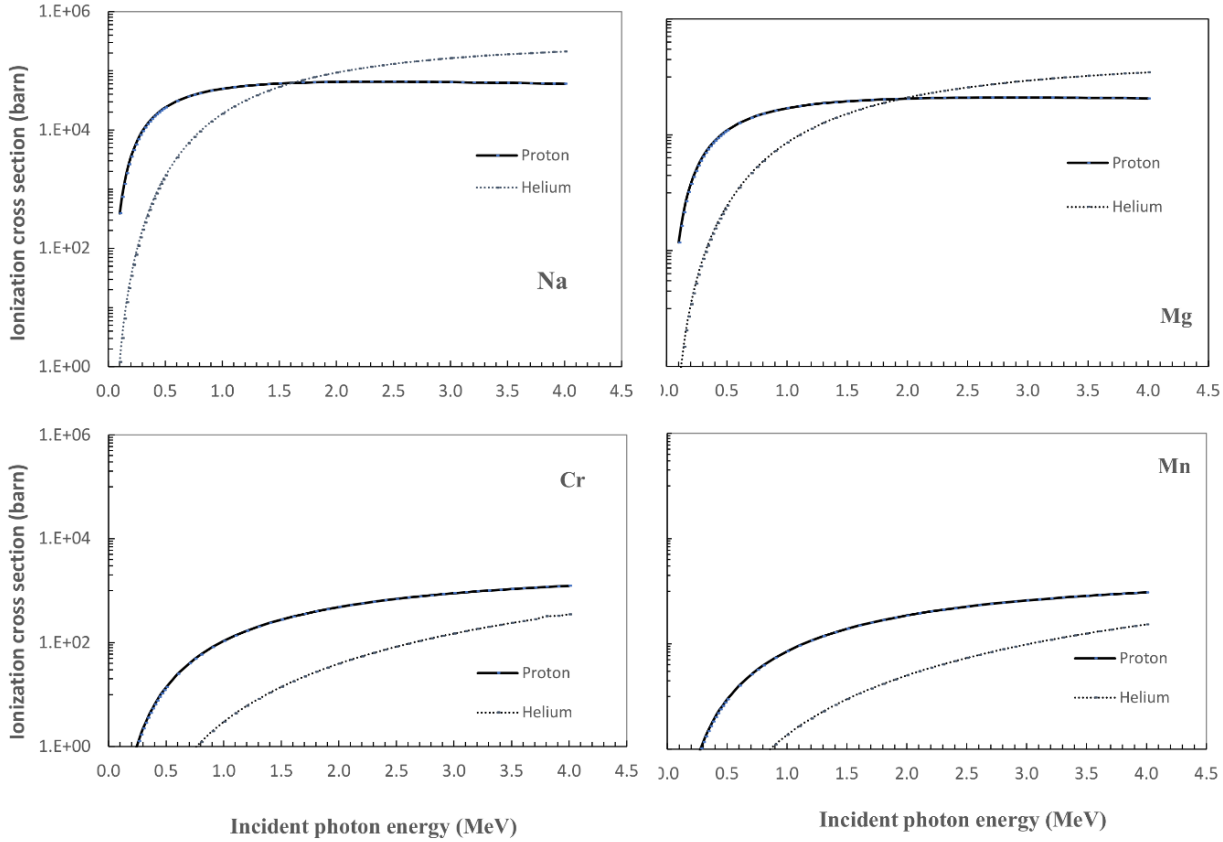

Figure 5. 2 Ionization cross section based on the ECPSSR theory for Na, Mg, Cr and Mn

The ionization cross-sections for several elements obtained through Cohen and Harrigan's calculations based on the ECPSSR theory for protons and helium are displayed in Figure 5. 2. The overall trend confirms that protons generally possess a higher ionization capability compared to helium ions [Cohen and Harrigan 1985; Beck et al. 2002]. However, it's noteworthy that the cross-sections have a similar order of magnitudes for light elements. Moreover, for incident photons with energies exceeding 1.8 MeV, helium ions exhibit higher efficiency than protons, as evidenced by the ionization cross-sections of Na and Mg. Figure 5. 3 displays the ionization cross section as a function of the atomic number (Z) to compare the differences between 1.8 MeV protons and helium ions. Additionally, it allows us to compare the ionization cross sections of 1.8 MeV and 2.5 MeV protons which not differ significantly. In the main plot, it is evident that the ionization cross section by 1.8 MeV proton showed higher than 1.8 MeV helium, except for Na. In the internal plot, a zoom-out reveals that for heavier elements (Z>20), the K-shell ionization is more effective when protons are used, as illustrated in Figure 5. 3.

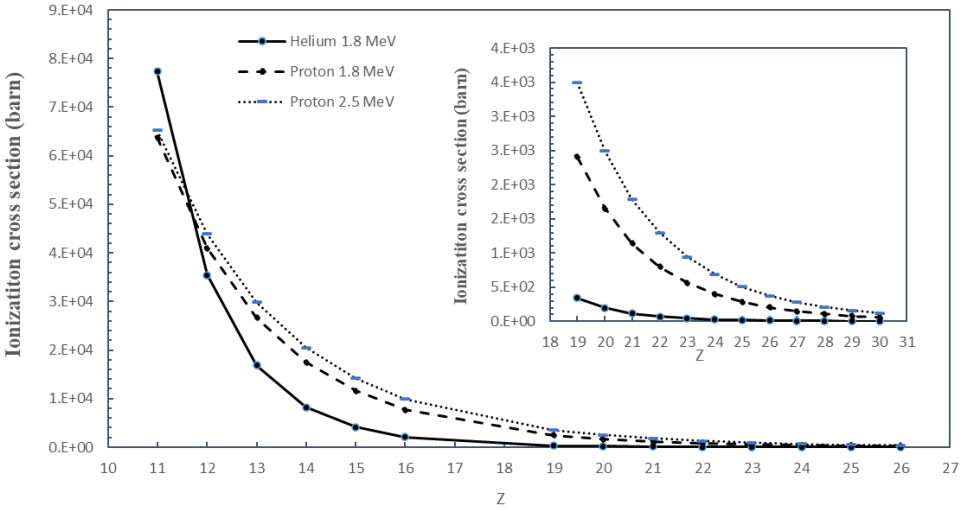

Figure 5. 3 Ionization cross section by proton (1.8 MeV and 2.5 MeV) and helium (1.8 MeV)

Moreover, the transmission of photons through the film absorber used in the experiment also affected the X-ray yield. The absorber employed in this experiment is Mylar with helium and proton beams with thicknesses of 2.0 and 38 μm, respectively. The transmission of the photon through Mylar was obtained from the atomic data and nuclear data table by Henke [Henke et al. 1993], and the ionization cross section was resumed for selected light and heavier elements in Table 5. 2 (Figure 5. 4). The X-ray detection yields

for He-PIXE and H-PIXE were proportional to the ionization cross section and transmission factor. The effects of the absorber on the PIXE analysis were reported in Kasahara's study on airborne particulate matter in which the thickness of the Mylar absorber was compared, which concluded that optimal measurements could be achieved for lighter elements using a thinner absorber (16-μm-thick Mylar) and a thicker absorber (78.6-μm-thick Mylar) for heavier elements [Kasahara et al. 1993]. In this study, we used a thinner absorber for light elements and a thicker Mylar absorber for heavier elements to obtain effective PIXE conditions for airborne particulate matter analysis. As demonstrated by the results in Table 5. 2, based on the yield of transmission and ionization cross section values, Na could not be detected, and the probability of detecting Al using H-PIXE was low. However, both H-PIXE and He-PIXE showed the ability to detect heavier elements such as Ca, Cr, and Fe, with H-PIXE exhibiting better sensitivity. Consequently, the X-ray yields induced by helium for light elements Na to Si are superior. On the contrary, when dealing with heavier elements, K-shell ionization clearly demonstrates greater effectiveness with protons.

Table 5. 2 Transmission factor of the photon by the Mylar thickness and ionization cross section for selected elements

Element	Na	Mg	Al	Ca	Cr	Fe
Transmission factor						
38-μm-thick Mylar	9.73×10^{-7}	2.25×10^{-4}	0.005	0.689	0.890	0.933
2-μm-thick Mylar	0.483	0.643	0.759	0.981	0.994	0.996
Ionization cross section,						
1.8 MeV H	6.38×10^{4}	4.10×10^{4}	2.66×10^{4}	1.65×10^{3}	1.14×10^{3}	7.98×10^{2}
1.8 MeV He	7.73×10^{4}	3.55×10^{4}	1.69×10^{4}	1.96×10^{2}	1.15×10^{2}	6.99×10^{1}
Transmission x Ionization						
H-PIXE	6.20×10^{-3}	9.22	1.33×10^{2}	1.14×10^{3}	1.01×10^{3}	7.44×10^{2}
He-PIXE	3.73×10^{4}	2.28×10^{4}	1.28×10^{4}	1.92×10^{2}	1.14×10^{2}	6.96×10^{1}

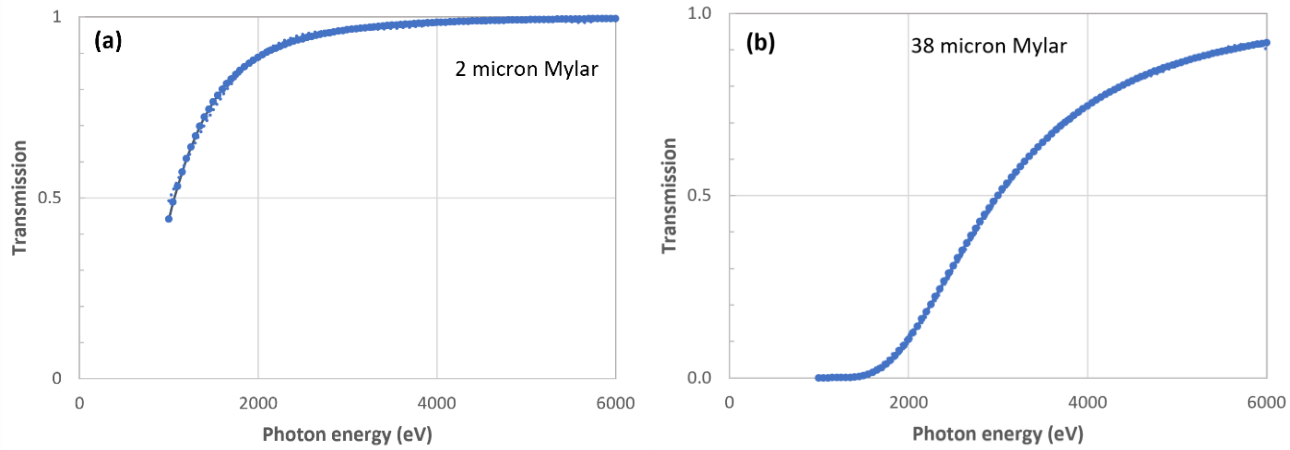

Figure 5. 4 Transmission factor through Mylar with a thickness of (a) 2 μm and (b) 38 μm

Higher energy is desirable for He and H-PIXE. However, the current performance condition of the Van de Graaff facility at Kyoto University only allows it to reach a maximum energy of 1.8 MeV. Furthermore, it is constrained to operate under 2.5 MV due to radiation regulations. Considering this fact with the calculations of ionization cross-section and transmission factors, we have decided to optimize the utilization of both helium and proton beams within the 1.8 MeV energy range. This choice becomes crucial for conducting our experiment effectively to achieve the most optimal analysis results. Notably, the results of calculation showed that at 1.8 MeV for helium is optimal, rendering its energy increase unnecessary, and we choose to use proton to complement the results for other heavier elements. This leads to the use of both helium and proton particle-induced X-ray emission methods in our study.

5.2.3 Sample measurement

The PIXE measurements were performed using a 4-MV Van de Graaff accelerator at Kyoto University. An analysing beam of protons or helium was injected at 45° to the surface of the sample, and the X-rays emitted from the sample were detected using a silicon drift detector SDD (Amptek XR-100 SDD) which placed at 90° relative to the beam direction (Figure 5. 5). The distance from the sample to the SDD was 35.4 mm, the detection area was 25 mm^2 which is collimated to 17 mm^2, and the solid angle was 2.0×10^{-2} sr. The window material of the SDD was Be with a thickness of 12.5 μm and energy resolution was 141 eV at Mn-Kα. To eliminate the noise caused by the scattered incident ions, Mylar film thickness of 2 μm for He-PIXE and 38 μm for H-PIXE were placed in front of the SDD. To minimise X-ray noise derived from the chamber materials (Fe, Cr, Ni, etc.), the sample holder and

surrounding chamber wall were shielded using high-purity carbon sheets. The shielding materials confirmed that there was no significant spectral noise by directly irradiating the beam in advance. The experimental setup is shown in Figure 5. 5. A 1.8 MeV proton or helium beam focused to 1×2 mm^2 was used for the experiments. The chamber was electrically isolated, and the beam current was measured using a micro ammeter connected to the chamber. GUPIX software was used for the deconvolution of the PIXE spectra and the quantification of elemental concentrations [Campbell et al. 2010]. GUPIX has the ability to perform absolute measurements and provide accurate quantitative results without the need for external calibration standards. All the input data related to a sample, including the spectrum, experimental setup, detector details, sample type, fit element list, and results, can be stored as an ASCII text file called the "PAR" file, allowing to analyze multiple spectra in sequence, streamlining the analysis process and increasing efficiency [Campbell et al. 2010].

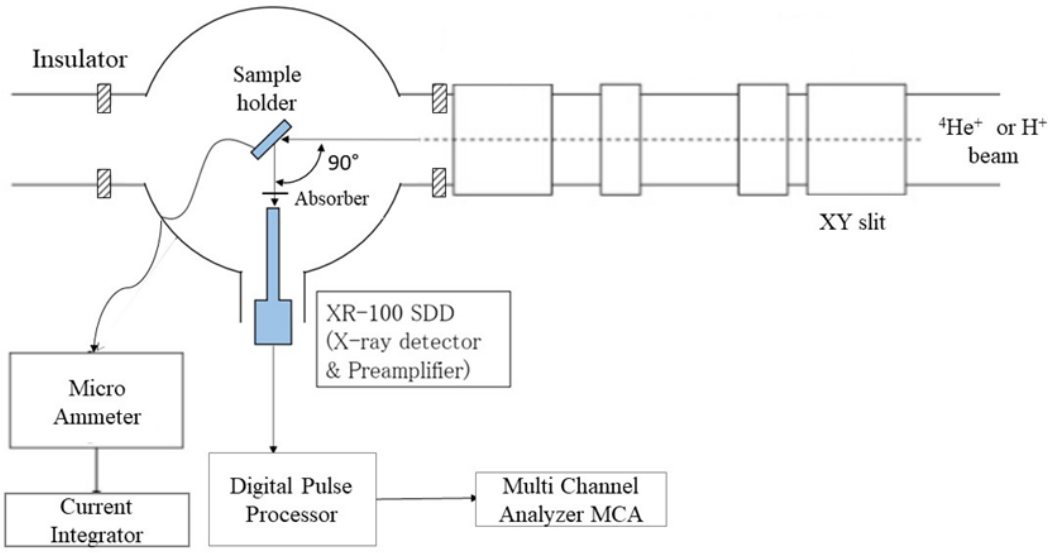

Figure 5. 5 PIXE experimental setup at Kyoto University

5.3 Results and Discussion

5.3.1 PIXE spectra from helium and proton

Standards reference material from the national institute of standard and technology NIST SRM 2783 air filter on media and micro matter) and airborne particulate samples were measured using a 1.8-MeV helium and proton beam for 300–600 s until 0.6 ×3.4 μC of samples were collected. Figure 5. 6 presents a typical spectrum obtained from the 1.8 MeV He and H-PIXE from a $PM_{2.5}$ and $PM_{2.5\text{-}10}$ sample with the same charges of 1.2 and 1.5 μC, respectively.

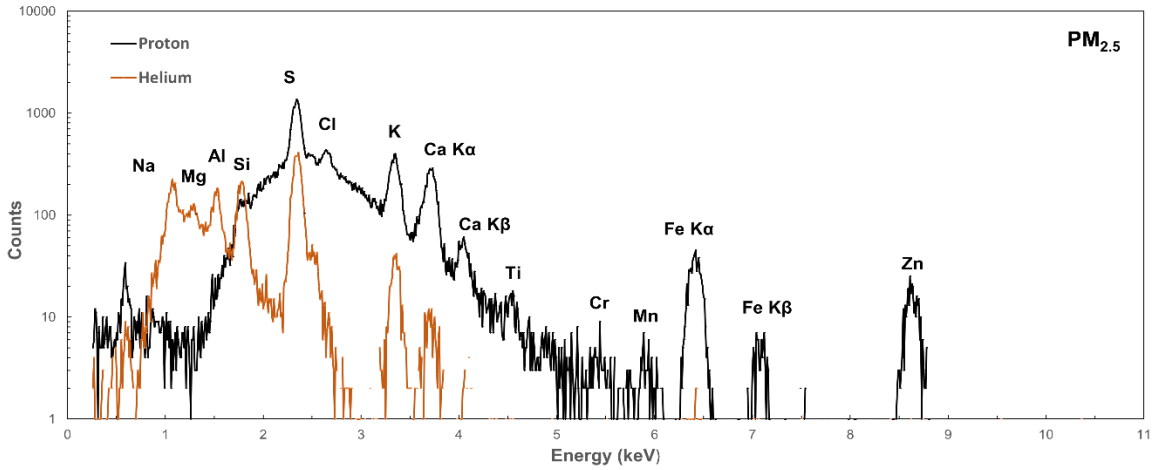

(a)

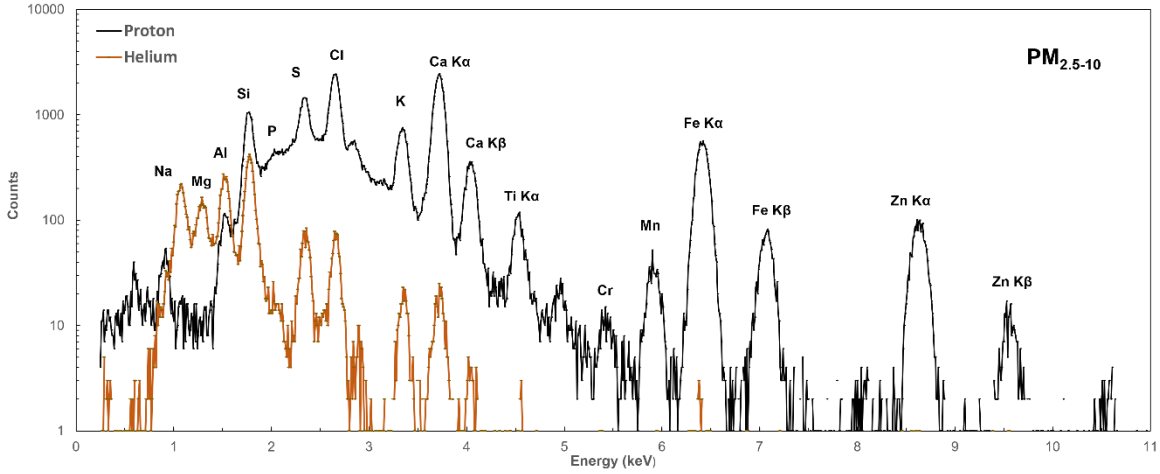

(b)

Figure 5. 6 The PIXE spectrum of $PM_{2.5}$ and $PM_{2.5\text{-}10}$ using helium and proton.

In Figure 5. 6, the peaks corresponding to Na, Mg, Al, and Si from the helium beam are observable. These peaks are superimposed on a low background and are easily discernible due to the elevated signal-to-background ratio. The background originating from the secondary electron bremsstrahlung can be attenuated using a Mylar absorber [Beck 2005; Olise et al. 2010]. However, for the heavier elements, their concentrations were found to be below the detection limit of the helium beam, resulting in limited detection capability. In contrast, when employing a proton beam, elements ranging from S to Pb are effectively detected.

The comparison of analytical results of helium and proton beam in several $PM_{2.5}$ samples is shown in whisker plot in Figure 5. 7. The whisker box plot provides a visual representation of the dataset. It showcases the lower and upper box lines, which correspond

to the values at the 25th and 75th percentiles, respectively, outliers, indicating the median (depicted as a solid black line at the box's center), and displaying the mean (represented by the cross mark). Error bars are incorporated to illustrate the values at the 5th and 95th percentiles. Figure 5. 7 showed the capability of both beams in detecting the light elements and heavier elements. It presents element concentrations in main part displays an overall of all elements. The zoomed-in image was created to focus on elements with lower concentrations, allowing for a clearer observation of details. Specifically, Na and Mg were effectively detected using the helium beam, rather than the proton beam. On the other hand, Al and Si were detectable with both beams, but the helium beam offered a better limit of detection for Al and Si. Heavier elements such as Cr, As, Mn, Zn, and Pb were not detected using helium, but were well detected using proton. From this result, it can be inferred that light elements such as Na, Mg, Al, and Si are more readily detectable when using a helium beam, whereas heavier elements such as K, Ca, Cr, Fe, Zn, and Pb, are more suitable and promptly detected using proton beams.

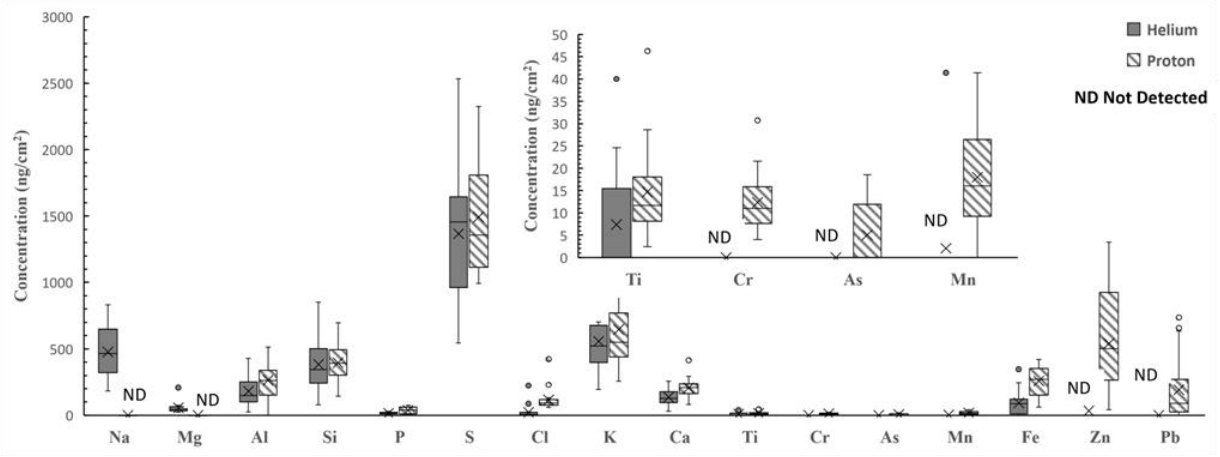

Figure 5. 7 Comparison of analytical results obtained by helium and proton

5.3.2 Limit of detection

Table 5. 3 presents the limit of detection (LOD) for selected elements, which has been calculated through GUPIX analysis. This calculation based on 3 times the square root of the background over 1 full width half maximum (FWHM) centred about the principal peak's centroid for a given element. Observably, the limits of detection for Na and Mg are remarkably improved. The reduction in the X-ray background in helium measurements allows for a better limit of detection for light elements [Beck 2005; Beck et al. 2002]. The LOD values indicate that helium beams are better suited also for Al and Si compared to

protons, while heavier elements like K, Ca, Cr, Fe, and Pb might be more effectively detected using protons.

Table 5. 3 Limit of detection (ng/cm^2) of selected elements using 1.8 MeV helium and proton beams as incident particles

Element	Helium	Proton
Na	0.53	44512
Mg	0.26	131
Al	0.49	10.9
Si	0.12	3.85
P	0.21	2.64
S	0.14	1.72
Cl	0.32	1.30
K	0.63	0.39
Ca	0.95	0.53
Sc	1.53	0.40
Ti	2.32	0.39
V	3.28	0.30
Cr	2.26	0.22
Mn	7.00	0.45
Fe	4.73	0.40
Co	14.7	0.56
Ni	19.8	0.38
Cu	29.2	0.74
Zn	42.1	1.17
As	793	4.96
Pb	68.3	3.76

5.3.3 Method validation

The PIXE spectra were analysed using GUPIX software to quantify the absolute concentration [Campbell et al. 2010]. The software was operated using a batch mode option for smooth analysis of all spectra. A correction factor to ensure absolute concentration was applied by analysing thin single-element standards deposited on polycarbonate filters (Micromatter Inc). The obtained concentration values were verified by analysing the NIST® SRM 2783 air particulates on the reference material of the filter media. The use of SRMs is a well-established practice in analytical chemistry to ensure the accuracy and reliability of analytical results. The concentrations of the light elements Na, Mg, Al, and Si were obtained via the helium beam, whereas those of heavier elements (from S to Pb) were obtained through measurements using a proton beam. The result of NIST® SRM 2783 air filter on media is plotted in Figure 5. 8. The recovery was determined by dividing the analytical results by the certified value. The vertical bar shows error bars derived from the relative

standard deviation to represent variability in the results. For most of the detected elements, the recovery range is 86–112%, except for trace elements such as V, Ni, and Cu, which exist at ppb levels and have recovery 81%, 133% and 80%, respectively. The recovery on V, Ni and Cu are acceptable due to the low level of their concentration [Olise et al. 2010; AOAC 2016]. Moreover, Sc, Co, and As were not detected optimally because their concentrations were below the LOD. Method comparison with other methods such as XRF is not carried out here, since validation method using SRM NIST and single standards Micromatter have been carried out and demonstrating good agreement.

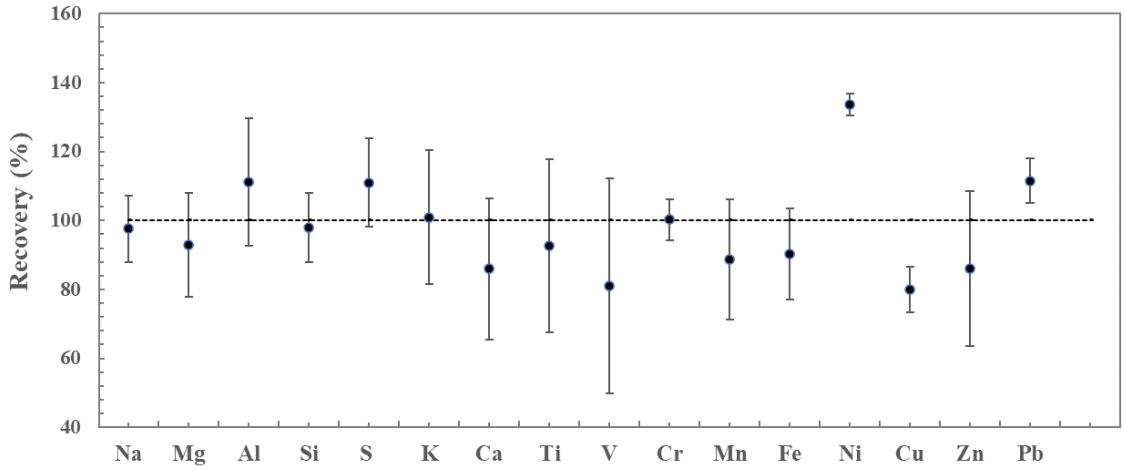

Figure 5. 8 The ratio of certificate value and analysis results using PIXE

5.3.4 Elemental concentrations

$PM_{2.5}$ and $PM_{2.5\text{-}10}$ samples were analysed. The elemental concentrations of $PM_{2.5}$ are summarised in Table 5. 4, and the elemental distribution is illustrated in the whisker plot in Figure 5. 9. Both helium and proton beams were used in the analysis to obtain optimal results, and 21 elements were detected in the samples. Helium beam used to detect light elements Na, Mg, Al, and Si, while proton beam used for S, K, Ca, Ti, V, Cr, Mn, Fe, Ni, Cu, Zn, and Pb.

Table 5. 4 The elemental concentrations (ng/cm^2) in $PM_{2.5}$ and $PM_{2.5-10}$ samples collected in Surabaya, Indonesia using helium and proton PIXE

	$PM_{2.5}$ (ng/m^3)				**$PM_{2.5-10}$ (ng/m^3)**			
	Mean	**Std. Dev.**	**Min**	**Max**	**Mean**	**Std. Dev.**	**Min**	**Max**
Na	635.6	552.3	35.8	4548.3	407.69	235.60	28.78	1244.74
Mg	83.6	90.7	15.3	678.5	129.68	68.54	26.99	318.91
Al	270.3	212.8	26.2	1059.6	553.14	404.50	36.13	1638.83
Si	586.6	457.2	44.2	2334.4	1143.82	822.28	121.31	3646.60
P	28.5	20.9	2	95.7	29.37	12.16	6.41	60.95
S	1172.9	739.7	278.6	6940.3	336.88	136.64	78.65	714.20
Cl	218.5	278.3	57.5	2544.3	761.49	537.80	54.91	2933.28
K	527.6	304.3	104.4	1974	236.78	116.32	53.35	686.75
Ca	236.6	99.6	82.7	638.8	657.42	274.51	65.14	1420.40
Sc	3.25	2.35	0.43	11.88	8.19	3.37	2.82	18.81
Ti	17.3	10.8	2.5	69.4	39.87	19.07	6.66	86.59
V	2.67	1.96	0.65	9.17	3.90	1.43	1.62	8.46
Cr	9.44	6.68	0.47	40.58	7.08	3.76	1.88	19.65
Mn	17.7	19.5	2.9	171.8	25.45	17.78	1.64	89.48
Fe	235.2	107.6	44.8	578.5	581.44	314.96	47.30	1632.62
Co	5.85	3.71	0.95	15.3	9.65	5.16	2.65	32.95
Ni	4.69	2.93	1.1	14.7	3.17	1.79	0.96	10.64
Cu	10.6	6.5	1.64	40.4	7.15	4.27	1.68	25.70
Zn	521.9	478.5	24.5	3651.1	531.83	445.86	15.47	2436.05
As	24.5	16.8	6.3	86.7	24.04	18.67	2.79	82.07
Pb	203	185	16.1	736.5	97.51	91.97	5.90	341.87

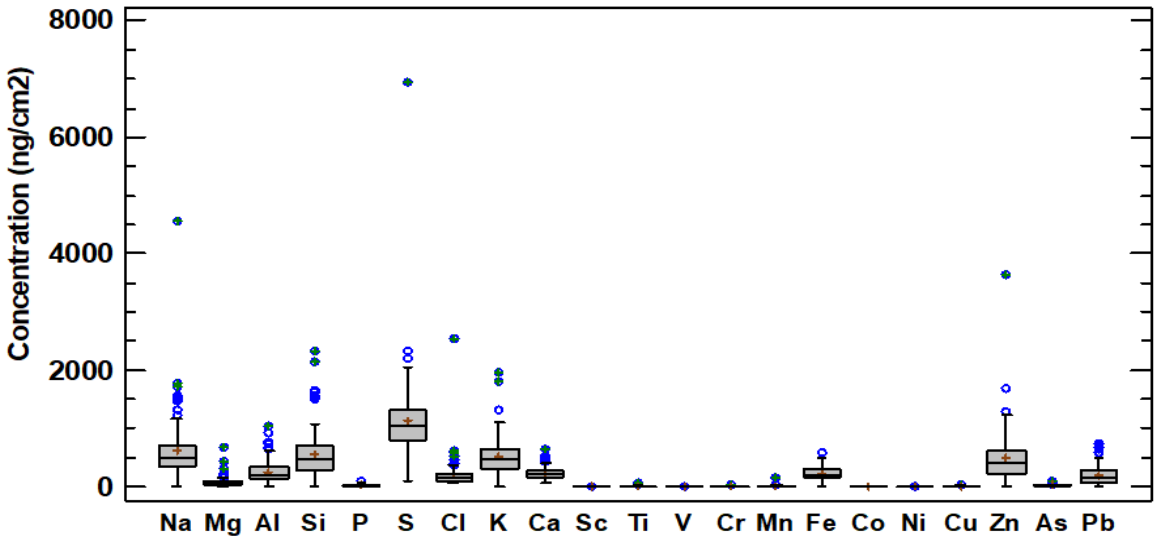

Figure 5. 9 Whisker plot of the elemental concentration in $PM_{2.5}$

In $PM_{2.5}$, certain major elements such as S, K, Zn, Fe, and Pb are dominant, and elements of crustal origin such as Al, Si, and Ca are identified. In $PM_{2.5\text{-}10}$, crustal elements (Al, Si, Ca and Fe) are dominant, followed by Cl, Zn and Na. The presence of sulfur in fine particulate matter is primarily attributed to the atmospheric conversion of SO_2 into sulphate particulates through homogeneous processes [Hopke et al. 2008]. The high sulfur content fuel utilized in diesel vehicles could contribute to these concentrations [Santoso et al. 2020b]. The key elements Al and Si consistently show high correlation coefficients ($r > 0.97$), indicating natural pollutant sources from soil and crustal dust [Ho et al. 2006; Taiwo et al. 2014; Santoso et al. 2020b]. This dataset also revealed the tendency of heavy metal pollution in the ambient air at the sampling site, as the concentrations of certain heavy metals such as Zn, Fe and Pb are high. A comparative analysis with other sites, both within and outside Indonesia, holds potential, necessitating additional investigation to elucidate this observation. Further analysis using receptor modeling to identify the sources, conditional probability function to identify the possible source location, as well as health risk assessment is necessary to comprehensively understand the origins, impact, and potential risks associated with these elevated heavy metal concentrations. Notably, particulate matter contains carbon and organic compounds, such as ammonium, nitrates, and sulfates [Lucarelli et al. 2011; Vega et al. 2021], which cannot be measured solely through PIXE; however, the information obtained via PIXE analysis yields a significant database and early notification. The PIXE method can obtain invaluable data for major, minor, and trace elements in aerosol

studies involving large numbers of samples. Those data of elements are needed to estimate the source identification and the contributions of pollutant sources.

5.4 Conclusions

Helium and proton particle-induced X-ray emissions were used for the elemental characterisation of airborne particulate matter samples collected in Indonesia. Both combinations yielded optimal results, especially for detecting light elements using helium and for detecting heavier elements using a proton beam, with a total of 21 elements detected. This elemental analysis revealed the major, minor, and trace elements in $PM_{2.5}$ and $PM_{2.5-10}$ yielding significant and important information. As revealed by the data, the heavy metals, crustal elements, and other elements showed the characteristics of $PM_{2.5}$ and $PM_{2.5-10}$ collected in Surabaya, which could be an early indicator of the air quality condition at the sampling site. This study also showed that the combination of He-PIXE and H-PIXE can produce a significant dataset to be utilized in aerosol studies. A dataset of elemental concentrations obtained through PIXE analysis is required for further statistical analysis and receptor modeling to identify the possible pollutant sources in $PM_{2.5}$ and $PM_{2.5-10}$. This makes PIXE is still a valuable tool in providing the chemical composition datasets of elements, for studying the sources and transport of atmospheric particulate matter, as well as its potential health effects. In conclusion, PIXE stands out as the preferred choice when analysing highly size-resolved aerosol samples or when demanding high time resolution in aerosol analysis. This study shows that PIXE still making a significant and valuable contributions to aerosol research.

CHAPTER 6 Assessment of Industrial Activities and Their Impact on Air Quality and Health Risk Assessment of $PM_{2.5}$ in Industrial Area of Surabaya, Indonesia

6.1 Introduction

Industrial activities, such as manufacturing/industrial processes, power generation, transportation and logistics, waste and incinerator, have a substantial impact on air quality degradation [Gallon et al. 2006; Sylvestre et al. 2017; Vega et al. 2021]. The emissions from industrial activities contribute significantly to the presence of fine particulate matter in the atmosphere [Alias et al., 2020; Vega et al., 2021; Yu and Park, 2021] . These activities often involve the burning of fossil fuels, resulting in the release of various pollutants. Fine particulate matter with a diameter less than 2.5 μm (referred to as $PM_{2.5}$) is particularly concerning because its size closely aligns with particles that can effectively enter the airways and alveoli of the lungs [Wang et al., 2019; Dysart et al., 2014]. Multiple studies have consistently demonstrated a strong correlation between elevated levels of fine particulate matter in the air and an increased risk of mortality from various causes, particularly cardiovascular and respiratory diseases [Dockery et al., 1993; Samet et al., 2000; Wang et al., 2020]. Residents of low- and middle-income countries bear a disproportionate burden of outdoor air pollution, with a striking 89% of the 4.2 million premature deaths occurring in these regions [WHO 2022]. The highest impact is observed in the World Health Organization's South-East Asia and Western Pacific Regions.

Addressing air pollution is crucial to protect public health, as it stands as the second highest risk factor for noncommunicable diseases [WHO 2022]. Effectively identifying and allocating air pollutants is crucial for air quality management as it provides valuable information to guide decision-making processes and address pollution sources. To identify the sources of pollution, observed PM composition data can be analysed using multivariate receptor models [Santoso et al. 2008]. Positive matrix factorization (PMF), developed by Paatero and Tapper is one such multivariate receptor modeling technique [Paatero and Tapper 1994]. PMF offers a flexible modeling approach that efficiently utilizes the information contained within the data. PMF has proven successful in various atmospheric studies, including those conducted in several countries [Reff et al. 2007].

Furthermore, research on APM in East Java has indicated concerning levels of air particulate matter, especially regarding potentially toxic elements. Our study on air quality

in several cities in Indonesia 2010–2017 revealed that concentrations of $PM_{2.5}$ in the industrial areas of Surabaya exceeded the Indonesian annual ambient air quality standard (15 $\mu g/m^3$). Additionally, significantly higher concentrations of potentially toxic elements such as Fe, Zn, and Pb were identified. These findings highlight a similar air quality condition to that in the Serpong area, which is contaminated with high levels of Pb in the air. Another investigation conducted by Humairoh, part of our continuous research efforts in monitoring air quality in East Java, showed the elevated of potentially toxic elements, including Pb, in air particulate matter samples collected from industrial zones in Waru, East Java [Humairoh et al. 2020]. They utilized principal component analysis (PCA) to identify four possible sources. In light of the high Pb contamination affecting several regions in East Java, further research was conducted in the vicinity of a lead smelter in Lamongan to assess the impact of the lead smelter industry on $PM_{2.5}$ and soil in the surrounding environment [Lestiani et al. 2023b, c]. We found that the concentrations of atmospheric lead in Serpong and Lamongan were higher than in Jakarta. In Serpong and Lamongan, Pb is attributed similarly to an average of 2.7% of $PM_{2.5}$. A study by Haryanto found that very high blood lead levels (BLLs) have been identified in children living near used lead acid batteries recycling smelters [Haryanto 2016; Prihartono et al. 2019]. It was found that many children in the area had learning difficulties and poor grades in school, and some had physical development problems such as stunting or other problems. Another study by Hindratmo also reported that the BLL in elementary school children collected from Tangerang (60 children) and Lamongan (69 children) who lived near the lead smelter industries, all the values of BLL were found above the CDC standard for BLL (5 μg/dL), and some children's BLL were out of the measurement range (above 65 ug/dL) [Hindratmo et al. 2018].

Surabaya has one of the largest industrial sites in Indonesia. It is known for its diverse industrial activities, including metal working, coal combustion, and transportation, which collectively contribute to air pollution [Santoso et al. 2020b]. Despite the significant air pollution burden associated with industrial activities in Surabaya, there is limited research publication specifically focused on air quality and pollutant sources in these industrial sites. Recent studies have indicated concerns about the levels of air particulate matter in Surabaya. A study conducted by Santoso et al. found that the concentrations of $PM_{2.5}$ in the industrial areas of Surabaya exceeded the Indonesian annual ambient air quality standard (15 $\mu g/m^3$), and significantly higher concentrations of heavy metals Fe, Zn, and Pb were identified [Santoso et al. 2020b]. Another investigation by Humairoh et al. highlighted the presence of

toxic heavy metals, such as lead in the air particulate matter samples collected from industrial zones in Waru, East Java [Humairoh et al. 2020] and utilized principal component analysis to identify four possible sources. Previous study on sources identification using principal component analysis in two semi industrial area in Bandung also reported [Lestiani et al. 2013a]. Based on review on receptor modeling by Hopke (2015), PCA is considered not a true receptor model because it allocates variances from the mean value rather than the precise values, thus lacking the ability to offer source apportionment for pollutants. PMF or hybrid receptor models for more accurate source identification are suggested to obtain better results on source apportionment [Hopke 2015; Saksakulkrai et al. 2023].

However, none of the studies have focused on the comprehensive identification of content for potentially toxic elements, utilization of receptor modeling to specifically pinpoint sources of pollutants, and health risk assessment to evaluate the respiratory hazards on human health. This knowledge gap underscores the necessity for further studies and investigations to enhance the understanding of and address the air quality challenges faced in Indonesia's industrial areas. This study involves analysing airborne particulate matter samples collected over a two-year period in an industrial area in Surabaya using particle-induced X-ray emission. The objective of the study is to identify the sources of fine particulate matter, the types of pollutants, and evaluate their contributions to particulate air pollution in the industrial area. Additionally, the study aims to assess the health risks associated with particulate-bound potentially toxic elements, considering both children and adults.

6.2 Methodology

6.2.1 Sampling

Sampling was carried out in Surabaya, which is located in the East Java province. The coordinates of the sampling site were S 07°20′46.43″ S and 112°44′03.12″ E as shown in Figure 6. 1. Surabaya, Indonesia's second-largest city, has a population of over 2.8 million and is known for its diverse industrial activities, which include manufacturing, shipbuilding, petrochemical, electronics, textiles, cement factories, smelters, and other metal industries [Santoso et al. 2020b]. It is a major economic center in Indonesia and serves as a regional trading hub and has a busy seaport. The mapping of industrial activities in Surabaya is shown in Figure 6. 1, with a coloured dot for each industry: steel (grey), galvanizing (red), aluminium and mineral industry (blue), plastic (green), and fertilizer (orange). A dichotomous sampler the Gent stacked filter unit (SFU) sampler was utilized to collect

particulate matter in $PM_{2.5}$ and $PM_{2.5\text{-}10}$ size fractions [Hopke et al. 1997]. The sampler was positioned on the rooftop of a building, approximately 4–5 meters above ground level. The coarse fraction sample was collected using an 8 µm pore coated nucleopore filter, while the fine fraction sample was collected using a 0.4 µm pore nucleopore filter. Sampling was conducted over a period of 24 hours once a week, from March 2021 to December 2022, resulting in a total of 86 pairs of samples. These samples were stored in clean plastic petri dishes and kept in a controlled environment to ensure mass stabilization [US EPA 2006].

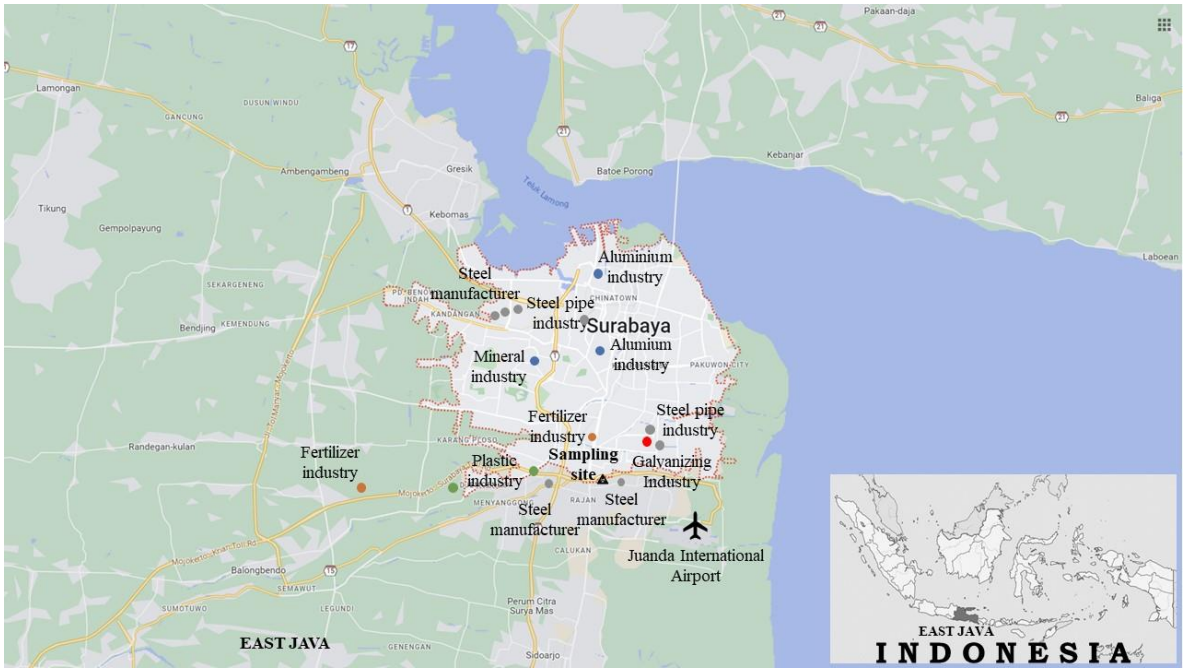

Figure 6. 1 Location of sampling site and industrial area in Surabaya, East Java

6.2.2 Sample characterization

The mass concentrations of $PM_{2.5}$ and $PM_{2.5\text{-}10}$ were determined by gravimetric analysis in environmentally controlled room. Moisture content can affect filter weight, therefor the filters were equilibrated for a minimum of 24 hours in prior to pre- and post-weighing. During the equilibration period, relative humidity was maintained at a 45±5%, and air temperature at 20±2°C. The filters were weighing before and after sampling using microbalance with ± 0.001 mg precision (MX5 Mettler Toledo), then divided by the volume of air passing through the filter to obtain the concentration of $PM_{2.5}$ ($\mu g/m^3$). PM_{10} was the sum of $PM_{2.5}$ and $PM_{2.5\text{-}10}$.

The BC concentrations were determined by measuring reflectance with an EEL model 43D smoke stain reflectometer (Diffusion Systems Ltd.), which measures the

reduction in reflected white light [Biswas et al. 2003; Begum and Hopke 2019]. The amount of light reflected or absorbed in the filter sample is determined by particle concentration, density, refractive index, and particle size. The BC loading is estimated by measuring the reflectance of light from a tungsten bulb. The uncertainty of the measurement was mainly dependent on the R_0 reflectance before and R_1 reflectance after sampling [Cohen et al. 2000]. The BC detection limit was 0.02 μg/m^3, based on the approach described by the U.S. Environmental Protection Agency [Salako et al. 2012]. From our replicate three measurements of sample analyses showed a typical relative percentage difference of 5%. The uncertainty in estimated BC mass could be as high as 15% which, when combined in quadrature with an uncertainty of 5% in $\ln(R_0/R_1)$, results in an uncertainty of ±15% in the values for mass absorption efficiency [Taha et al. 2007]. The reflectance value of the sample filter was measured three times after it was placed on a white standard. The difference between the reflected light obtained from the filter sample and that of a blank filter is directly proportional to the concentration of black carbon (BC) on the filter. The reflectometer calibration was carried out using the white (100%) and grey (33 ± 1.5%) standards with known reflectance values provided by the manufacturer [Biswas et al. 2003; Begum et al. 2010]. For the BC calculation, a mass absorption coefficient used was 5.7 m^2/g, this value was established by Maenhaut experimentally determined for reflectance using white light measurement in 47 mm diameter Nucleopore filters [Seneviratne et al. 2011].

The samples were analysed by PIXE using a 4-MV van de Graaff accelerator at Kyoto University. The measurements were performed using both helium ions and protons as incident projectiles to obtain optimal results. The experiments employed a focused beam of 1.8 MeV protons or helium ions, with a beam spot size of 1×2 mm^2. The chamber was electrically isolated, and the beam current was accurately monitored using a micro ammeter connected to the chamber. Helium was used to analyse light elements Na, Mg, Al and Si, while proton was used to determine other heavier elements (S, K, Cl, Ca, Ti, V, Cr, Mn, Fe, Co, Ni, Cu, As, Zn, and Pb) (Lestiani et al., 2023a). To deconvolute the PIXE spectra and determine the elemental concentrations, the spectra obtained were analysed using the computer code GUPIX [Campbell et al. 2010]. The accuracy of the analysis was evaluated by assessing the measured concentrations of a standard reference material from the National Institute of Standards and Technology SRM NIST 2783 air particulate on filter media and single elements of Micromatter standards. For most of the identified elements, the recovery range lies between 86 to 112%, with the exception of trace elements like V, Ni, and Cu,

which exhibit recoveries ranging from 80% to 133%, still considered acceptable due to their low concentrations [AOAC, 2002; Lestiani et al., 2023a].

6.2.3 Data analysis

Reconstructed mass

The reconstructed mass (RCM) is an estimation of the overall sample mass obtained by summing the measured chemical constituents. Mass closure or reconstructed mass was calculated based on eight components: crustal matter, sea salt, ammonium sulphate, nitrate, elemental carbon, organic matter, smoke, and lead bromide as described by Chan [Chan et al. 1997]. Chow et al. (2015) extended the list of major PM components to include major inorganic ions (e.g., SO_4^{2-}, NO_3^-, and NH_4^+), organic matter (OM) or organic carbon OC, elemental carbon EC, geological minerals (dust/soil/crustal material), salt, other trace elements, and the remaining mass [Chow et al. 2015].

In this study, the reconstructed mass (RCM) was determined by considering the following components: crustal matter/geological mineral, sea salt, ammonium sulphate, smoke, black carbon BC and other trace elements. For crustal elements/geological minerals containing Al, Si, Ca, and Fe compounds, they are assumed to be Al_2O_3, SiO_2, CaO, and Fe_2O_3, respectively. The IMPROVE "soil" formula applies a factor of 1.16 to account for unmeasured compounds [Malm et al. 1994; Chan et al. 1997; Chow et al. 2015], for the exclusion of MgO, Na_2O, K_2O and H_2O from the crustal mass calculation, as shown in Eq. 6. 1:

$$\text{Crustal elements} = 1.16\,(1.90A1 + 2.15Si + 1.41Ca + 1.67Ti + 2.09Fe) \quad \text{Eq. (6. 1)}$$

Various methodologies were employed to estimate the contribution of sea salt since there is no standard method to estimate salt. Some studies multiplied the sodium concentration by 2.54 [Malm et al. 1994], and certain studies determined the sea salt contribution by summing the sodium and chloride concentrations [Pey et al. 2009; Chow et al. 2015]. In this study, we use the sum of calculation of sodium and chlorine.

The estimation of ammonium sulphate involved multiplying the sulfur content by a factor of 4.125 [Chan et al. 1997]. When only sulfur (S) is measured, it is assumed that it has been neutralized as $(NH_4)2SO_4$, hence the estimation of $(NH_4)2SO_4$ as 4.125 times the sulfur content [Malm et al. 1994; Chow et al. 2015] as described in Eq. 6. 2.

$$\text{Ammonium sulphate} = 4.125 \times S \qquad \text{Eq. (6. 2)}$$

Smoke is commonly associated with the combustion of biomass and incineration, and potassium is often utilized as a key tracer element. Potassium has a non-soil component from smoke, therefore, iron is used as a surrogate for soil potassium [Chan et al. 1997], and the formula of Eq. 6. 3 is used.

$$\text{Smoke} = K - 0.6\,Fe \qquad \text{Eq. (6. 3)}$$

$$\text{RCM} = \text{Crustal} + \text{Seasalt} + \text{Ammonium Sulfate} + \text{Smoke} + \text{BC} + \text{Other trace elements} \qquad \text{Eq. (6. 4)}$$

To achieve reliable source apportionment outcomes, the reconstructed mass (RCM) plays a significant indicator which describes the total of analysed mass. However, it is worth noting that in this study, the RCM does not include the organic compounds such as nitrates which not analysed and particle-bound water. Additionally, for the coarse fraction, the RCM calculation excludes smoke and black carbon due to their larger particle size, which the main contributors originating from natural rather than anthropogenic sources.

Positive Matrix Factorization

Multivariate approaches in source apportionment rely on the principle that chemical species originating from the same sources exhibit similar temporal behaviour at the receptor site. These approaches involve the measurement of chemical species in multiple samples collected over time at a single receptor site. By grouping together species with similar variability into a minimal number of factors, the dataset's variability can be effectively explained. In this study, receptor modeling and apportionment of particulate matter (PM) mass were performed using the Positive Matrix Factorization (PMF) method [Paatero and Tapper, 1994]. PMF constrains sources to have non-negative species concentrations, ensures that no sample has a negative source contribution, and utilizes error estimates for each observed data point as point-by-point weights. This aspect is advantageous as it accommodates missing and below detection limit data, which is common in environmental monitoring results [Paatero and Hopke, 2003]. The signal-to-noise ratio of individual elemental measurements significantly impacts receptor models and modeling results. For species with weak signals (close to the detection limit), the variance may be primarily attributed to noise [Paatero and Hopke 2002]. To address this, Paatero and Hopke (2003) recommend down-weighting or excluding noisy variables based on their signal-to-noise ratio

[Paatero and Hopke 2003]. Variables that consistently remain below the detection limit or exhibit high measurement uncertainty relative to their concentrations are screened out. In this analysis, the data were evaluated based on their signal-to-noise ratio (S/N ratio). Variables with very low S/N ratios (≤ 0.2) were excluded from the analysis, while weak variables ($0.2 \leq S/N \leq 2$) were down weighted. To explore and control the rotational freedom in solutions, the FPEAK method was employed, and the impact on Q values (chi-squared), G-vector plots, and residual plots was observed [Paatero et al., 2005]. Several examinations with number of factors between 5 and 10 were applied to find a meaningful and significant solution. Only solutions that linked with physical sources were acceptable in the results. In this study, any missing data were replaced with the geometric mean of the corresponding components. For values below the detection limit, half of detection limit was utilized, and its associated uncertainty was substituted at 5/6 of the detection limit value as per EPA PMF 5.0 user guide.

Conditional Bivariate Probability Function

Conditional bivariate probability function (CBPF) is used to identify and characterize emission sources region in the local scale. It is an extension of the commonly used conditional probability function (CPF), which only considers wind direction. The application of the CPF methodology is expanded to include the bivariate scenario, resulting in the generation of a conditional bivariate probability function (CBPF) plot [Althuwaynee et al. 2021]. In this plot, wind speed is incorporated as a third variable, represented on the radial axis. The bivariate analysis offers additional insights into the nature of identified sources by providing essential information on dispersion characteristics. By considering concentration intervals, the enhanced CPF or CBPF approach reveals a source information that is not captured in the standard CPF or CBPF analysis [Uria-Tellaetxe and Carslaw 2014]. CBPF adds wind speed as a third variable, which provides more information about the type of sources being identified and their dispersion characteristics [Uria-Tellaetxe and Carslaw 2014]. CBPF is calculated by first dividing the observation site into a grid of cells, each with a specific range of wind direction and wind speed. Then, the probability of a high concentration of pollutant being observed in each cell is calculated. This probability is then plotted as a function of wind direction and wind speed, creating a CBPF plot. The CBPF plot can be used to identify the source regions that are most likely to be contributing to high pollutant concentrations at the observation site. The shape of the CBPF plot can also provide information about the type of sources being identified. For example, a CBPF plot with a

sharp peak in one direction suggests that a point source is in that direction. A high probability of CBPF at both low and high wind speeds implies the existence of potential emission sources at ground-level and stack sources, respectively. In general, low wind speeds tend to disperse atmospheric pollutants to a limited geographical or small area, indicating local-scale dispersion. Conversely, high wind speeds increase the dispersal of the dispersion of pollutants over larger distances, potentially leading to their transportation to remote regions [Uria-Tellaetxe and Carslaw 2014]. Hence, the occurrence of high CBPF probabilities at both low and high wind speeds can suggest the presence of local and non-local emission sources, respectively [Zhou et al. 2019]. CBPF has been made readily accessible through the openair R package [Carslaw and Ropkins 2012; Uria-Tellaetxe and Carslaw 2014].

6.2.4 Health Risk Assessment

The average daily dose (ADD) is used in the health risk assessment process to estimate the dose of the air pollutant that a person is likely to be exposed to over a period of time [US EPA 1989, 2011]. It is calculated by multiplying the concentration of the pollutant in the air by the amount of time that a person is exposed to the pollutant. The dose is then used to calculate the risk of adverse health effects from exposure to the air pollutant. Health risk assessment involves the evaluation of potential health risks to individuals exposed to certain hazards. It encompasses the estimation of parameters like the Average Daily Dose (ADD), Hazard Quotient (HQ), and Health Index (HI), which provide insights into the level of exposure, potential adverse effects, and overall health impact associated with the given hazards. For calculating the Average Daily Dose (ADD), Hazard Quotient (HQ), and Hazard Index (HI) as per the approach described by the US Environmental Protection Agency (EPA) in 1989 and 2011 [US EPA 1989, 2011]. The Average Daily Dose represents the estimated value for exposure, is calculated by multiplying the concentration of the pollutant in the air by the amount of time that a person is exposed to the pollutant using the formula in Eq. (3. 1).

Hazard quotient (HQ) is a measure of the potential for adverse health effects from exposure to a hazardous substance. It is calculated by dividing the average daily dose (ADD) of the substance by the reference dose (RfD) for the substance. The RfD is an estimate of the amount of a substance that is expected to have no adverse health effects in 50% of the exposed population over a lifetime. RfD is typically expressed in milligrams of substance per kilogram of body weight per day. An HQ of 1 or less indicates that the ADD is below the RfD and that there is no significant risk of adverse health effects. An HQ greater than 1

indicates that the ADD is above the RfD and that there is a potential for adverse health effects [US EPA 1989]. While Hazard Index (HI) assesses the overall potential for chronic effects caused by multiple substances/chemicals or heavy metals. It is calculated by summing up the hazard quotients for each substance. The specific values used for variables such as concentration, inhalation rate, exposure frequency, etc., would depend on elemental data being evaluated. This study included the analysis of toxic elements As, Co, Cr, Ni, and Pb which have been classified by the International Agency for Research on Cancer (IARC) as potentially or probably carcinogenic to humans [US EPA 2011]. Previous studies have suggested that the proportion of carcinogenic Chromium (VI) to non-carcinogenic Chromium (III) concentrations in the ambient air is 1:6 [Hsu et al. 2016] and the concentration of Chromium (VI) represents approximately 1/7 of the total chromium concentration [Park et al. 2008; Vega et al. 2021]. The individuals residing in the study area, including both adults and children, were considered as potential recipients.

Within the context of carcinogens, the assessment of risk is evaluated based on the probability attributed to an individual's potential development of cancer over their lifetime as a result of being exposed to potential carcinogenic agents. The evaluation of potential risks associated with carcinogenesis involves the utilization of the subsequent equations [Alias et al., 2020; US EPA, 1989].

$$CR = LADD \times SF \qquad \text{Eq (6.5)}$$

Here, CR denotes the dimensionless probability of carcinogenic risk, while SF represents the carcinogenic slope factor specific to each metal (day kg/mg). The cumulative carcinogenic risk is computed as the sum of risks originating from all individual metals. LADD (Lifetime Average Daily Dose) for the metal's exposure concentrations concerning carcinogenic risk, its computation employs equation (1), adopting an averaging time (AT_{car}) for cancer risk spanning 70 years multiplied by 365 days. The precise SF values correspond to the chosen potentially toxic elements by US EPA [US EPA, 2011, 1989].

$$SF = IUR \times \frac{1}{IR} \times BW \qquad \text{Eq (6.6)}$$

The IUR value, sourced from the Integrated Risk Information System (IRIS) — a repository dispensed by the US EPA (Environmental Protection Agency) provides human health risk information — is expressed in units of $m^3/\mu g$ and signifies the increased risk of cancer per microgram of exposure. The CR value indicates the likelihood of an individual

developing any form of cancer following lifelong exposure to carcinogenic metals. In the context of regulatory requisites, the acceptable range for the cumulative risk falls within the range of 1×10^{-4} to 1×10^{-6} [US EPA, 2011]. A total CR that is equivalent to or lower than 10^{-6} denotes a state of regulatory safety, whereas a total CR that equals or exceeds 10^{-4} indicates a potentially noteworthy risk [US EPA, 2011].

6.3 Results and Discussion

6.3.1 Meteorological Condition

In most cities in Indonesia including Surabaya, the climate is characterized by high humidity and high temperature in the entire year (Figure 6. 2). It is important to understand that Indonesia is a tropical country, thus having only two seasons, with a division of 4–5 months of dry season, 4–5 months of rainy season, and the remaining period as a transitional or interseason phase. The dry season (April – August) and wet season (November – March). However, the timing of these two seasons has become uncertain lately due to the changing global climate conditions. During the dry season, the relative humidity decreases and becomes lower than that of the wet season. In the wet season, rainfall and wind speed become stronger, leading to an increase in relative humidity. The rainy season in Indonesia is also characterized by more frequent rainfall, higher rain intensity, and greater precipitation compared to the dry season. The average temperature during the sampling period was 27.9°C, while the average relative humidity was 80.9%. Winds primarily originated from the east and west directions, with an average wind speed of 2.84 m/s.

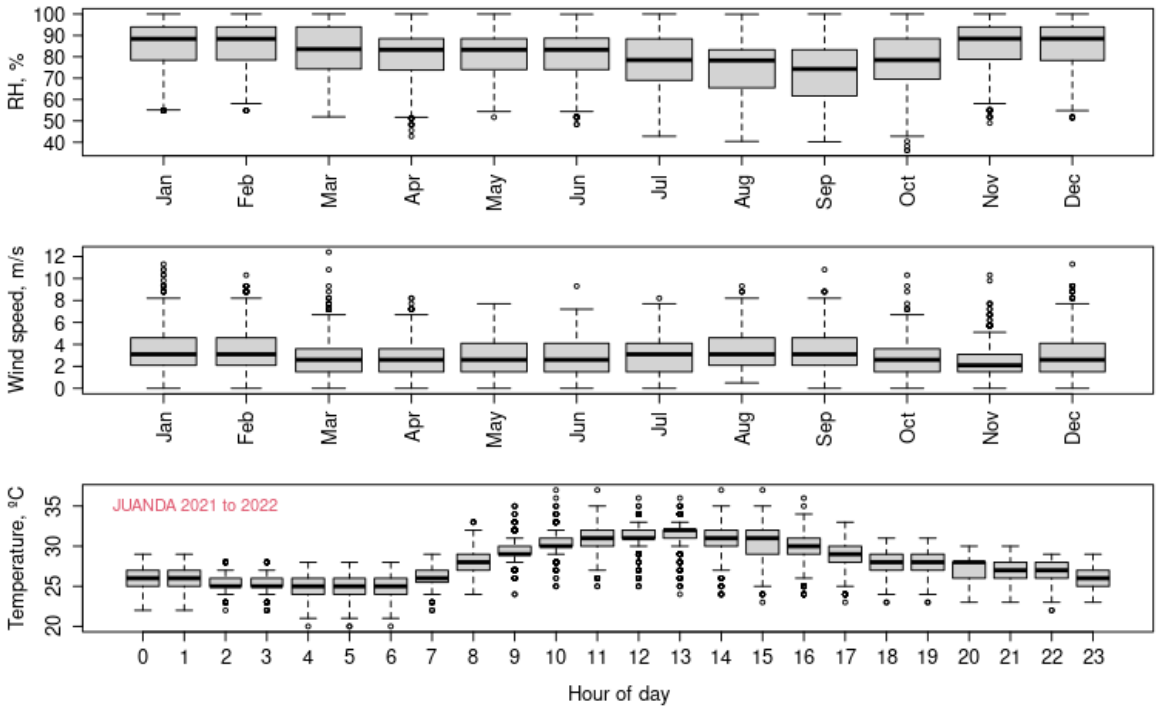

Figure 6. 2 The temperature, wind speed and humidity during the study period in Surabaya

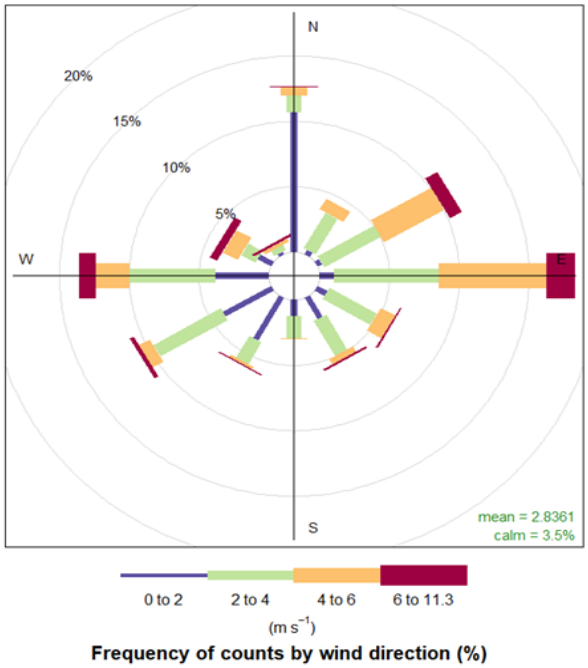

Figure 6. 3 The wind rose during 2021–2022 at Surabaya

6.3.2 Mass and black carbon concentrations

The summary of mass of $PM_{2.5}$, $PM_{2.5-10}$ and PM_{10} concentrations in sampling site Surabaya is resumed in Table 6. 1. The focus of this study is on $PM_{2.5}$; nevertheless, the

research also includes data on $PM_{2.5-10}$ and PM_{10} to offer a comprehensive understanding of the air quality at the sites, considering the varying composition of PM particles of different sizes.

Table 6. 1 Summary of mass and black carbon concentrations of PM in Surabaya and comparison with other sites

Year	n	$PM_{2.5}$	$PM_{2.5-10}$	PM_{10}	%$PM_{2.5}$ in PM_{10}	BC	%BC in $PM_{2.5}$
2021	41	14.8	24.0	38.8	39.1%	4.1	28.8%
2022	45	12.8	19.3	32.1	41.2%	3.5	25.4%

The annual average concentration of $PM_{2.5}$ in 2021 and 2022 were 14.8 and 12.8 $\mu g/m^3$, respectively, indicating compliance with the Indonesian standard for annual average $PM_{2.5}$ levels (15 $\mu g/m^3$). The $PM_{2.5}$ concentration from 2020–2021 ranged from 3.29 to 27.05 μg/m3 with an annual average value of 13.63 ± 4.54 $\mu g/m^3$. However, despite meeting the Indonesian standards, the annual average $PM_{2.5}$ concentration at this site exceeded the World Health Organization (WHO) annual standard of 5 $\mu g/m^3$. Additionally, approximately 28% of the daily $PM_{2.5}$ concentrations exceeded the WHO's 24-hour standard of 15 $\mu g/m^3$ [WHO 2021] as can be seen in Figure 6. 4. It is worth noted that the average during this period is lower than in previous years, which ranged from 15–17 $\mu g/m^3$ [Santoso et al. 2020b]. This decrease in $PM_{2.5}$ levels can be partially attributed to the COVID-19 pandemic and the resulting reduction in human activities and industrial operations. A similar trend was observed in Jakarta, where a significant decrease of approximately 40% in $PM_{2.5}$ levels was observed due to the impact of COVID-19 [Santoso et al. 2021]. The average ratio of $PM_{2.5}$ to PM_{10} during the study period was 40.2 ± 8.6%, this ratio was similar to other studies in Asia [Hopke et al., 2008; Begum and Hopke, 2019; Wimolwattanapun et al., 2011; Rahman et al., 2015; Pabroa et al., 2022; Santoso, Lestiani, Damastuti, et al., 2020] which suggesting similar characteristic of PM_{10}, a tendency for higher concentration in $PM_{2.5–10}$ coarse fraction than the $PM_{2.5}$ fine fraction. It worth noted that Hopke et al. (1997) demonstrated that the GENT sampler tends to underestimate $PM_{2.5}$ levels as its 50% collection point is closer to 2.2 μm instead of the intended 2.5 μm (Hopke et al., 1997).

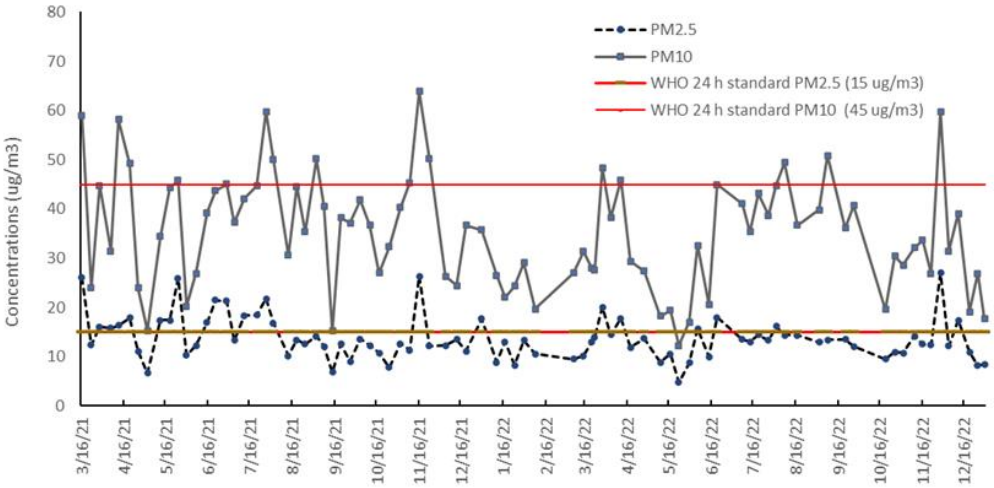

Figure 6. 4 Time variation of $PM_{2.5}$ and PM_{10} in Surabaya 2021–2022.

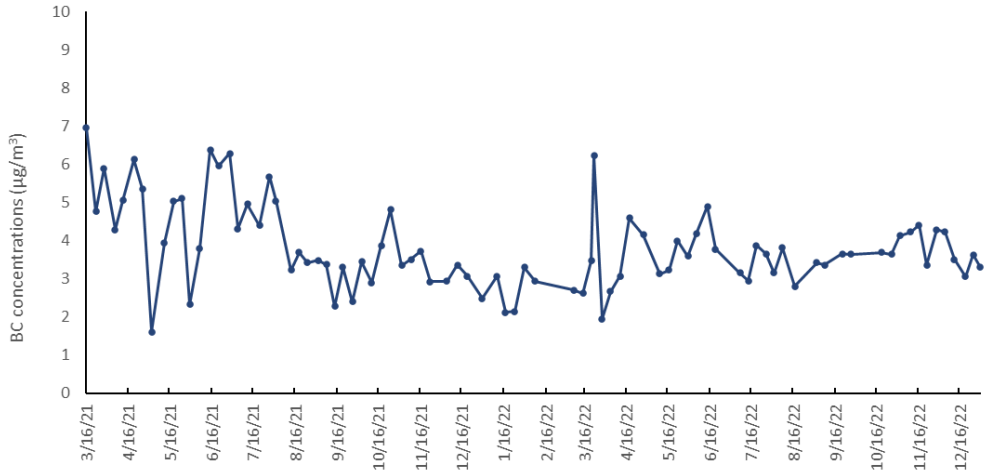

Figure 6. 5 Black carbon concentrations in Surabaya 2021-2022

Figure 6. 5 represents the time series of black carbon concentration during the study period. The annual average concentrations of BC in 2021 and 2022 were 4.1 and 3.5 µg/m^3, respectively. These levels were found to be similar to those reported in other Asian countries such as Kuala Lumpur, Malaysia [Rahman et al., 2015]; Pathum Thani, Thailand [Wimolwattanapun et al., 2011]; Ulaanbaatar, Mongolia [Davy et al., 2011; Gunchin et al., 2019]; and Mumbai, India [Salako et al., 2012]. When compared with other cities in Indonesia, Surabaya's black carbon is similar to that of Jakarta (3.54±1.27 µg/m^3) and Bandung (3.5 µg/m^3), but higher than in other cities in Java, such as Semarang (3.1 µg/m^3), Tangerang (2.5 µg/m^3) and Yogyakarta (2.4 µg/m^3) [Santoso et al., 2020b, 2020a]. It

suggests that Surabaya might have similar sources of black carbon emissions with these major urban areas Jakarta and Bandung. This could indicate the potential factors related to the economic and urban development, such as industrial activities, transportation, and population density. Black carbon is commonly emitted through high-temperature combustion, as observed in biomass burning and diesel engines. In the industrial site of Tangerang, a study conducted by Santoso (2011) reported that the source of BC was identified as a combination of biomass burning, diesel vehicle emissions, and road dust [Santoso et al., 2011]. Nevertheless, it is generally believed that BC emissions in Surabaya are predominantly contributed by vehicles emission and biomass combustion [Santoso et al., 2020b]. In this study, black carbon was identified as a major component of $PM_{2.5}$, comprising approximately 27% of the fine particle mass. The $PM_{2.5}$ and BC pollution roses have similar pattern and shown in Figure 6. 6. The plots show that the highest wind direction probabilities for high pollutant concentrations were from the west. The $PM_{2.5}$ and BC had frequencies of about 18% from west direction, 13% from north and east, and 11% from southwest and northeast, where there are several industries spreading from those directions.

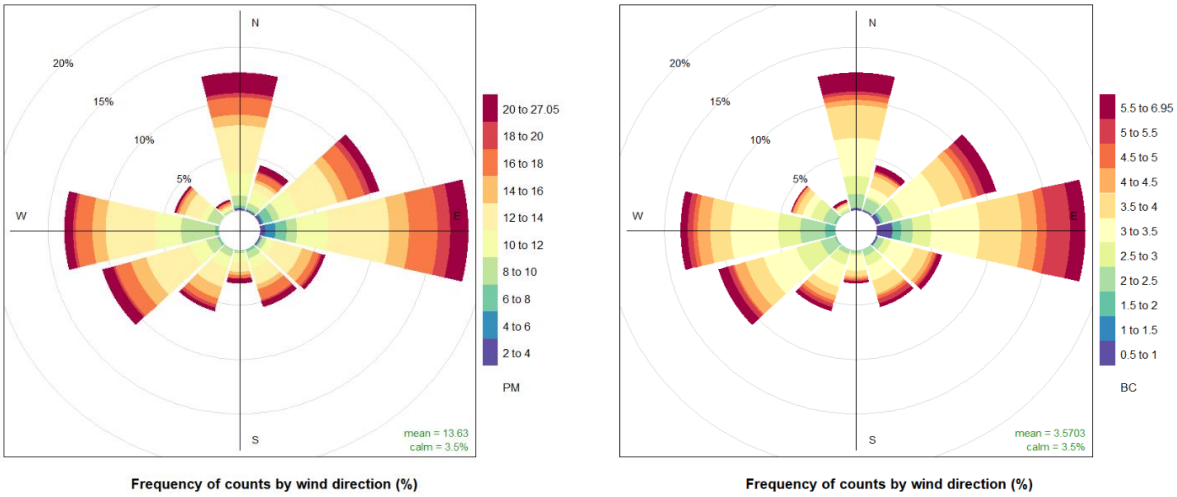

Figure 6. 6 Pollution wind roses of $PM_{2.5}$ and black carbon

Multiple peaks of $PM_{2.5}$ and black carbon were observed in March, June and October (Figure 6. 4 and Figure 6. 5). Additionally, the average monthly $PM_{2.5}$ and BC concentration reached its highest point in June, which corresponds to the peak period of the dry season. The daily concentration trends revealed that the highest $PM_{2.5}$ and black carbon concentrations occurred on Tuesdays and Wednesdays (Figure 6. 7). This pattern seems to be linked to increased mobility on these days, as human behaviour and activities contribute a significant influence on air pollution levels. Based on the Google Mobility Report 2021 in

East Java (https://www.google.com/covid19/mobility/?hl=id), mobility to retail and recreational areas, grocery stores, transit stations, and workplaces was notably elevated on Wednesdays, followed by Monday and Tuesday (Figure A. 1). The observed higher mobility on those three days contribute to increased traffic, primarily due to factors such as work commutes and shopping, resulting in elevated vehicular emissions. These emissions lead to elevated levels of black carbon and particulate matter on Tuesday and Wednesday. Despite a decrease in $PM_{2.5}$ concentrations due to the COVID-19 pandemic, the levels still exceeded the WHO standard. The $PM_{2.5}$ levels observed suggest there are likely to have potential health effects for the population [WHO, 2021], and it is essential to identify the sources of $PM_{2.5}$ and determine their relative contributions to strengthen emission control policies and implement measures aimed at reducing multiple pollutants effectively.

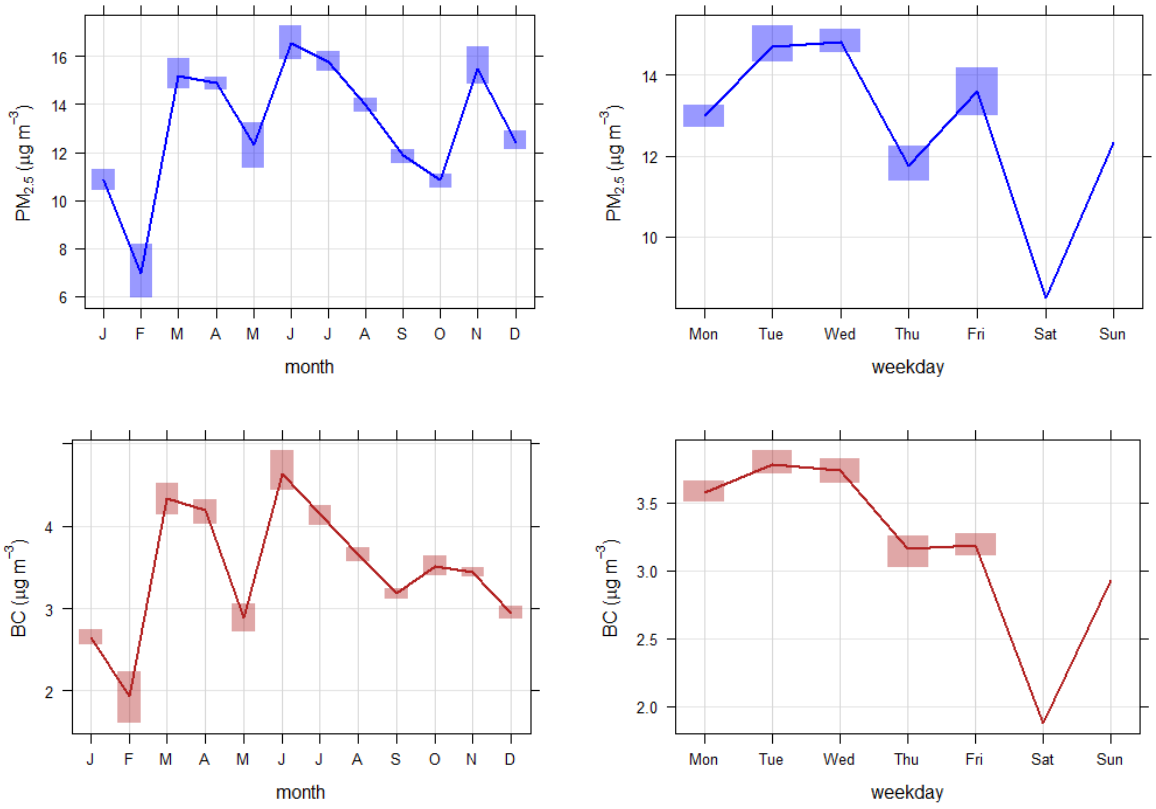

Figure 6. 7 Monthly and weekday averages of $PM_{2.5}$ and BC concentrations

6.3.3 Chemical composition

The elemental concentrations that will be used for source apportionment are summarised in Table 6. 2. which includes information on average values, standard deviations, as well as the minimum and maximum concentrations. The elemental distribution is illustrated in the whisker plot in Figure 6. 8. The whisker plot provides a visual

representation of the data, illustrating the 25th and 75th percentile values, identifying outliers, displaying the median (represented by a solid black line in the middle of the box), and showing the mean (depicted by + mark). Additionally, error bars are included to represent the 5th and 95th percentile values.

Table 6. 2 The elemental concentrations of $PM_{2.5}$ in Surabaya 2021-2022 in ng/m^3

	Mean	Stdev	Min	Max
Na	317.3	276.9	84.0	2311.6
Mg	41.8	45.6	7.8	344.9
Al	134.6	96.7	13.4	457.3
Si	293.0	210.2	28.5	1159.6
P	14.3	10.7	1.0	48.9
S	590.6	383.9	143.6	3527.4
Cl	109.5	144.8	29.6	1300.0
K	266.2	157.1	53.8	1013.4
Ca	117.8	52.5	41.0	328.7
Ti	8.7	5.7	1.2	37.7
V	1.3	1.0	0.3	4.6
Cr	4.7	3.4	0.2	20.3
Mn	9.0	10.0	1.4	87.3
Fe	117.9	52.9	23.1	287.0
Co	2.9	1.8	0.4	7.6
Ni	2.4	1.5	0.5	7.5
Cu	5.4	3.4	0.8	20.7
Zn	264.6	243.3	12.6	1855.7
As	12.3	8.6	3.7	44.6
Pb	100.3	92.7	8.0	367.3

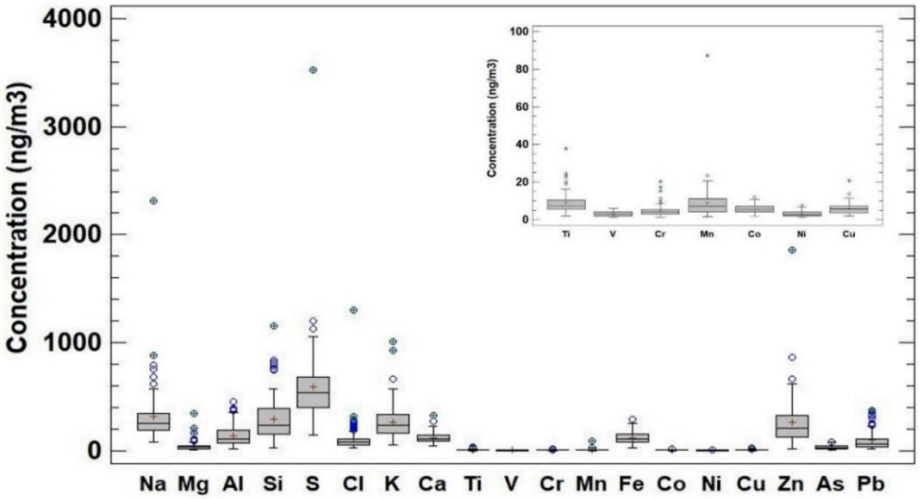

Figure 6. 8 Whisker plot of elemental concentrations of $PM_{2.5}$ in Surabaya 2021-2022.

Figure 6. 8 shows that the highest concentration of elements was found to be S, followed by Si, K, Zn, Fe, and Pb. Sulfur was the highest concentration, averaging 590.6 ng/m^3 with a maximum value of 3527 ng/m^3. The existence of sulfur in particulate matter is primarily attributed to the atmospheric transformation of SO_2 into sulfate particles through homogenous mechanism [Hopke et al. 2008]. The utilization of high-sulfur content fuel in diesel vehicles might potentially add to these concentration levels [Davy et al. 2011b; Santoso et al. 2020b]. However, it is worth noting that starting from 2021, the Indonesian government has implemented measures to reduce the sulfur content in diesel fuel to 500 ppm, which is lower than the previous level of 2500 ppm [Ministry of Energy And Mineral 2013]. Regulation SK 978/2013 introduced increasingly stringent sulfur limits for diesel fuel type cetane number CN48, with targets set at 3,000 ppm by 2016, 2,500 ppm by 2017, 500 ppm by 2021, and further reducing to 50 ppm by 2025 [Ministry of Energy And Mineral 2013; Xie and Harjono 2020]. The high sulfur content observed during the study period from 2021 to 2022 was likely also associated with other various sources, including coal-fired power plants, refineries, and industrial activities [Cohen et al. 2010]. Since the 2000s, in Indonesia coal has outstripped natural gas as the dominant technology in the power sector, with an increasing number of coal power plants. Indonesia is currently ranked fifth among global leaders in terms of future coal-fired capacity development, with 35 Gigawatts (GW) of coal-fired capacity in the pre-construction or construction phase [Ordonez et al. 2021].

The high concentration of K could be attributed to several possible sources. Some potential sources of elevated K concentrations in $PM_{2.5}$ was likely from biomass burning, such as the combustion of wood, crop residues, or other organic materials [Begum and

Hopke 2019; Almeida et al. 2020; Vuong et al. 2023]. Additionally, K can also originate from industrial emissions, such as those produced by certain manufacturing processes or power plants. It is also worth considering the contribution of natural sources, such as dust or soil particles that contain potassium compounds [Chow et al. 2015]. To determine the exact cause of the high K concentration, further investigation and analysis would be required, including examining specific emission sources and conducting source apportionment studies. $PM_{2.5}$ compositions exhibited elevated levels of crustal elements, including Al, Si, Ca, Ti, and Fe. It is noteworthy that the key elements Al and Si consistently showed strong correlation coefficients ($r > 0.97$), indicating their natural origin from soil and crustal dust as pollutant sources. Moreover, high concentrations of Pb, Fe, and Zn were also observed. Due to the high levels of Fe, Zn, and Pb in $PM_{2.5}$ concentrations, a comparison was conducted between the concentrations of Fe, Zn, and Pb and those reported in previous studies conducted in industrial sites in Indonesia, as well as in other sites around the world. The comparison of these elements in Surabaya with those in other Indonesian and Asian countries is summarized in Table 6. 3

Table 6. 3 Fe, Zn and Pb concentrations in $PM_{2.5}$ from Surabaya and several sites in Indonesia and other countries in the world in ng/m^3

Sampling sites	Description	Fe	Zn	Pb	Ref
Surabaya, East Java	Industrial area	117.9	264.6	100.3	This study
Lamongan, East Java	Industrial area	29.8	27.9	457.7	[Lestiani et al. 2023b]
Tangerang, Industry 1, Banten	Industrial area	155-528*	44-129*	670.0	[Santoso et al. 2011]
Tangerang, Industry 2, Banten	Industrial area	92-509*	20-386*	170.0	[Santoso et al. 2011]
Jakarta	Metropolitan	117.5	125.7	49.6	[Santoso et al. 2020a]
Other countries in Asia					
Dhaka, Bangladesh	Urban area	260	463	131	[Rahman et al. 2021]
Kuala Lumpur, Malaysia	Urban area	140	47	24	[Rahman et al. 2015]
Gwangju, Korea	Urban area	250	67	31	[Yu and Park 2021]
Ulsan, Korea	Industrial area	153	46	17	[Park et al. 2008]
Kitakyushu, Japan	Urban area	140	30	11	[Zhang et al. 2021]
Delhi, India	Urban area	780	380	300	[Jain et al. 2020]
Valenzuela, Philippines	Industrial area		93	40	[Pabroa et al. 2022]
Karachi, Pakistan	Urban area	3175	1117	529	[Mansha et al. 2012]
Damascus, Syria	Urban area	580	470	150	[Ahmad et al. 2020]
Baoshan, China	Industrial area	1187	681	149	[Chen et al. 2008]
Nanjing, China	Megacity	577	199	51	[Yang et al. 2019]
Beijing, China	Industrial area	1910	630	200	[Sun et al. 2004]
Taiwan	Industrial area	171	103	23	[Hsu et al. 2016]
Segzi Isfahan, Iran	Industrial area	-	-	62	[Soleimani et al. 2018]

Note: * range concentrations

Table 6. 3 presents the results of this comparison, revealing that the average lead concentration in Surabaya at 100.3 ng/m³, is lower compared to the levels observed in industrial Tangerang site 1, site 2 and Lamongan East Java, where the respective average values were 170, 670 and 457.7 µg/m³ [Santoso et al. 2011]. However, the daily concentration of highest value of Pb in Surabaya (357.7 ng/m^3) has exceeded the US EPA standard on 150 ng/m^3 [Hopke et al. 2008]. Additionally, the contribution of lead to $PM_{2.5}$ in Surabaya was on average of 0.7%. Despite the research study being conducted during the pandemic period, the observed values of Pb in Surabaya were found to be significantly higher than those in other cities in Java, such as Jakarta, Bandung, Semarang, and Yogyakarta [Santoso et al. 2020b]. Compared to other countries in Asia, Surabaya's lead levels surpass those of Asian counterparts, such as Malaysia, Korea, Japan, Taiwan and Iran. This discrepancy between Surabaya and cities of similar urbanization levels within Asia highlights a concerning environmental issue. The highest of Pb level were found in industrial area in Karachi, Damascus, Delhi, Baoshan and Beijing. Similar trends for Fe and Zn were also appeared higher in these cities.

Comparing the values of Fe concentrations to other cities in Indonesia, Surabaya's Fe appears to be relatively moderate. It has a similar level to Jakarta and Tangerang, but ishigher than Lamongan. While for Zn with maximum level of 1855 ng/m^3, compared with other industrial cities in Indonesia, it's evident that Zn levels in Surabaya fall within a high range, with potential variations in comparison to different industrial zones. Further research and analysis are required to understand the specific factors contributing to this source of Zn in Surabaya.

6.3.4 Reconstructed Mass

The relationship between the reconstructed mass and measured masses of $PM_{2.5}$ is depicted in Figure 6. 9. The slope of the graph suggests that the average reconstructed masses accounted for 61% of the measured masses. However, it is important to note that mass closure was relatively low due to the absence of measurements for organic compounds such nitrates and organic carbon. Figure 6. 9 presents the distribution of reconstructed mass components in the calculated RCM values for $PM_{2.5}$. The average RCM for $PM_{2.5}$ was found to be 64.7 ± 11.4%, indicating that the mass reconstruction only accounted for approximately 65% of the total $PM_{2.5}$ mass. The composition of average $PM_{2.5}$ mass in Surabaya comprised

27% black carbon, 18% sulfate, 12% soil, 3% sea-salt, 1% smoke, and 3% trace elements. The missing mass (35%) was assumed mainly consist of nitrates and organic matter. According to another study [Cohen et al. 2010], organic matter contributes approximately 28% of the mass, whereas nitrates contribute within the range of 5-15% of the mass. Black carbon and sulfate were found to be the dominant contributors to the fine particulate RCM, together accounting for a total of 45%.

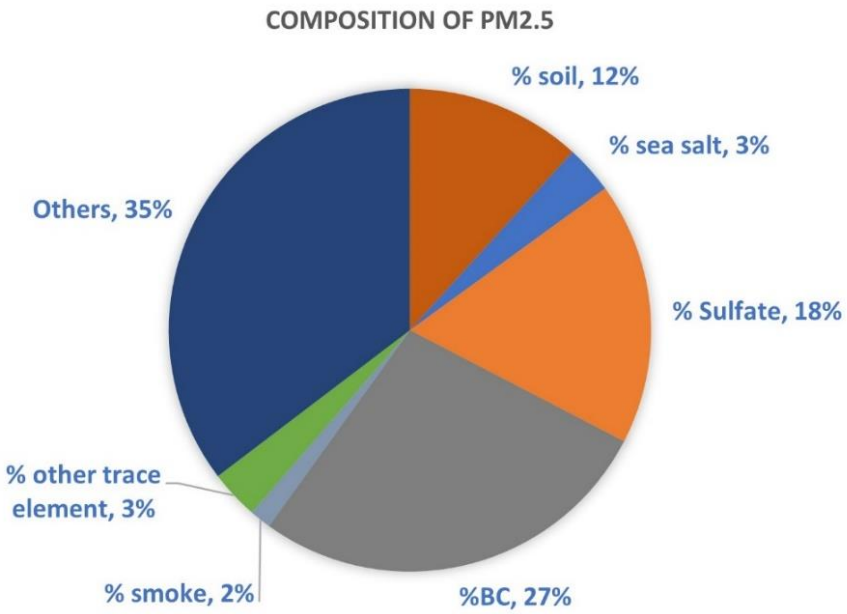

Figure 6. 9 Distribution of component from RCM calculation of $PM_{2.5}$ in Surabaya 2021-2022

This preliminary analysis of RCM offers valuable insights into potential sources of $PM_{2.5}$ in Surabaya, as well as an evaluation of the dataset reconstructed from the measured element composition. The RCM estimates over 50% which shows that the data is sufficient and reasonable to do source apportionment.

6.3.5 Source profile

To enhance the accuracy of source identification and apportionment, this study employed Positive Matrix Factorization (PMF) and to identify the potential source directions, Conditional Bivariate Probability function (CBPF) was employed. The distribution of each sources identified is shown in Figure 6. 12. In this study, PMF analysis revealed eight factors associated with the galvanizing industry, ammonium chloride, secondary sulfate, biomass burning, soil, steel industry, traffic emissions, and lead smelting sources, as presented in Figure 6. 10.

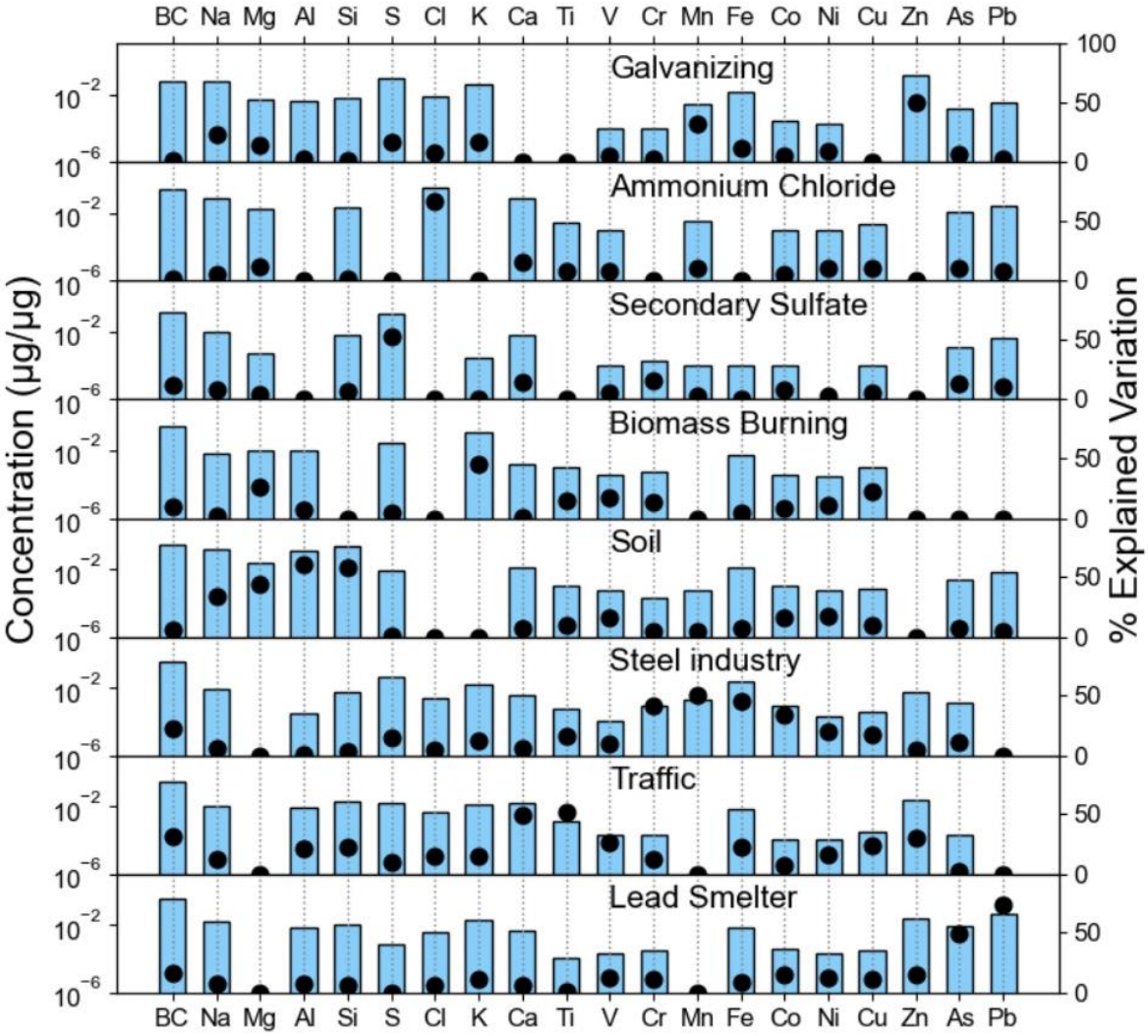

Figure 6. 10 Source profiles of PMF for $PM_{2.5}$ at Surabaya from 2021-2022.

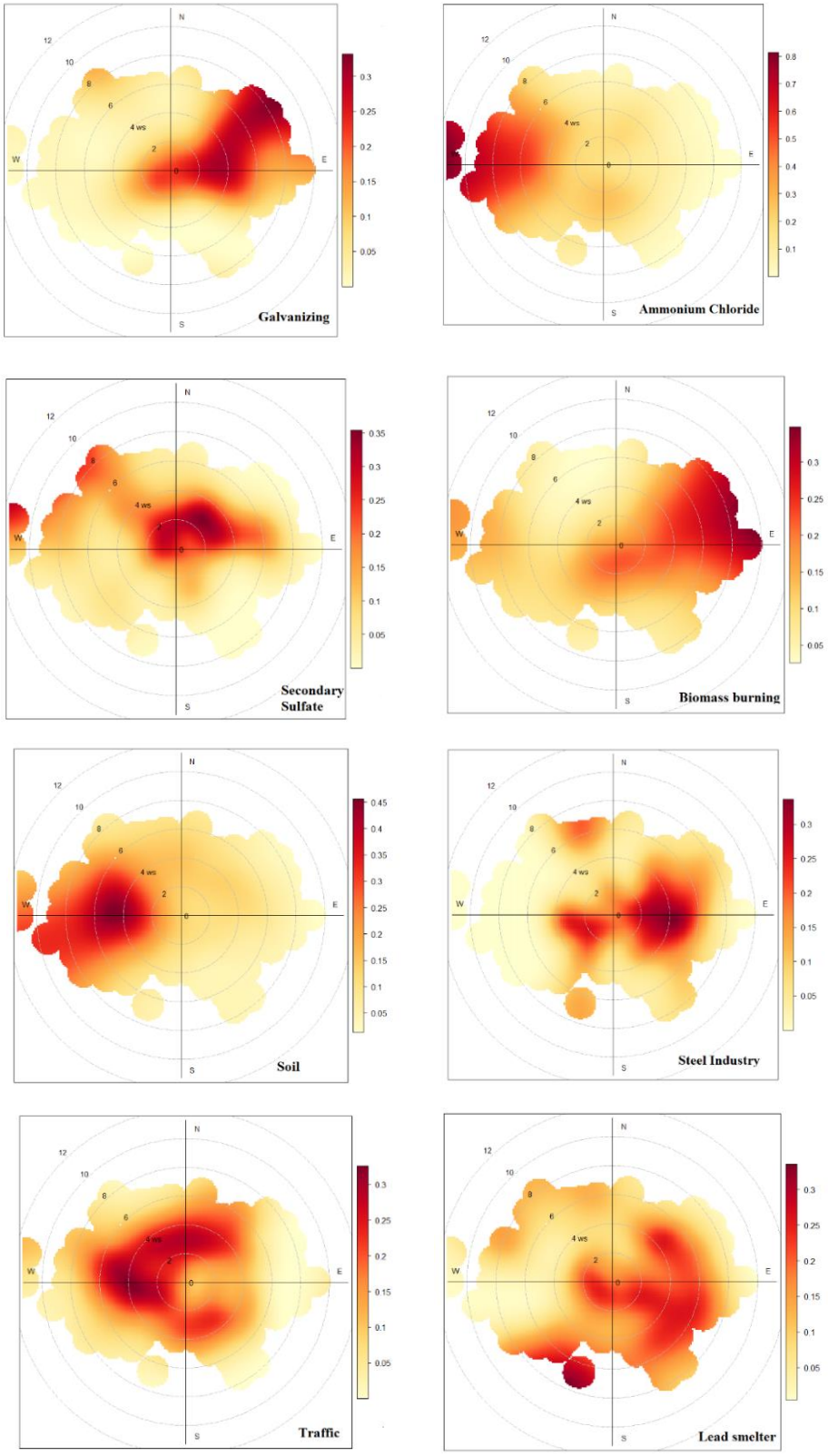

Figure 6. 11 The plot of CBPF for each profile of pollutant sources in Surabaya 2021-2022

The first factor shows elevated Zn concentrations and demonstrates characteristics consistent with a Zn-related source, accounting for 7.8% of fine particulate mass (Figure 6. 12). Zinc could be released from municipal solid waste, galvanizing, and two-stroke emissions [Hopke et al. 2008]. The galvanizing industry is a known source of zinc (Zn) emissions. Galvanizing involves the process of coating steel or iron products with a layer of zinc to protect them from corrosion. There is a large galvanizing industry that provides hot-dip galvanizing services, which involve immersing the metal in a bath of molten zinc, potentially releasing zinc vapor. The galvanizing industry might contribute to the fine particle Zn in the study area, supported by the CBPF plot (Figure 6. 11), which shows high probability sources originating from the northeast side where the galvanizing industry is located (Figure 6. 1).

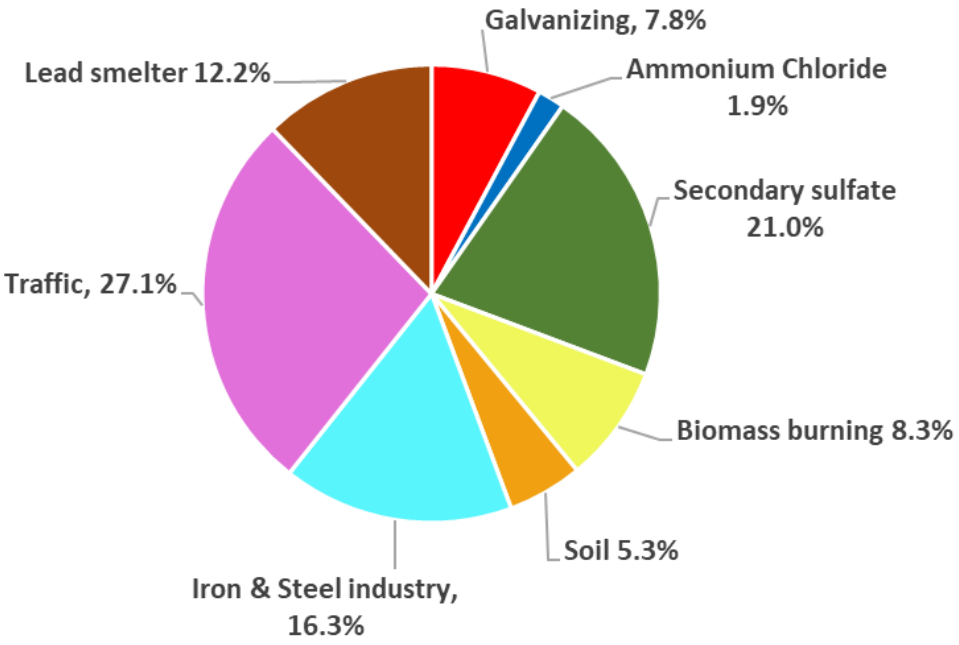

Figure 6. 12 Distribution of the source identified for $PM_{2.5}$ in Surabaya

The second factor contains high levels of Cl. This factor contributes small portion of 1.9%. This factor is mainly affected by the west wind direction, which show the probability of sources of Cl from industrial that emits Cl such as fertilizer industry or plastic industry. This Cl in this profile, does not have correlation with Na, which eliminates the possibility of seasalt sources, and the direction is come from west side not east side or south direction which the seasalt windblown from the ocean could occurred. In the west side, there is a cluster of domestic tofu industries that use plastic fuel for cooking the tofu [Paddock 2019; Aryani et al. 2021]. The emission from the waste plastic burning could release the chlorine

into the air [Yuan et al. 2014; Verma et al. 2016], and it can potentially react with the ammonium form ammonium chloride [Gunthe et al. 2021].

The third factor was dominated by high S, moderate BC and the comparatively lower levels of certain other elements (such as As, Pb, Si, V, Cr, Ca) within the identified factor, as being representative of secondary sulfates [Wimolwattanapun et al. 2011]. Secondary sulfate was recognized through the predominant presence of S concentrations. Secondary aerosols, like sulfates, are difficult in accurately tracing their origins as they resulted from the atmospheric reactions of emitted pollutants [Pabroa et al. 2022]. This factor likely received contributions from industrial or coal-fired power plants, as well as diesel vehicles that burned high S fuel [Wimolwattanapun et al. 2011]. A high CBPF area may refer places where secondary particle formation is intensified. This factor contributes to 21% of $PM_{2.5}$ and is primarily influenced by the wind from the northern and northwest directions.

The fourth factor exhibited a high loading of potassium (K) and moderate levels of black carbon (BC). The presence of potassium and BC serves as indicative markers for biomass burning emissions, which are known to produce elevated concentrations of carbonaceous particles [Han et al., 2023; Park et al., 2022; Santoso et al., 2008]. In Indonesia, open dumping, the burning of waste materials (such as wood, paper, cardboard, and biomaterial, including vegetation), and the practice of burning agricultural residue after rice harvest remain common practices. These activities result in substantial emissions as biomass burning. This biomass burning contributes to 8.3% of $PM_{2.5}$ levels in Surabaya, which is lower than Bandung (20%) and Lembang (40%) [Santoso et al., 2008; Santoso et al., 2013]. The similar typical habits of open burning in Malaysia, found that biomass burning contributed 9.3% of fine particulate in Kuala Lumpur, Malaysia [Rahman et al. 2015]. While in Hanoi, Vietnam based on long-term measurements (2001–2008) showed that biomass burning constituted 13%, while automobiles and various transport modes contributed 40%, industry accounted for 19%, and coal combustion 17% [Cohen et al. 2010]. The dominant source direction of biomass burning in Surabaya was influenced primarily by the east and southeast sides, as shown in Figure 6. 11. In these areas, a zoo is located to the south, and slums are found to the south and west, generating a significant amount of tree branches and domestic waste. Consequently, biomass burning from these areas might have contributed significantly to the overall emissions.

The fifth factor exhibits a high loading of crustal elements, including Al, Si, and Mg, and moderate loadings of Ca and Ti. These elements are typically associated with soil. The

soil-related factors account for approximately 60% of Al, 57% of Si, 44% of Mg in this profile. Although the concentration of Fe in this profile is not notably high, it is worth noting that steel industry sources, as discussed earlier, are known to contribute significant amounts of Fe to the environment. These crustal elements are frequently employed as tracers for identifying the soil source in many studies [Chan et al. 1997; Begum and Hopke 2019; Almeida et al. 2020]. The contribution of soil to $PM_{2.5}$ was 5.3%. However, the soil profiles contain an abundance of Co, Cr, V, and Ni, indicating the presence of deposited anthropogenic emissions, such as those from traffic and industry, or fugitive emissions. Similar soil profiles were also found in Dushanbe, Tajikistan, and Krakow, Poland [Almeida et al. 2020]. This soil source is found to be influenced by the western wind, which originates from agricultural areas around the sampling site and the nearby road.

The sixth factor comprises high loadings of Fe, Cr, Co, Cu, Mn, and Ni, which are indicative of industrial emissions primarily originating from ferrous metal sources [Hopke 1999; Mansha et al. 2012]. High loadings of Cr, Cu, and Mn would be expected to be associated with iron/steel works [Hopke 1999; Taiwo et al. 2014; Suvarapu and Baek 2017], and this is more consistent with a high presence of Fe in this profile. Several large iron/steel works in Surabaya were located around the sampling site in the north, east, and west sides. The possible source for this profile may be industrial emissions from the iron/steel industry. The CBPF plot shows that the steel industry source is mainly influenced by the winds blowing from the northeast, east, and west sides, where the iron/steel industries are distributed in that area. This factor was attributed to 16.3% of the total $PM_{2.5}$.

The seventh factor is traffic emission and has high BC, and signature of the road dust from Al, Si, Ca and Ti. The traffic-related factor represented the largest share of BC, which is a common indicator of vehicle exhaust emissions. However, it also featured significant contributions from elements typically associated with the wear tire of vehicles, such as Cr, Cu, Fe, and Zn [Mukherjee and Agrawal 2017; Silva et al. 2021; Chatoutsidou and Lazaridis 2022]. This profile represents 27.1 % which is the major source that contributes to the $PM_{2.5}$. The CBPF shows the influenced by the west and surrounding direction of the sampling site except from the east direction. The large intercity highway which connects the northern, southern and western parts of the city is located in this direction.

The eighth factor is characterized by a high concentration of Pb and As, along with moderate BC levels. Pb is the predominant element, contributing to 73.7% of this factor. Other heavy metals, such as Fe, Cr, Zn, Ni, and Cu, were found in smaller concentrations.

The source of this factor is lead smelting, which is influenced by the south and southwest directions, as illustrated in Figure 6. 11. The Pb smelter in Lamongan which is in the northwest does not seem to have a significant impact on the high Pb pollution in Surabaya. The Pb sources in Surabaya seem to be more affected by the direction from the north and southwest direction. The illegal recycling of lead-acid batteries through lead smelting activities was identified not only in the Lamongan region (56 km away from the sampling site) [Lestiani et al. 2023b], but also in Sidoarjo, which is situated 13.8 km to the south of the sampling site [Asnawi 2022]. Legal recycling of lead batteries industries was also found in Pasuruan, located 25 km to the southeast of the sampling site [Asnawi 2022]. These industries could be the main sources of the elevated Pb in Surabaya based on the CBPF results.

6.3.6 Health Risk Assessment

Non carcinogenic risk

All parameters used in this calculation are resumed in supplementary in Table A. 2 and Table A. 3. A comprehensive non carcinogenic risk assessment of potentially toxic elements in $PM_{2.5}$ was calculated using Hazard Quotients (HQs) and Hazard Index (HI) for adults and children. Table 6. 4 presents the summarized maximum of ADD, HQ and HI for As, Cr (VI), Cu, Ni, Pb and Zn in both children and adults, and Figure 6. 12 shows the comparison of HQ of each element for both. These results showed that all potentially toxic elements have HQ values below 1, thus there is a minimal possibility of occurrence for noncancerous health risks. Among both adults and children, the highest HQ was observed for As, while the lowest was Co. This reveals that As poses a comparatively greater potential hazard to human health in comparison to the other metals. The hazard levels of each element by their HQ values were As>Pb>Cr>Zn>Cu>Ni>Co. The highest HQ value was associated with As for both adults and children, with the adult value exceeding that of children by more than two times. Despite the HQ value was still below 1, it should be paid more attention to children regarding potential health impacts.

Table 6. 4 Resume of ADD, HQ and HI

Element	ADD (ng/kg.day)		HQ		HI	
	Adults	Children	Adults	Children	Adults	Children
As	9.59	23.23	0.0319	0.0772		
Co	1.63	3.95	8.15×10^{-6}	1.97×10^{-5}		
Cr	0.62	1.51	0.0218	0.0528		
Cu	4.46	10.79	0.0001	0.0003		
Ni	0.11	0.27	5.63×10^{-6}	1.36×10^{-5}		
Pb	78.99	191.23	0.0224	0.0543	0.078	0.188
Zn	399.10	966.24	0.0013	0.0032		

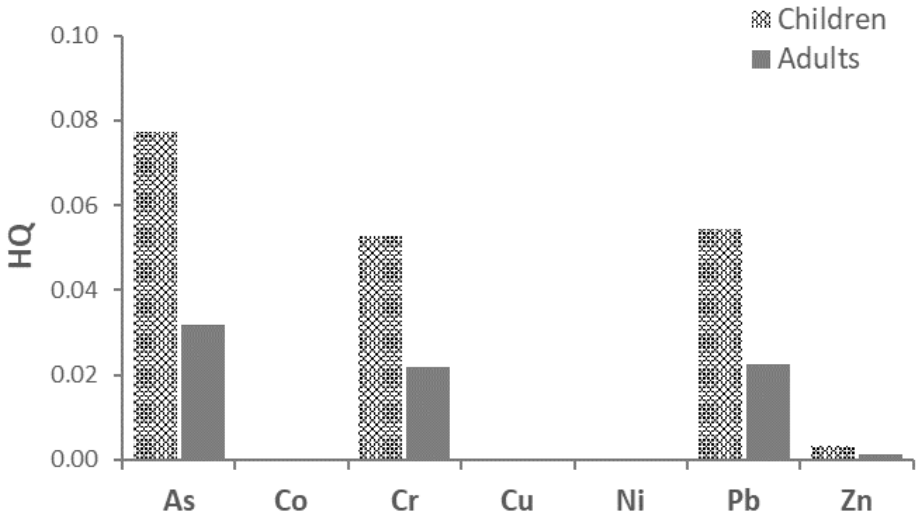

Figure 6. 13 Comparison of HQ for each element for adults and children

Carcinogenic health risk

The health risk associated with carcinogenic contaminants was estimated based on assumption that inhalation is the major exposure pathways following the criteria established by US EPA 2011. A carcinogenic risk was assessed for As, Co, Cr, Ni and Pb representing the carcinogenic elements in $PM_{2.5}$ (Table 6. 5).

Table 6. 5 The summary of LADD and carcinogenic risk (CR)

	LADD (ng/kg/day)		CR	
Element	**Adults**	**Children**	**Adults**	**Children**
As	3.29	1.99	6.31E-05	1.58E-05
Co	0.56	0.34	1.90E-05	4.76E-06
Cr	0.21	0.13	1.14E-05	2.86E-06
Ni	0.04	0.02	4.13E-08	1.03E-08
Pb	27.08	16.39	1.45E-06	3.62E-07
Sum			**9.50E-05**	**2.38E-05**

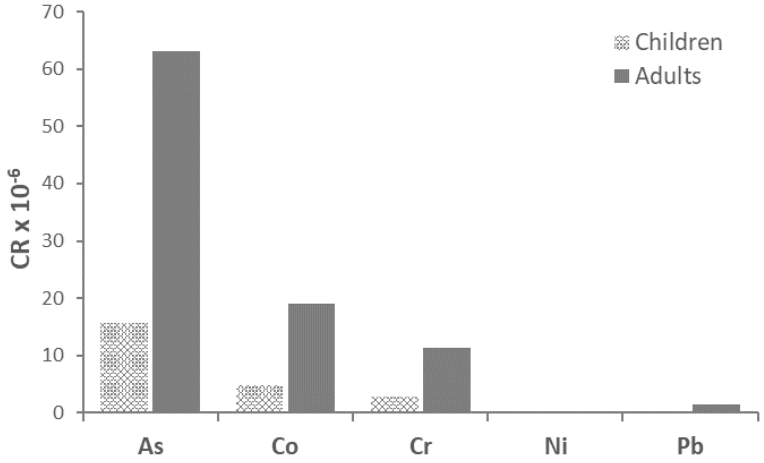

Figure 6. 14 Carcinogenic risk from all potentially toxic elements

From the value of LADD, the results show that Pb was the highest exposure concentrations for both adults and children. While for the estimation for the carcinogenic risk as shown in Figure 6. 13, the CR value for As, Co, Ni and Pb have exceeded the minimal acceptable risk level of one in 1000,000 population (1×10^{-6}). The total CR value for all calculated potentially toxic elements for adults and children were 9.50×10^{-5} and 2.38×10^{-5}, respectively. These values indicated that the number cases of cancer can occur per 100,000 were 10 adults and 3 children in population. Adults was higher than children since the adults get exposure to the pollution in longer time compared to children.

6.4 Conclusions

The study conducted in Surabaya, Indonesia, revealed insights into the city's air quality, as the impact of industrial activities, particulate matter composition over the years 2021-2022 and its health risk assessment. Surabaya experiences a high elevated contamination of several potentially toxic elements in the air. The annual average $PM_{2.5}$ levels complied with Indonesian standards, but they exceeded the stricter WHO guidelines, posing potential health risks. Black carbon which serves as a distinctive marker for incomplete combustion, accounted for 27% of $PM_{2.5}$ composition. A seasonal variation was found that highest $PM_{2.5}$ and BC were observed during the dry season and highest peak in June. Among the elevated elements in $PM_{2.5}$, the highest concentration was observed for S, followed by Si, K, Zn, Fe, and Pb. The PMF revealed eight factors: galvanizing industry, ammonium chloride, secondary sulfate, biomass burning emission, road dust, steel industry, vehicles emissions, and lead smelting. Metal industries such as galvanizing, steel industry and lead smelting were found to be a significant contributor to $PM_{2.5}$ with a total of % 37.3%. Industrial and vehicular sources significantly contribute to the fine particulate pollution. The human health assessment indicated that both adults and children living at the sampling site encountered a carcinogenic risk with total risk 9.50×10^{-5} and 2.38×10^{-5}, respectively. These values indicate 10 and 3 cases of cancer in the adult and child populations per 100,000 individuals, respectively. Carcinogenic risks from As, Co, Ni, and Pb, although below regulatory upper limits (10^{-4}), but already exceeded the lower limit and emphasized the importance of continued monitoring and mitigation efforts to protect public health in Surabaya to avoid greater loss. The results of this study emphasize the significance of managing sources linked to industry and transportation related sources is crucial in decreasing the high $PM_{2.5}$ levels and minimalizing the health impact in the industrial area Surabaya, Indonesia. The results will enhance our comprehension of air quality challenges in Indonesia's industrial regions. Furthermore, these findings will be beneficial in formulating effective strategies for managing air pollution and mitigating the adverse health effects linked to air pollution in industrial areas.

CHAPTER 7 Conclusions and Recommendations

7. 1. Conclusions

Several conclusions and key findings can be drawn from this research. The introductory statement emphasizes the lack of a comprehensive study on air quality and environmental impact assessments of industrial activities in Indonesia. This highlights the need for further research in this area. From the results in Chapter 2 which several research activities conducted in 17 sampling sites in Indonesia, indicating that some cities especially in Java Island the air quality parameter of $PM_{2.5}$ have violated the national standard for annual average of $PM_{2.5}$. The research not only focusing on the compliance with the standard, but more important is the level of heavy metals that pose health impact to human health. Particularly Surabaya and Tangerang, have elevated concentrations of heavy metals such as lead (Pb) in the air, which exceed international air quality standards. Especially in Surabaya not only Pb, but other heavy metals such as Fe and Zn were high. These high levels of Pb, Fe and Zn may be linked to industrial activities in these areas, such as lead battery recycling, smelter and other industries.

Further research in Chapter 3 was carried out to identify the sources of lead by focusing on the vicinity of a lead smelter in Lamongan, East Java, which is suspected to be a significant source of lead pollution in the region. The characterization in airborne particulate matter collected near the lead smelter industry showed high levels of lead in the air. Pb was found as the dominant heavy metal, with an average concentration of 0.46 $\mu g/m^3$, followed by other elements S, K, Fe, and Zn. Pb almost reached the limit of WHO 0.5 $\mu g/m^3$ and exceeded the US EPA standards 0.15 $\mu g/m^3$. Pb is attributed to an average of 2.7% of $PM_{2.5}$. The results from PCA suggested that the lead smelter and metal industry have a major influence on the study area. The health risk assessment was carried out using the hazard quotient (HQ) and cancer risk (CR) for Pb, Cr, and Ni. The HQ value and the CR value of Pb were found to be slightly higher than the permissible acceptable level. The CR value of 1.81×10^{-6} indicates that approximately two cases of cancer per 1000,000 adult population at Lamongan may occur due to Pb contamination. The conclusion drawn from the results is that the lead smelter in Lamongan, East Java, is a significant source of lead pollution in the region. This pollution poses health risks to the local population, with a potential increase in cancer cases that should be mitigated for further action.

To assess the impact of the lead smelter on the surrounding soil, the investigation the characteristics of potentially toxic elements in soils collected from the vicinity of the lead smelter was carried out in Chapter 4. The sampling points encompassed approximately 80.11% of the area dedicated to crops or agricultural land. The study reveals severe Pb contamination within a 1.5 km radius of the smelter, with an average contamination factor (Cf) of 22.0, posing a significant health risk. Soil analysis indicates heavy pollution by As and Pb, and moderate pollution by Cu, Ni, and Zn. PCA results confirm the smelter as the primary source of potentially toxic elements in the soil, accounting for 66.2%. Health risk assessment highlights non-carcinogenic risks from As and Pb exposure, primarily through oral ingestion compared with inhalation and dermal contact, affecting both children and adults. Carcinogenic risks from these elements in the soil exceed acceptable levels for both age groups in the study area. The results in APM and soil in Lamongan showed the significant impact of lead pollution on the surrounding environment and the potential impact on human health. In conclusion, it showed that the lead smelter in Lamongan has caused severe Pb contamination in the surrounding soil, posing significant health risks to both children and adults, with additional heavy pollution by As and moderate pollution by Cu, Ni, and Zn, highlighting the urgent need for environmental remediation and health protection measures.

We continued to conduct separate research focus on Surabaya, the capital city of East Java to assess the impact of the lead smelter in Lamongan to other sites in East Java. We collected $PM_{2.5}$ and $PM_{2.5\text{-}10}$ samples in Surabaya near industrial sites from 2021 to 2022. These samples were characterized using PIXE at Kyoto University. This analysis revealed the presence of various elements in the particulate matter providing essential information about their chemical composition (Chapter 5). Both helium and protons were used in the analysis to obtain optimal results, and 21 elements were detected in the samples. Notably, the use of helium particle-induced X-ray emission was more suitable for Na, Mg, Al, and Si than protons. The combination of He-PIXE and H-PIXE provides significant datasets to be utilized in aerosol studies. Overall, the method validation using SRM showed a good agreement which shows that the PIXE system offers reliable data. A dataset of elemental concentrations by PIXE analysis is obtained for further statistical analysis and receptor modeling to identify the possible pollutant sources. This result makes PIXE is a valuable tool and still encouraging in providing the chemical composition datasets of elements, for

studying the sources and transport of atmospheric particulate matter, as well as its potential health effects.

Based on the PIXE results, it demonstrates strong evidence and reaffirms that Surabaya continues to experience elevated air contamination with potentially toxic elements. The research also suggests that $PM_{2.5}$ concentrations exceed the World Health Organization's annual standards, highlighting the health impact of these pollutants. Utilizing the receptor modeling method Positive Matrix Factorization PMF and Conditional bivariate probability function (CBPF), we identified several sources of $PM_{2.5}$, including industrial activities such as galvanizing as a source of Zn, steel production as a source of Fe, and lead smelting as a source of Pb contamination in the air. These metal industries were found to be a significant contributor to $PM_{2.5}$ and located in the surroundings of the sampling sites. When compared to other cities in Indonesia and global, it also reveals a high degree of contamination occurring in Surabaya. For health risk assessment, the total CR value for all calculated potentially toxic elements As, Co, Cr, Ni and Pb for adults and children were 2.38×10^{-5} and 9.50×10^{-5}, respectively. These values indicated that the number of cancer cases can occur per 1,000,000 were 24 adults and 10 children in the population. Adults were higher than children since the adults get exposure to the pollution in longer time compared to children. The conclusion in this Chapter 6 is that Surabaya is still facing significant air pollution with potentially harmful elements, particularly $PM_{2.5}$, originating from industrial sources. It is worth noting that this pollution surpasses international health standards and poses a notable cancer risk for both adults and children.

Overall, this dissertation concludes that industrial activities, especially those related to lead smelting and metal industries, have a substantial impact on air quality in East Java, Indonesia, leading to elevated levels of potentially toxic elements in the air and soil. The degree of heavy metal pollution has already reached a very concerning level, endangering the health of humans and the surrounding environment. The main sources of this pollution must be controlled in order to prevent the worsening of air and soil environmental conditions. Several actions need to be taken to minimize the impact, and proper measures to harmonize industrial and economic activities should be considered. This research, by utilizing nuclear analytical techniques in greater use in environmental fields, emphasizes the importance of comprehending and addressing these environmental challenges and provides valuable data for the development of air quality policies in the region.

7. 2. Recommendations

Based on the research results that have been carried out, several recommendations can be made:

1. Increased Monitoring and Regulation

Given the findings of elevated heavy metal concentrations in the air, particularly in Surabaya and Tangerang, there is an urgent need for enhanced air quality monitoring and regulatory measures. The Indonesian government should consider implementing stricter controls and regular monitoring of industrial emissions to ensure compliance with national and international air quality standards.

2. Source Identification and Mitigation

It is essential to identify specific pollution sources contributing to the elevated levels of heavy metals, such as lead, iron, and zinc. In the case of Surabaya, further investigation into the lead battery recycling and smelting industries should be conducted to pinpoint the exact sources. Once identified, targeted mitigation strategies should be implemented to reduce emissions and minimize environmental and health impacts.

3. Community Awareness and Health Protection

Local communities residing near industrial areas with elevated heavy metal levels, particularly in Surabaya, should be made aware of potential health risks associated with exposure to these pollutants. Educational campaigns and health protection measures, such as promoting personal protective equipment, should be developed and implemented.

4. Ecological Impact Assessment

Beyond human health concerns, it is crucial to assess the ecological impact of heavy metal contamination in soil and air. Research on potential harm to local ecosystems and wildlife should be initiated to develop conservation and remediation strategies. Some remediation research has been applied to the soil environment that contaminated with Pb, but further collaboration research is needed to ensure and accelerate the results. In soil research, the elemental concentration in topsoil and subsurface soil does not differ significantly. This phenomenon may be unique to Indonesia characteristic and warrants further study to determine its underlying causes. Further research related to soil sampling should be conducted in Surabaya, East Java. This is crucial for evaluating comprehensive

health risk assessments, especially considering that ingestion is the primary pathway for risk assessment.

5. Collaborative Research and International Cooperation

Collaborative research efforts with international partners can provide valuable insights and expertise. Sharing data and research findings with organizations and countries facing similar environmental challenges, especially those in Asia, can lead to effective strategies for mitigating industrial pollution.

6. Policy Development

The research underlines the necessity of comprehensive environmental policies that encompass industrial emissions, air quality standards, and pollution control. These policies should be designed to ensure long-term sustainability and environmental protection.

7. Further Research

Continuous research is vital to monitor the progress of pollution reduction measures and to assess their effectiveness. Future studies should focus on tracking changes in air quality and the environment and reevaluating the health and ecological impacts. Especially for the evaluation of some policies including the industrialization, the improvement of industrial technologies, and the improvement of air quality status. Research focus also needs to be developed towards the analysis of organic compounds due to indications of various other hazardous pollutants, and to obtain more comprehensive results for the characteristics of the pollutants. High resolution of time sampling will provide more significant information.

For health risk assessment, several parameters such as skin absorption etc were based in US EPA (Environmental Protection Agency, USA) values. Using the parameter values from the US EPA may not be appropriate, and it would be more suitable to employ parameters specific to Indonesia. Therefore, future research is warranted to determine the country-specific parameters for Indonesia. In future research, it would be beneficial to investigate EPA parameters, determining which ones are common and which are influenced by local climate and lifestyles. This approach would enhance the characteristics of Indonesia specific health risk assessments.

Other risks associated with food such as vegetables and other sources should also be taken into consideration. Additional research in the field of health risk assessment from food

intake affected by industrial areas has been conducted by other researchers, some of which is yet to be published, a thorough and comprehensive risk assessment is necessary to fully complete the evaluation.

Future research on the determination of Pb, As and Cr chemical form or speciation is essential for a comprehensive understanding of their behavior in the soil. This knowledge is crucial for assessing the bioavailability, mobility, and potential environmental and health impacts of these elements. Additionally, it can provide valuable insights that will contribute to the development of effective environmental management and remediation strategies.

8. Alternative Technologies

Encourage industries, especially those contributing to high heavy metal emissions, to explore and adopt cleaner and more environmentally friendly technologies that reduce pollution at the source.

By implementing these recommendations, we hope that it can work towards improving air quality, protecting the health of its citizens, and preserving its natural environment while continuing its industrial growth. International collaboration and knowledge sharing will be instrumental in addressing the shared challenge of industrial pollution in the region.

REFERENCES

Adventini N, Santoso M, Lestiani DD, et al. 2017. Lead identification in soil surrounding a used lead acid battery smelter area in Banten, Indonesia. J Phys Conf Ser 860:. https://doi.org/10.1088/1742-6596/860/1/012006

Ahmad M, Rihawy MS, Haydr R, et al. 2020. PIXE and statistical analysis of fine airborne particulate matter ($PM_{2.5}$) in Damascus. Nucl Instruments Methods Phys Res Sect B Beam Interact with Mater Atoms 462:75–81. https://doi.org/10.1016/j.nimb.2019.11.003

Akopyan K, Petrosyan V, Grigoryan R, Melkom Melkomian D. 2018. Assessment of residential soil contamination with arsenic and lead in mining and smelting towns of northern Armenia. J Geochemical Explor 184:97–109. https://doi.org/10.1016/j.gexplo.2017.10.010

Alias N, Khan MF, Sairi N., et al. 2020. Characteristics, Emission Sources, and Risk Factors of Heavy Metals in $PM_{2.5}$ from Southern Malaysia. ACS Earth Sp Chem 4:1309–1323. https://doi.org/10.1021/acsearthspacechem.0c00103

Almeida SM, Manousakas M, Diapouli E, et al. 2020. Ambient particulate matter source apportionment using receptor modelling in European and Central Asia urban areas. Environ Pollut 266:. https://doi.org/10.1016/j.envpol.2020.115199

Althuwaynee OF, Pokharel B, Aydda A, et al. 2021. Spatial identification and temporal prediction of air pollution sources using conditional bivariate probability function and time series signature. J Expo Sci Environ Epidemiol 31:709–726. https://doi.org/10.1038/s41370-020-00271-8

AOAC. 2016. Appendix F : Guidelines for Standard Method Performance Requirements. AOAC Off Methods Anal 1–18

AOAC. 2002. AOAC International Guidelines for Single Laboratory Validation (2002).

Aryani MI, Mara A, Caesar D. 2021. Political Economy of Import Waste Regulations in East Java : Implications of Indonesia's Role as Waste Importer Country. 5th Int Semin Res Mon 2020, NST Proc 2021:195–205. https://doi.org/http://dx.doi.org/10.11594/nstp.2021.0930

Asnawi A. 2022. Investigating Illegal Lead-Producing Battery Melting Businesses in Lamongan [2] (In Indonesia). In: Mongabay. https://www.mongabay.co.id/2022/03/04/menyelisik-bisnis-peleburan-aki-ilegal-

penghasil-timbal-di-lamongan-2/

Atanacio A, Cohen D, Begum B, et al. 2016. The APAD and ASFID: Long-term fine and coarse ambient particulate matter and source fingerprint databases for the Asia-Pacific region. Air Qual Clim Chang 50:41

Bacon JR, Dinev NS. 2005. Isotopic characterisation of lead in contaminated soils from the vicinity of a non-ferrous metal smelter near Plovdiv, Bulgaria. Environ Pollut 134:247–255. https://doi.org/10.1016/j.envpol.2004.07.030

BAPPENAS TM of NDP. 2006. National Strategy and Action Plans for Improving Urban Air Quality in 5 Major Cities (In Indonesian)

Bashir A, Suhel S, Azwardi A, et al. 2019. The Causality Between Agriculture, Industry, and Economic Growth: Evidence from Indonesia. Etikonomi 18:155–168. https://doi.org/10.15408/etk.v18i2.9428

Beck L. 2005. Improvement in detection limits by using helium ions for particle-induced x-ray emission. X-Ray Spectrom 34:393–399. https://doi.org/10.1002/xrs.854

Beck L, Bassinot F, Gehlen M, et al. 2002. Detection limit improvement for Mg in marine foraminiferal calcite by using helium induced X-ray emission. Nucl Instruments Methods Phys Res Sect B Beam Interact with Mater Atoms 190:482–487. https://doi.org/10.1016/S0168-583X(01)01264-2

Begum BA, Biswas SK, Markwitz A, Hopke PK. 2010. Identification of sources of fine and coarse particulate matter in Dhaka, Bangladesh. Aerosol Air Qual Res 10:345–353. https://doi.org/10.4209/aaqr.2009.12.0082

Begum BA, Hopke PK. 2019. Identification of sources from chemical characterization of fine particulate matter and assessment of ambient air quality in Dhaka, Bangladesh. Aerosol Air Qual Res 19:118–128. https://doi.org/10.4209/aaqr.2017.12.0604

Behrooz R., Kaskaoutis DG, Grivas G, Mihalopoulos N. 2021. Human health risk assessment for toxic elements in the extreme ambient dust conditions observed in Sistan, Iran. Chemosphere 262:127835. https://doi.org/10.1016/j.chemosphere.2020.127835

Bermudez GMA, Jasan R, Plá R, Pignata ML. 2012. Heavy metals and trace elements in atmospheric fall-out: Their relationship with topsoil and wheat element composition. J Hazard Mater 213–214:447–456. https://doi.org/10.1016/j.jhazmat.2012.02.023

Biswas SK, Tervahattu H, Kupiainen K, Khaliquzzaman M. 2003. Impact of Unleaded Gasoline Introduction on the Concentration of Lead in the Air of Dhaka, Bangladesh.

J Air Waste Manag Assoc 53:1355–1362. https://doi.org/10.1080/10473289.2003.10466299

Bowen H. 1979. Environmental Chemistry of the Elements. Academic Press

BPS Statistics Indonesia. 2013. Indonesia Population Projection 2010-2035

BPS Statistics Indonesia. 2015. Statistic of Lamongan Regency 2015

BPS Statistics Indonesia. 2020. Kependudukan Jawa Timur 2020

Brauer M, Freedman G, Frostad J, et al. 2016. Ambient Air Pollution Exposure Estimation for the Global Burden of Disease 2013. Environ Sci Technol 50:79–88. https://doi.org/10.1021/acs.est.5b03709

Brodjonegoro BPS. 2019. Policies to Support The Development of indonesia's Manufacturing Sector During 2020–2024

Budiyono, Haryanto B, Hamonangan E, Hindratmo B. 2016. Correlation Blood Lead Levels and Inteligence Levels Among Elementary School Students Living At Surrounding Used Battery Smelter in the Regency of Tangerang and Lamongan (in Indonesian). Ecolab 10:41–47

Campbell JL, Boyd NI, Grassi N, et al. 2010. The Guelph PIXE software package IV. Nucl Instruments Methods Phys Res Sect B Beam Interact with Mater Atoms 268:3356–3363. https://doi.org/10.1016/j.nimb.2010.07.012

Cao J, Chow JC, Lee FSC, Watson JG. 2013. Evolution of PM2.5 measurements and standards in the U.S. And future perspectives for China. Aerosol Air Qual Res 13:1197–1211. https://doi.org/10.4209/aaqr.2012.11.0302

Carslaw DC, Ropkins K. 2012. Openair - An r package for air quality data analysis. Environ Model Softw 27–28:52–61. https://doi.org/10.1016/j.envsoft.2011.09.008

Cartwright B, Merry RH, Tiller KG. 1977. Heavy metal contamination of soils around a lead smelter at Port Pirie, South Australia. Soil Res 15:69–81

Chan YC, Simpson RW, McTainsh GH, et al. 1997. Characterisation of chemical species in PM2.5 and PM10 aerosols in Brisbane, Australia. Atmos Environ 31:3773–3785. https://doi.org/10.1016/S1352-2310(97)00213-6

Chatoutsidou SE, Lazaridis M. 2022. Mass concentrations and elemental analysis of $PM_{2.5}$ and PM_{10} in a coastal Mediterranean site: A holistic approach to identify contributing sources and varying factors. Sci Total Environ 838:. https://doi.org/10.1016/j.scitotenv.2022.155980

Chen J, Tan M, Li Y, et al. 2008. Characteristics of trace elements and lead isotope ratios

in $PM_{2.5}$ from four sites in Shanghai. J Hazard Mater 156:36–43. https://doi.org/10.1016/j.jhazmat.2007.11.122

Chiari M, Yubero E, Calzolai G, et al. 2018. Comparison of PIXE and XRF analysis of airborne particulate matter samples collected on Teflon and quartz fibre filters. Nucl Instruments Methods Phys Res Sect B Beam Interact with Mater Atoms 417:128–132. https://doi.org/10.1016/j.nimb.2017.07.031

Chow JC. 1995. Measurement methods to determine compliance with ambient air quality standards for suspended particles. J Air Waste Manag Assoc 45:320–382. https://doi.org/10.1080/10473289.1995.10467369

Chow JC, Lowenthal DH, Chen LWA, et al. 2015. Mass reconstruction methods for $PM_{2.5}$: a review. Air Qual Atmos Heal 8:243–263. https://doi.org/10.1007/s11869-015-0338-3

Cohen DD. 1999. Accelerator Based Ion Beam Techniques for Trace Element Aerosol Analysis. In: Landsberger S, Creatchman M (eds) Elemental Analysis of Airborne Particles. Amsterdam, Netherland, pp 139–196

Cohen DD, Crawford J, Stelcer E, Bac VT. 2010. Characterisation and source apportionment of fine particulate sources at Hanoi from 2001 to 2008. Atmos Environ 44:320–328. https://doi.org/10.1016/j.atmosenv.2009.10.037

Cohen DD, Harrigan M. 1985. K- and L-shell ionization cross sections for protons and helium ions calculated in the ecpssr theory. At Data Nucl Data Tables 33:255–343. https://doi.org/10.1016/0092-640X(85)90004-X

Cohen DD, Taha G, Stelcer E, et al. 2000. The Measurement and Sources of Fine Particle Elemental Carbon at Several Key Sites in NSW over the Past Eight Years . 15th Int Clean Air Conf 485–490

Cohen JE, Amon JJ. 2012. Lead poisoning in china: A health and human rights crisis. Health Hum Rights 14:

Damayanti S, Lestari P. 2020. Receptor Modelling of particulate matter at residential area near industrial region in Indonesia using Positive Matrix Factorization. E3S Web Conf 148:0–5. https://doi.org/10.1051/e3sconf/202014803003

Davy PK, Gunchin G, Markwitz A, et al. 2011a. Air particulate matter pollution in Ulaanbaatar, Mongolia: Determination of composition, source contributions and source locations. Atmos Pollut Res 2:126–137. https://doi.org/10.5094/APR.2011.017

Davy PK, Gunchin G, Markwitz A, et al. 2011b. Air particulate matter pollution in

Ulaanbaatar, Mongolia: Determination of composition, source contributions and source locations. Atmos Pollut Res 2:126–137. https://doi.org/10.5094/APR.2011.017

De Vleeschouwer F, Le Roux G, Shotyk W. 2010. Peat as an archive of atmospheric pollution and environmental change: a case study of lead in Europe. PAGES news 18:20–22. https://doi.org/10.22498/pages.18.1.20

Dimitrijević MD, Nujkić MM, Alagić S, et al. 2016. Heavy metal contamination of topsoil and parts of peach-tree growing at different distances from a smelting complex. Int J Environ Sci Technol 13:615–630. https://doi.org/10.1007/s13762-015-0905-z

Dockery D., Pope A, Xu X, et al. 1993. An Association between Air Pollution and Mortality in Six US cities. N Engl J Med 329:1753–1759

Douay F, Pruvot C, Waterlot C, et al. 2009. Contamination of woody habitat soils around a former lead smelter in the North of France. Sci Total Environ 407:5564–5577. https://doi.org/10.1016/j.scitotenv.2009.06.015

Douay F, Roussel H, Pruvot C, Waterlot C. 2008. Impact of a smelter closedown on metal contents of wheat cultivated in the neighbourhood. Environ Sci Pollut Res 15:162–169. https://doi.org/10.1065/espr2006.12.366

Duruibe JO, Ogwuegbu MOC, Egwurugwu JN. 2007. Heavy metal pollution and human biotoxic effects. Int J Phys Sci 2:112–118. https://doi.org/10.1016/j.proenv.2011.09.146

Dysart MM, Galvis BR, Russell AG, Barker TH. 2014. Environmental particulate (PM2.5) augments stiffness-induced alveolar epithelial cell mechanoactivation of transforming growth factor beta. PLoS One 9:. https://doi.org/10.1371/journal.pone.0106821

Ebong GA, Dan EU, Inam E, Offiong NO. 2018. Journal of King Saud University – Science Total concentration , speciation , source identification and associated health implications of trace metals in Lemna dumpsite soil , Calabar , Nigeria. J King Saud Univ - Sci. https://doi.org/10.1016/j.jksus.2018.01.005

Engel-Di Mauro S. 2021. Atmospheric sources of trace element contamination in cultivated urban areas: A review. J Environ Qual 50:38–48. https://doi.org/10.1002/jeq2.20078

Ettler V. 2015. Soil contamination near non-ferrous metal smelters: A review. Appl Geochemistry 64:56–74. https://doi.org/10.1016/j.apgeochem.2015.09.020

Flocchini RG, Feeney PJ, Sommerville RJ, Cahill TA. 1972. Sensitivity versus target backings for elemental analysis by alpha excited X-ray emission. Nucl Instruments

Methods 100:397–402. https://doi.org/10.1016/0029-554X(72)90813-0

Gallon C, Tessier A, Gobeil C, Carignan R. 2006. Historical perspective of industrial lead emissions to the atmosphere from a Canadian smelter. Environ Sci Technol 40:741–747. https://doi.org/10.1021/es051326g

Galvão ES, Santos JM, Lima AT, et al. 2018. Trends in analytical techniques applied to particulate matter characterization: A critical review of fundaments and applications. Chemosphere 199:546–568. https://doi.org/10.1016/j.chemosphere.2018.02.034

Gao Y, Guo X, Ji H, et al. 2016. Potential threat of heavy metals and PAHs in PM2.5 in different urban functional areas of Beijing. Elsevier B.V.

Gonsior B, Roth M. 1983. Trace Element Analysis by Particle and Photon-Induced X-Ray Emission Spectroscopy. Talanta Rev 30:385–400

Gunchin G, Manousakas M, Osan J, et al. 2019. Three-year long source apportionment study of airborne particles in ulaanbaatar using X-ray fluorescence and positive matrix factorization. Aerosol Air Qual Res 19:1056–1067. https://doi.org/10.4209/aaqr.2018.09.0351

Gunthe SS, Liu P, Panda U, et al. 2021. Enhanced aerosol particle growth sustained by high continental chlorine emission in India. Nat Geosci 14:77–84. https://doi.org/10.1038/s41561-020-00677-x

Han Y, Eun D, Lee G, et al. 2023. Enhancement of PM 2 . 5 source appointment in a large industrial city of Korea by applying the elemental carbon tracer method for positive matrix factorization (PMF) model. Atmos Pollut Res 14:101910. https://doi.org/10.1016/j.apr.2023.101910

Haryanto B. 2018. Climate Change and Urban Air Pollution Health Impacts in Indonesia. Springer Clim 215–239. https://doi.org/10.1007/978-3-319-61346-8_14

Haryanto B. 2016. Lead exposure from battery recycling in Indonesia. Rev Environ Health 31:1–4. https://doi.org/10.1515/reveh-2015-0036

Hasan GMMA, Das AK, Satter MA, Asif M. 2023. Distribution of Cr, Cd, Cu, Pb and Zn in organs of three selected local fish species of Turag river, Bangladesh and impact assessment on human health. Emerg Contam 9:100197. https://doi.org/10.1016/j.emcon.2022.11.002

Henke B, Gullikson E, Davis J. 1993. X-ray Interactions: Photoabsorption, scattering, transmission and reflection E=50-30,000 eV, Z=1-92. At Data Nucl Data Tables 54:. https://doi.org/10.1016/s0961-1290(05)71235-7

Hindratmo B, Rahmani R, Mukhtar R. 2018. Blood Levels of Elementary Students Around Used Battery Smelters in Tangerang and Lamongan Regency. Ecolab 12:93–101

Ho KF, Cao JJ, Lee SC, Chan CK. 2006. Source apportionment of $PM_{2.5}$ in urban area of Hong Kong. J Hazard Mater 138:73–85. https://doi.org/10.1016/j.jhazmat.2006.05.047

Hopke P. 1999. An Introduction to Source Receptor Modeling. In: Landsberger S, Creatchman M (eds) Elemental Analysis of Airborne Particles Vol.1, 1st edn. Gordon and Breach Science Publishers, Amsterdam, Netherland, p 273

Hopke PK. 2015. It is time to drop principal components analysis as a "receptor model." J Atmos Chem 72:127–128. https://doi.org/10.1007/s10874-015-9309-1

Hopke PK, Cohen DD, Begum BA, et al. 2008. Urban air quality in the Asian region. Sci Total Environ 404:103–112. https://doi.org/10.1016/j.scitotenv.2008.05.039

Hopke PK, Xie Y, Raunemaa T, et al. 1997. Characterization of the gent stacked filter unit pm10 sampler. Aerosol Sci Technol 27:726–735. https://doi.org/10.1080/02786829708965507

Horvath H. 1997. Experimental calibration for aerosol light absorption measurements using the integrating plate method - Summary of the data. J Aerosol Sci 28:1149–1161. https://doi.org/10.1016/S0021-8502(97)00007-4

Hsu CY, Chiang HC, Lin SL, et al. 2016. Elemental characterization and source apportionment of PM_{10} and $PM_{2.5}$ in the western coastal area of central Taiwan. Sci Total Environ 541:1139–1150. https://doi.org/10.1016/j.scitotenv.2015.09.122

Hu B, Jia X, Hu J, et al. 2017. Assessment of heavy metal pollution and health risks in the soil-plant-human system in the Yangtze river delta, China. Int J Environ Res Public Health 14:. https://doi.org/10.3390/ijerph14091042

Hu W, Huang B, He Y, Kalkhajeh YK. 2016. Assessment of potential health risk of heavy metals in soils from a rapidly developing region of China. Hum Ecol Risk Assess 22:211–225. https://doi.org/10.1080/10807039.2015.1057102

Hubbell JH, Seltzer SM. 2004. X-Ray Mass Attenuation Coefficients. In: NIST Stand. Ref. Database 126. https://www.nist.gov/pml/x-ray-mass-attenuation-coefficients

Humairoh GP, Syafei AD, Santoso M, et al. 2020. Identification of trace element in ambient air case study: Industrial estate in Waru, Sidoarjo, East Java. Aerosol Air Qual Res 20:1910–1921. https://doi.org/10.4209/aaqr.2019.11.0590

International Atomic Energy Agency. 2004. Ion beam techniques for the analysis of light

elements in thin films, including depth profiling : final report of a co-ordinated research project 2000-2003. 126

Ishii K. 2019. Pixe and its applications to elemental analysis. Quantum Beam Sci 3:. https://doi.org/10.3390/qubs3020012

Ivošević T, Mandić L, Orlić I, et al. 2014. Comparison between XRF and IBA techniques in analysis of fine aerosols collected in Rijeka, Croatia. Nucl Instruments Methods Phys Res Sect B Beam Interact with Mater Atoms 337:83–89. https://doi.org/10.1016/j.nimb.2014.07.020

Ivošević T, Stelcer E, Orlić I, et al. 2016. Characterization and source apportionment of fine particulate sources at Rijeka, Croatia from 2013 to 2015. Nucl Instruments Methods Phys Res Sect B Beam Interact with Mater Atoms 371:376–380. https://doi.org/10.1016/j.nimb.2015.10.023

Jain S, Sharma SK, Vijayan N, Mandal TK. 2020. Seasonal characteristics of aerosols ($PM_{2.5}$ and PM_{10}) and their source apportionment using PMF: A four year study over Delhi, India. Environ Pollut 262:114337. https://doi.org/10.1016/j.envpol.2020.114337

Jaishankar M, Tseten T, Anbalagan N, et al. 2014. Toxicity, mechanism and health effects of some heavy metals. Interdiscip Toxicol 7:60–72. https://doi.org/10.2478/intox-2014-0009

Jallad KN. 2015. Heavy metal exposure from ingesting rice and its related potential hazardous health risks to humans. Environ Sci Pollut Res 22:15449–15458. https://doi.org/10.1007/s11356-015-4753-7

Ji A, Wang F, Luo W, et al. 2011. Lead poisoning in China: A nightmare from industrialisation. Lancet 377:1474–1476. https://doi.org/10.1016/S0140-6736(10)60623-X

Johansson SAE. 1992a. Optimization of the sensitivity in PIXE analysis. Int J PIXE 2:33–46

Johansson SAE. 1992b. Particle induced X-ray emission and complementary nuclear methods for trace element determination Plenary lecture. Analyst 117:259–265. https://doi.org/10.1039/AN9921700259

Johansson SAE, Johansson TB. 1976. Analytical application of particle induced X-ray emission. Nucl Instruments Methods 137:473–516. https://doi.org/10.1016/0029-554X(76)90470-5

Johansson TB, Akselsson R, Johansson SAE. 1970. X-ray analysis: Elemental trace analysis at the 10-12 g level. Nucl Instruments Methods 84:141–143. https://doi.org/10.1016/0029-554X(70)90751-2

Jolly YN, Islam A, Akbar S. 2013. Transfer of metals from soil to vegetables and possible health risk assessment. Springerplus 2:1–8. https://doi.org/10.1186/2193-1801-2-385

Kafle HK, Khadgi J, Ojha RB, Santoso M. 2022. Concentration, Sources, and Associated Risks of Trace Elements in the Surface Soil of Kathmandu Valley, Nepal. Water Air Soil Pollut 233:. https://doi.org/10.1007/s11270-021-05444-1

Kang MJ, Kwon YK, Yu S, et al. 2019. Assessment of Zn pollution sources and apportionment in agricultural soils impacted by a Zn smelter in South Korea. J Hazard Mater 364:475–487. https://doi.org/10.1016/j.jhazmat.2018.10.046

Kasahara M, Yoshida K, Takahashi K. 1993. Sampling and measurement conditions for PIXE analysis of atmospheric aerosols. Nucl Inst Methods Phys Res B 75:240–244. https://doi.org/10.1016/0168-583X(93)95651-K

Kelly FJ, Fussell JC. 2012. Size, source and chemical composition as determinants of toxicity attributable to ambient particulate matter. Atmos Environ 60:504–526. https://doi.org/10.1016/j.atmosenv.2012.06.039

Kim HK, Jang TI, Kim SM, Park SW. 2015. Impact of domestic wastewater irrigation on heavy metal contamination in soil and vegetables. Environ Earth Sci 73:2377–2383. https://doi.org/10.1007/s12665-014-3581-2

Kim Oanh NT, Upadhyay N, Zhuang YH, et al. 2006. Particulate air pollution in six Asian cities: Spatial and temporal distributions, and associated sources. Atmos Environ 40:3367–3380. https://doi.org/10.1016/j.atmosenv.2006.01.050

Koelmans AA, Jonker MTO, Cornelissen G, et al. 2006. Black carbon: The reverse of its dark side. Chemosphere 63:365–377. https://doi.org/10.1016/j.chemosphere.2005.08.034

Kristiansen NI, Prata AJ, Stohl A, Carn SA. 2015. Stratospheric volcanic ash emissions from the 13 February 2014 Kelut eruption. Geophys Res Lett 42:588–596. https://doi.org/10.1002/2014GL062307

Kurniawati S, Kusmartini I, Adventini N, Lestiani DD. 2012. Applicability of ED-XRF Spectrometer for Sediment Analysis. In: Nasional Seminar Nuclear Analytical Technique. Center for Applied Nuclear Science and Technology, pp 152–158

Lelieveld J, Klingmüller K, Pozzer A, et al. 2019. Cardiovascular disease burden from

ambient air pollution in Europe reassessed using novel hazard ratio functions. Eur Heart J 40:1590–1596. https://doi.org/10.1093/eurheartj/ehz135

Lestari P, Mauliadi YD. 2009. Source apportionment of particulate matter at urban mixed site in Indonesia using PMF. Atmos Environ 43:1760–1770. https://doi.org/10.1016/j.atmosenv.2008.12.044

Lestiani D., Santoso M, Kurniawati S, et al. 2015. Characteristics of Feed Coal and Particulate Matter in the Vicinity of Coal-fired Power Plant in Cilacap, Central Java, Indonesia. Procedia Chem 16:216–221. https://doi.org/10.1016/j.proche.2015.12.044

Lestiani DD, Apryani R, Lestari L, et al. 2018. Characteristics of trace elements in volcanic ash of kelud eruption in East Java, Indonesia. Indones J Chem 18:457–463. https://doi.org/10.22146/ijc.26876

Lestiani DD, Kijin S, Santoso M, Takagi I. 2023a. Helium and Proton Particle-Induced X-Ray Emission (PIXE) for Characterization of PM2.5 from Surabaya , Indonesia. Anal Lett 0:1–14. https://doi.org/10.1080/00032719.2023.2248307

Lestiani DD, Santoso M, Kurniawati S, et al. 2019. Chemical Composition of Fine Particulate Matter from Peat Forest Fires at Palangka Raya and Its Dispersion using HYSPLIT. IOP Conf Ser Earth Environ Sci 303:. https://doi.org/10.1088/1755-1315/303/1/012035

Lestiani DD, Santoso M, Kurniawati S, et al. 2023b. Heavy Metals, Sources, and Potential Risk Assessment of PM2.5 in the Vicinity of a Lead Smelter in Indonesia. Aerosol Sci Eng. https://doi.org/10.1007/s41810-023-00179-4

Lestiani DD, Santoso M, Kurniawati S, Markwitz A. 2013a. Characteristic of airborne particulate matter samples collected from two semi industrial sites in Bandung, Indonesia. Indones J Chem 13:

Lestiani DD, Santoso M, Trompetter WJ, et al. 2013b. Determination of chemical elements in airborne particulate matter collected at Lembang, Indonesia by particle induced X-ray emission. J Radioanal Nucl Chem 297:. https://doi.org/10.1007/s10967-012-2348-z

Lestiani DD, Syahfitri WYN, Adventini N, et al. 2023c. Impacts of a lead smelter in East Java, Indonesia: degree of contamination, spatial distribution, ecological risk, and health risk assessment of potentially toxic elements in soils. Environ Monit Assess 195:1165. https://doi.org/10.1007/s10661-023-11745-1

Leung AOW, Duzgoren-Aydin NS, Cheung KC, Wong MH. 2008. Heavy metals

concentrations of surface dust from e-waste recycling and its human health implications in southeast China. Environ Sci Technol 42:2674–2680

Li L, Zhang Y, Ippolito JA, et al. 2020a. Lead smelting effects heavy metal concentrations in soils, wheat, and potentially humans. Environ Pollut 257:113641. https://doi.org/10.1016/j.envpol.2019.113641

Li P, Lin C, Cheng H, et al. 2015. Contamination and health risks of soil heavy metals around a lead/zinc smelter in southwestern China. Ecotoxicol Environ Saf 113:391–399. https://doi.org/10.1016/j.ecoenv.2014.12.025

Li Q, Cheng H, Zhou T, et al. 2012. The estimated atmospheric lead emissions in China, 1990-2009. Atmos Environ 60:1–8. https://doi.org/10.1016/j.atmosenv.2012.06.025

Li Z, Feng X, Li G, et al. 2011. Mercury and other metal and metalloid soil contamination near a Pb/Zn smelter in east Hunan province, China. Appl Geochemistry 26:160–166. https://doi.org/10.1016/j.apgeochem.2010.11.014

Li Z, Lu H, Zhoug F. 2020b. Lead exposure characteristics and pollution evaluation of indoor and outdoor dust in primary school campuses of Baoji city in northwest China. IOP Conf Ser Earth Environ Sci 545:. https://doi.org/10.1088/1755-1315/545/1/012024

Li Z, Ma Z, van der Kuijp TJ, et al. 2014. A review of soil heavy metal pollution from mines in China: Pollution and health risk assessment. Sci Total Environ 468–469:843–853. https://doi.org/10.1016/j.scitotenv.2013.08.090

Liu G, Yu Y, Hou J, et al. 2014. An ecological risk assessment of heavy metal pollution of the agricultural ecosystem near a lead-acid battery factory. Ecol Indic 47:210–218. https://doi.org/10.1016/j.ecolind.2014.04.040

Lockitch G. 1993. Perspectives on Lead Toxicity. 26:371–381

Loska K, Wiechułła D, Korus I. 2004. Metal contamination of farming soils affected by industry. Environ Int 30:159–165. https://doi.org/10.1016/S0160-4120(03)00157-0

Lucarelli F, Nava S, Calzolai G, et al. 2011. Is PIXE still a useful technique for the analysis of atmospheric aerosols? The LABEC experience. X-Ray Spectrom 40:162–167. https://doi.org/10.1002/xrs.1312

Malm C, Sisler JF, Cahill A. 1994. Spatial and seasonal trends in particles concentration and optical extinction in the United States. 99:1347–1370

Mansha M, Ghauri B, Rahman S, Amman A. 2012. Characterization and source apportionment of ambient air particulate matter (PM2.5) in Karachi. Sci Total

Environ 425:176–183. https://doi.org/10.1016/j.scitotenv.2011.10.056

Markus J, McBratney AB. 2001. A review of the contamination of soil with lead. Environ Int 27:399–411. https://doi.org/10.1016/S0160-4120(01)00049-6

Matawle JL, Pervez S, Dewangan S, et al. 2014. PM2.5 chemical source profiles of emissions resulting from industrial and domestic burning activities in India. Aerosol Air Qual Res 14:2051–2066. https://doi.org/10.4209/aaqr.2014.03.0048

Mboi N, Syailendrawati R, Ostroff SM, et al. 2022. The state of health in Indonesia's provinces, 1990–2019: a systematic analysis for the Global Burden of Disease Study 2019. Lancet Glob Heal 10:e1632–e1645. https://doi.org/10.1016/S2214-109X(22)00371-0

Ministry of Energy And Mineral. 2013. Standard and Quality (specification) of diesel fuel type 48 which is marketed domestically. No. 978.K/10/DJM. S/2013

Ministry of Industry. 2023. Dominant and Surging Contribution, Manufacturing Industry Still Confident. In: Press Release. https://kemenperin.go.id/artikel/24036/Kontribusi-Dominan-dan-Melonjak,-Industri-Manufaktur-Masih-Pede-. Accessed 6 Oct 2023

Mitkova T, Markoski M. 2015. Phytoremediation of Soils Contaminated with Heavy Metals in the Vicinity of the Smelter for Lead and Zinc in Veles. 80:53–57

MOFA M of FAI. 2018. Indonesia. https://kemlu.go.id/harare/en/read/indonesia/2729/etc-menu

Mohammed TI, Chang-Yen I, Bekele I. 1996. Lead pollution in East Trinidad resulting from lead recycling and smelting activities. Environ Geochem Health 18:123–128. https://doi.org/10.1007/BF01771288

Mukherjee A, Agrawal M. 2017. World air particulate matter: sources, distribution and health effects. Environ Chem Lett 15:283–309. https://doi.org/10.1007/s10311-017-0611-9

Murray CJL, Afshin A, Alam T, et al. 2020. Global burden of 369 diseases and injuries in 204 countries and territories, 1990–2019: a systematic analysis for the Global Burden of Disease Study 2019. Lancet 396:1204–1222. https://doi.org/10.1016/S0140-6736(20)30925-9

Nagajyoti PC, Lee KD, Sreekanth TVM. 2010. Heavy metals, occurrence and toxicity for plants: A review. Environ Chem Lett 8:199–216. https://doi.org/10.1007/s10311-010-0297-8

Ni M, Huang J, Lu S, et al. 2014. A review on black carbon emissions, worldwide and in

China. Chemosphere 107:83–93. https://doi.org/10.1016/j.chemosphere.2014.02.052

Ogrizek M, Jaćimović R, Šala M, Kroflič A. 2021. No more waste at the elemental analysis of airborne particulate matter on quartz fibre filters. Talanta 226:. https://doi.org/10.1016/j.talanta.2021.122110

Ogrizek M, Kroflič A, Šala M. 2022. Critical review on the development of analytical techniques for the elemental analysis of airborne particulate matter. Trends Environ Anal Chem 33:. https://doi.org/10.1016/j.teac.2022.e00155

Olise FS, Owoade OK, Olaniyi HB. 2010. An optimization of PIXE procedure for high-Z species in a lower Z matrix. Appl Radiat Isot 68:1030–1034. https://doi.org/10.1016/j.apradiso.2010.01.034

Ordonez JA, Jakob M, Steckel JC, Fünfgeld A. 2021. Coal, power and coal-powered politics in Indonesia. Environ Sci Policy 123:44–57. https://doi.org/10.1016/j.envsci.2021.05.007

Oreščanin V, Mikelić IL, Mikelić L, Lulić S. 2008. Applicability of MiniPal 4 compact EDXRF spectrometer for soil and sediment analysis. X-Ray Spectrom 37:508–511. https://doi.org/10.1002/xrs.1079

Paatero P, Hopke PK. 2003. Discarding or downweighting high-noise variables in factor analytic models. Anal Chim Acta 490:277–289. https://doi.org/10.1016/S0003-2670(02)01643-4

Paatero P, Hopke PK. 2002. Utilizing wind direction and wind speed as independent variables in multilinear receptor modeling studies. Chemom Intell Lab Syst 60:25–41. https://doi.org/10.1016/S0169-7439(01)00183-6

Paatero P, Hopke PK, Begum BA, Biswas SK. 2005. A graphical diagnostic method for assessing the rotation in factor analytical models of atmospheric pollution. Atmos Environ 39:193–201. https://doi.org/10.1016/j.atmosenv.2004.08.018

Paatero P, Tapper U. 1994. Positive matrix factorization: A non-negative factor model with optimal utilization of error estimates of data values. Environmetrics 5:111–126. https://doi.org/10.1002/env.3170050203

Pabroa PCB, Racho JMD, Jagonoy AM, et al. 2022. Characterization, source apportionment and associated health risk assessment of respirable air particulates in Metro Manila, Philippines. Atmos Pollut Res 13:101379. https://doi.org/10.1016/j.apr.2022.101379

Pacyna JM, Pacyna EG, Aas W. 2009. Changes of emissions and atmospheric deposition

of mercury, lead, and cadmium. Atmos Environ 43:117–127. https://doi.org/10.1016/j.atmosenv.2008.09.066

Paddock R. 2019. To Make This Tofu, Start by Burning Toxic Plastic. New York Times

Park EJ, Kim DS, Park K. 2008. Monitoring of ambient particles and heavy metals in a residential area of Seoul, Korea. Environ Monit Assess 137:441–449. https://doi.org/10.1007/s10661-007-9779-y

Park J, Kim H, Kim Y, et al. 2022. Source apportionment of PM2.5 in Seoul, South Korea and Beijing, China using dispersion normalized PMF. Sci Total Environ 833:155056. https://doi.org/10.1016/j.scitotenv.2022.155056

Permadi DA, Kim Oanh NT. 2013. Assessment of biomass open burning emissions in Indonesia and potential climate forcing impact. Atmos Environ 78:250–258. https://doi.org/10.1016/j.atmosenv.2012.10.016

Pey J, Querol X, Alastuey A. 2009. Variations of levels and composition of PM10 and PM2.5 at an insular site in the Western Mediterranean. Atmos Res 94:285–299. https://doi.org/10.1016/j.atmosres.2009.06.006

Phalen R., Cuddihy R., Fisher G., et al. 1991. Main Features of the Proposed NCRP Respiratory Tract Model. 179–184

Pönkä A. 1998. Lead in the ambient air and blood of children in Helsinki. Sci Total Environ 219:1–5. https://doi.org/10.1016/S0048-9697(98)00209-5

Prihartono NA, Djuwita R, Mahmud PB, et al. 2019. Prevalence of blood lead among children living in battery recycling communities in greater Jakarta, Indonesia. Int J Environ Res Public Health 16:1–11. https://doi.org/10.3390/ijerph16071276

Qiu K, Xing W, Scheckel KG, et al. 2016. Temporal and seasonal variations of As, Cd and Pb atmospheric deposition flux in the vicinity of lead smelters in Jiyuan, China. Atmos Pollut Res 7:170–179. https://doi.org/10.1016/j.apr.2015.09.003

Qu CS, Ma ZW, Yang J, et al. 2012. Human Exposure Pathways of Heavy Metals in a Lead-Zinc Mining Area, Jiangsu Province, China. PLoS One 7:. https://doi.org/10.1371/journal.pone.0046793

Rahman MS, Bhuiyan SS, Ahmed Z, et al. 2021. Characterization and source apportionment of elemental species in $PM_{2.5}$ with especial emphasis on seasonal variation in the capital city “Dhaka”, Bangladesh. Urban Clim 36:100804. https://doi.org/10.1016/j.uclim.2021.100804

Rahman SA, Hamzah MS, Elias MS, et al. 2015. A long term study on characterization and

source apportionment of particulate pollution in klang valley, kuala lumpur. Aerosol Air Qual Res 15:2291–2304. https://doi.org/10.4209/aaqr.2015.03.0188

Rahman SA, Hamzah MS, Wood AK, et al. 2011. Sources apportionment of fine and coarse aerosol in Klang Valley, Kuala Lumpur using positive matrix factorization. Atmos Pollut Res 2:197–206. https://doi.org/10.5094/APR.2011.025

Ramanathan V, Carmichael G. 2008. Global and regional climate changes due to black carbon. Nat Geosci 1:221–227. https://doi.org/10.1038/ngeo156

Reff A, Eberly SI, Bhave P V. 2007. Receptor modeling of ambient particulate matter data using positive matrix factorization: Review of existing methods. J Air Waste Manag Assoc 57:146–154. https://doi.org/10.1080/10473289.2007.10465319

Roumié M, Nsouli B, Zahraman K, Reslan A. 2004. First accelerator based ion beam analysis facility in Lebanon: Development and applications. Nucl Instruments Methods Phys Res Sect B Beam Interact with Mater Atoms 219–220:389–393. https://doi.org/10.1016/j.nimb.2004.01.088

Saksakulkrai S, Chantara S, Shi Z. 2023. Airborne particulate matter in Southeast Asia: a review on variation, chemical compositions and source apportionment. Environ Chem 19:401–431. https://doi.org/10.1071/en22044

Salako GO, Hopke PK, Cohen DD, et al. 2012. Exploring the variation between EC and BC in a variety of locations. Aerosol Air Qual Res 12:1–7. https://doi.org/10.4209/aaqr.2011.09.0150

Samet JM, Dominici F, Curriero FC, et al. 2000. Fine Particulate Air Pollution and Mortality in 20 U.S. Cities 1987-1994. N Engl J Med 343:1742–1749

Santoso M, Hopke PK, Hidayat A, Diah Dwiana L. 2008. Sources identification of the atmospheric aerosol at urban and suburban sites in Indonesia by positive matrix factorization. Sci Total Environ 397:229–237. https://doi.org/10.1016/j.scitotenv.2008.01.057

Santoso M, Hopke PK, Permadi DA, et al. 2021. Multiple air quality monitoring evidence of the impacts of large-scale social restrictions during the covid-19 pandemic in Jakarta, Indonesia. Aerosol Air Qual Res 21:. https://doi.org/10.4209/aaqr.200645

Santoso M, Lestiani DD. 2014. IAEA XRF Newsletter: X ray Fluorescence in Member States

Santoso M, Lestiani DD, Damastuti E, et al. 2020a. Long term characteristics of atmospheric particulate matter and compositions in Jakarta, Indonesia. Atmos Pollut

Res 11:2215–2225. https://doi.org/10.1016/j.apr.2020.09.006

Santoso M, Lestiani DD, Kurniawati S, et al. 2020b. Assessment of urban air quality in Indonesia. Aerosol Air Qual Res 20:2142–2158. https://doi.org/10.4209/aaqr.2019.09.0451

Santoso M, Lestiani DD, Markwitz A. 2013. Characterization of airborne particulate matter collected at Jakarta roadside of an arterial road. J Radioanal Nucl Chem 297:. https://doi.org/10.1007/s10967-012-2350-5

Santoso M, Lestiani DD, Mukhtar R, et al. 2011. Preliminary study of the sources of ambient air pollution in Serpong, Indonesia. Atmos Pollut Res 2:. https://doi.org/10.5094/APR.2011.024

Sattar Y, Rashid M, Ramli M, Sabariah B. 2014. Black carbon and elemental concentration of ambient particulate matter in Makassar Indonesia. IOP Conf Ser Earth Environ Sci 18:. https://doi.org/10.1088/1755-1315/18/1/012099

Seneviratne MCS, Waduge VA, Hadagiripathira L, et al. 2011. Characterization and source apportionment of particulate pollution in Colombo, Sri Lanka. Atmos Pollut Res 2:207–212. https://doi.org/10.5094/APR.2011.026

Silva HF, Silva NF, Oliveira CM, Matos MJ. 2021. Heavy metals contamination of urban soils—a decade study in the city of lisbon, portugal. Soil Syst 5:. https://doi.org/10.3390/soilsystems5020027

Siregar S, Idiawati N, Lestari P, et al. 2022. Chemical Composition, Source Appointment and Health Risk of $PM_{2.5}$ and $PM_{2.5-10}$ during Forest and Peatland Fires in Riau, Indonesia. Aerosol Air Qual Res 22:. https://doi.org/10.4209/aaqr.220015

Smith AH, Goycolea M, Haque R, Biggs ML. 1998. Marked Increase in Bladder and Lung Cancer Mortality in a Region of Northern Chile due to Arsenic in Drinking Water. 147:2–7

Smith C. 2020. Encyclopedia of Global Archaeology

Soleimani M, Amini N, Sadeghian B, et al. 2018. Heavy metals and their source identification in particulate matter ($PM_{2.5}$) in Isfahan City, Iran. J Environ Sci (China) 72:166–175. https://doi.org/10.1016/j.jes.2018.01.002

Stafilov T, Šajn R, Pančevski Z, et al. 2010. Heavy metal contamination of topsoils around a lead and zinc smelter in the Republic of Macedonia. J Hazard Mater 175:896–914. https://doi.org/10.1016/j.jhazmat.2009.10.094

Sterckeman T, Douay F, Proix N, Fourrier H. 2000. Vertical distribution of Cd, Pb and Zn

in soils near smelters in the North of France. Environ Pollut 107:377–389. https://doi.org/10.1016/S0269-7491(99)00165-7

Sullivan M. 2015. Reducing lead in air and preventing childhood exposure near lead smelters: Learning from the U.S. experience. New Solut 25:78–101. https://doi.org/10.1177/1048291115569027

Sun Y, Zhuang G, Wang Y, et al. 2004. The air-borne particulate pollution in Beijing - Concentration, composition, distribution and sources. Atmos Environ 38:5991–6004. https://doi.org/10.1016/j.atmosenv.2004.07.009

Susanto AD. 2020. Air pollution and human health. Med J Indones 29:8–10. https://doi.org/10.13181/mji.com.204572

Suvarapu LN, Baek SO. 2017. Determination of heavy metals in the ambient atmosphere: A review. Toxicol Ind Health 33:79–96. https://doi.org/10.1177/0748233716654827

Sylvestre A, Mizzi A, Mathiot S, et al. 2017. Comprehensive chemical characterization of industrial $PM_{2.5}$ from steel industry activities. Atmos Environ 152:180–190. https://doi.org/10.1016/j.atmosenv.2016.12.032

Taha G, Box GP, Cohen DD, Stelcer E. 2007. Black carbon measurement using laser integrating plate method. Aerosol Sci Technol 41:266–276. https://doi.org/10.1080/02786820601156224

Taiwo AM, Beddows DCS, Calzolai G, et al. 2014. Receptor modelling of airborne particulate matter in the vicinity of a major steelworks site. Sci Total Environ 490:488–500. https://doi.org/10.1016/j.scitotenv.2014.04.118

Taylor MP, Isley CF, Glover J. 2019. Prevalence of childhood lead poisoning and respiratory disease associated with lead smelter emissions. Environ Int 127:340–352. https://doi.org/10.1016/j.envint.2019.01.062

Tchounwou PB, Yedjou CG, Patlolla AK, Sutton DJ. 2012. Molecular, clinical and environmental toxicicology Volume 3: Environmental Toxicology. Mol Clin Environ Toxicol 101:133–164. https://doi.org/10.1007/978-3-7643-8340-4

Thomaidis NS, Bakeas EB, Siskos PA. 2003. Characterization of lead, cadmium, arsenic and nickel in $PM_{2.5}$ particles in the Athens atmosphere, Greece. Chemosphere 52:959–966. https://doi.org/10.1016/S0045-6535(03)00295-9

Tóth G, Hermann T, Da Silva MR, Montanarella L. 2016. Heavy metals in agricultural soils of the European Union with implications for food safety. Environ Int 88:299–309. https://doi.org/10.1016/j.envint.2015.12.017

Trompetter WJ, Markwitz A, Davy P. 2005. Air Particulate Research Capability At the New Zealand Ion Beam Analysis Facility Using Pixe and Iba Techniques. Int J PIXE 15:249–255. https://doi.org/10.1142/s0129083505000581

Uria-Tellaetxe I, Carslaw DC. 2014. Conditional bivariate probability function for source identification. Environ Model Softw 59:1–9. https://doi.org/10.1016/j.envsoft.2014.05.002

US EPA. 2006. 40 CFR Part 50 National Ambient Air Quality Standards for Particulate Matter; Final Rule

US EPA. 2023. Particulate Matter (PM) Basics. https://www.epa.gov/pm-pollution/particulate-matter-pm-basics#PM

US EPA. 2011. EPA-600-R-090-052F, Exposure Factors Handbook, 2011 Edition.

US EPA. 1989. Risk Assessment Guidance for Superfund Volume I Human Health Evaluation Manual (Part A). Off Emerg Remedial Response 1:1–291. https://doi.org/EPA/540/1-89/002

US EPA. 2022. Integrated Risk Information System. https://iris.epa.gov/AdvancedSearch/. Accessed 1 Jul 2022

Vadrucci M, Mazzinghi A, Gorghinian A, et al. 2019. Analysis of Roman Imperial coins by combined PIXE, HE-PIXE and μ-XRF. Appl Radiat Isot 143:35–40. https://doi.org/10.1016/j.apradiso.2018.10.016

Valko M, Morris H, Cronin M. 2005. Metals, Toxicity and Oxidative Stress. Curr Med Chem 12:1161–1208. https://doi.org/10.2174/0929867053764635

Vega E, López-Veneroni D, Ramírez O, et al. 2021. Particle-bound pahs and chemical composition, sources and health risk of $PM_{2.5}$ in a highly industrialized area. Aerosol Air Qual Res 21:1–24. https://doi.org/10.4209/AAQR.210047

Verma R, Vinoda KS, Papireddy M, Gowda ANS. 2016. Toxic Pollutants from Plastic Waste- A Review. Procedia Environ Sci 35:701–708. https://doi.org/10.1016/j.proenv.2016.07.069

Vuong QT, Bac VT, Thang PQ, et al. 2023. Trace element characterization and source identification of particulate matter of different sizes in Hanoi, Vietnam. Urban Clim 48:101408. https://doi.org/10.1016/j.uclim.2023.101408

Wang B, Eum K Do, Kazemiparkouhi F, et al. 2020. The impact of long-term $PM_{2.5}$ exposure on specific causes of death: Exposure-response curves and effect modification among 53 million U.S. Medicare beneficiaries. Environ Heal A Glob

Access Sci Source 19:1–12. https://doi.org/10.1186/s12940-020-00575-0

Wang Y, Yang L, Kong L, et al. 2015. Spatial distribution, ecological risk assessment and source identification for heavy metals in surface sediments from Dongping Lake, Shandong, East China. Catena 125:200–205. https://doi.org/10.1016/j.catena.2014.10.023

Wang Z, Zhao J, Wang T, et al. 2019. Fine-particulate matter aggravates cigarette smoke extract–induced airway inflammation via wnt5a–ERK pathway in COPD. Int J COPD 14:979–994. https://doi.org/10.2147/COPD.S195794

Watson JG. 2002. Visibility: Science and regulation. J Air Waste Manag Assoc 52:628–713. https://doi.org/10.1080/10473289.2002.10470813

Watson JG, Chow JC, Chen L-WA. 2005. Summary of Organic and Elemental Carbon/Black Carbon Analysis Methods and Intercomparisons

Watson RL, Sjurseth JR, Howard RW. 1971. An investigation of the analytical capabilities of X-ray emission induced by high energy alpha particles. Nucl Instruments Methods 93:69–76. https://doi.org/10.1016/0029-554X(71)90139-X

WHO. 2022. Ambient (outdoor) air pollution. https://www.who.int/news-room/fact-sheets/detail/ambient-(outdoor)-air-quality-and-health. Accessed 15 Mar 2023

WHO. 2018. Air Pollution and Child Health. Who 113:32

WHO. 2021. WHO global air quality guidelines

WHO. 2010. Exposure to Lead: A major public health concern. World Heal Organ 6

Wimolwattanapun W, Hopke PK, Pongkiatkul P. 2011. Source apportionment and potential source locations of $PM_{2.5}$ and $PM_{2.5-10}$ at residential sites in metropolitan Bangkok. Atmos Pollut Res 2:172–181. https://doi.org/10.5094/APR.2011.022

Wuana RA, Okieimen FE. 2011. Heavy Metals in Contaminated Soils: A Review of Sources, Chemistry, Risks and Best Available Strategies for Remediation. ISRN Ecol 2011:1–20. https://doi.org/10.5402/2011/402647

Wyzga RE. 1997. Ambient Particles and Health: Lines that Divide: Invited Discussions. J Air Waste Manag Assoc 47:995–1008. https://doi.org/10.1080/10473289.1997.10463950

Xiao M, Xu S, Yang B, et al. 2022. Contamination , Source Apportionment , and Health Risk Assessment of Heavy Metals in Farmland Soils Surrounding a Typical Copper Tailings Pond

Xie Y, Harjono M. 2020. The retail fuels market in Indonesia. Icct 1–13

Xing W, Zhang H, Scheckel KG, Li L. 2016. Heavy metal and metalloid concentrations in components of 25 wheat (Triticum aestivum) varieties in the vicinity of lead smelters in Henan province, China. Environ Monit Assess 188:23. https://doi.org/10.1007/s10661-015-5023-3

Yadav IC, Devi NL. 2019. Biomass burning, regional air quality, and climate change, 2nd edn. Elsevier Inc.

Yang Y, Ruan Z, Wang X, et al. 2019. Short-term and long-term exposures to fine particulate matter constituents and health: A systematic review and meta-analysis. Environ Pollut 247:874–882. https://doi.org/10.1016/j.envpol.2018.12.060

Yin P, Brauer M, Cohen A, et al. 2017. Long-term fine particulate matter exposure and nonaccidental and cause-specific mortality in a large national cohort of Chinese men. Environ Health Perspect 125:117002-1-117002–11. https://doi.org/10.1289/EHP1673

Yu GH, Park S. 2021. Chemical characterization and source apportionment of $PM_{2.5}$ at an urban site in Gwangju, Korea. Atmos Pollut Res 12:101092. https://doi.org/10.1016/j.apr.2021.101092

Yuan G, Chen D, Yin L, et al. 2014. High efficiency chlorine removal from polyvinyl chloride (PVC) pyrolysis with a gas-liquid fluidized bed reactor. Waste Manag 34:1045–1050. https://doi.org/10.1016/j.wasman.2013.08.021

Yuan Y, Wu Y, Ge X, et al. 2019. In vitro toxicity evaluation of heavy metals in urban air particulate matter on human lung epithelial cells. Sci Total Environ 678:301–308. https://doi.org/10.1016/j.scitotenv.2019.04.431

Zhai Y, Liu X, Chen H, et al. 2014. Source identification and potential ecological risk assessment of heavy metals in $PM_{2.5}$ from Changsha. Sci Total Environ 493:109–115. https://doi.org/10.1016/j.scitotenv.2014.05.106

Zhao J, Zhang Y, Xu H, Tao S, Wang R, Yu Q, et al. 2021 Trace elements from ocean-going vessels in East Asia: vanadium and nickel emissions and their impacts on air quality. Journal of Geophysical Research: Atmospheres. 2021 Apr 27;126(8):e2020JD033984.

Zhang X, Eto Y, Aikawa M. 2021. Risk assessment and management of $PM_{2.5}$-bound heavy metals in the urban area of Kitakyushu, Japan. Sci Total Environ 795:148748. https://doi.org/10.1016/j.scitotenv.2021.148748

Zhang ZH, Khlystov A, Norford LK, et al. 2017. Characterization of traffic-related ambient fine particulate matter ($PM_{2.5}$) in an Asian city: Environmental and health

implications. Atmos Environ 161:132–143. https://doi.org/10.1016/j.atmosenv.2017.04.040

Zhong C, Yang Z, Jiang W, et al. 2016. Ecological geochemical assessment and source identification of trace elements in atmospheric deposition of an emerging industrial area: Beibu Gulf economic zone. Sci Total Environ 573:1519–1526. https://doi.org/10.1016/j.scitotenv.2016.08.057

Zhou H, Hopke PK, Zhou C, Holsen TM. 2019. Ambient mercury source identification at a New York State urban site: Rochester, NY. Sci Total Environ 650:1327–1337. https://doi.org/10.1016/j.scitotenv.2018.09.040

Zhou Y, Jiang D, Ding D, et al. 2022. Ecological-health risks assessment and source apportionment of heavy metals in agricultural soils around a super-sized lead-zinc smelter with a long production history, in China. Environ Pollut 307:119487. https://doi.org/10.1016/j.envpol.2022.119487

ACKNOWLEDGEMENT

In the graceful and blessing of God, this dissertation has been completed, as a fulfillment of the requirements for the degree of Doctoral by Research in Department of Nuclear Engineering, Graduate School of Engineering at Kyoto University, Japan under Japan Society for the Promotion of Science Ronpaku Dissertation PhD Program.

I would like to express my deepest gratitude to my supervisor, Professor Ikuji Takagi, for his superb guidance, supervision, and support. I appreciate his willingness to provide me with the opportunity and chance to pursue my PhD program through the JSPS grant. I am truly fortunate to have such a dedicated supervisor who offers unwavering support, constantly encouraging and ensuring the smooth and successful execution of my research and experiments at Kyoto University.

I would like to acknowledge the student members in the Nuclear Engineering Department, Kyoto University, Sung Kijin for his collaboration and help in preliminary characterization and data analysis, Moriyama and Suzuki for their technical support with the accelerator start-up and operation during the experiments. Without their help, this research will not run smoothly. I also would like to express my thank to Mrs Souma the laboratory secretary who has been greatly support with administrative matters during my visit to Kyoto. Mrs. Souma's help and support have made my visit in Kyoto smooth and enjoyable. She makes building good relationships and connecting with people enjoyable in the midst of busy and stressful experiments.

Special appreciation is extended to my institutional supervisor from Research Organization for Nuclear Energy, National Research and Innovation Agency BRIN, Professor Muhayatun Santoso, for her inspiring, helpful discussion, motivational support and encouraging way to guide me in carrying out the final project and the preparation of this dissertation. Under her supervision and guidance, I grew and enhanced the capability as a researcher. I would especially like to thank my research team in BRIN, Natalia Adventini who already retired but her support has left a lasting impact on the research, Endah Damastuti, Syukria Kurniawati, Woro Yatu Niken Syahfitri, Djoko Prakoso Dwi Atmodjo, Indah Kusmartini, Dyah Kumala Sari, Feni Fernita Nurhaini and Moch. Faizal Ramadhani for their prayers and all the support given during the research and continuous encouragement for accomplishing this study. Many thanks to Ministry of Environmental and Forestry, Mrs. Rita Mukhtar the staff of Agency for Standardization of Environmental and Forestry

Instrumentation, and the team, East Java province environmental protection agency, Dimas Ageng Sutrisno and team for their time and technical support in airborne particulate matter sampling.

I gratefully acknowledge the support of Japan Society for the Promotion of Science, for their financial grant through Ronpaku Dissertation PhD Program JSPS toward my PhD study. This research was also received support through the research contract RCARP01/RC2 from the Regional Cooperative Agreement Research Organization (RCARO), and technical collaboration from International Atomic Energy Agency through the RAS and INS project.

I really appreciate the head of Research Center for Radiation Detection and Nuclear Analysis Technology, Research Organization for Nuclear Energy CRDNAT, Dr. Abu Khalid Rivai and all the administrative staffs in CRDNAT and BRIN for their support during my PhD program.

Last but not least, I would like to extend a special acknowledgment to my husband, Yayat. He has had to put up with my study activities, and his continuous support, patience, and understanding throughout this journey have been my greatest source of strength. My daughters, Zahrah, Salma, Alya, Kayla, and Nayla, have shown remarkable patience, support, and continuous prayers. Their encouragement and love have carried me through the challenges. I also want to express my gratitude to my father, my sister, and my brother for their prayers and support.

Many others have worked behind the scenes to encourage and support my efforts, although their names have not been mentioned.

This work wouldn't have been possible without the help of these people, organizations, and institutions. Being in a good teamwork is a blessing and it is a powerful motivator. May God bless you all.

PUBLICATIONS

Several papers from this dissertation have already been published, while others are currently in the drafting stage. Here are the working titles for a selection of papers in various stages of development at the time of this dissertation submission.

1. Santoso, M, Lestiani, D.D., Kurniawati, S., Damastuti, E., Kusmartini, I., Atmodjo, D.P.D., Sari, D.K., Hopke, P.K., Mukhtar, R., Muhtarom, T., Tjahyadi, A., Parian, S., Kholik, N., Sutrisno, D.A., Wahyudi, D., Sitorus, T.D., Djamilus, J., Riadi, A., Supriyanto, J., Dahyar, N., Sondakh, S., Hogendorp, K., Wahyuni, N., Gede Bejawan, I., Suprayadi, L.S., 2020. Assessment of urban air quality in Indonesia. Aerosol Air Qual. Res. 20, 2142–2158. https://doi.org/10.4209/aaqr.2019.09.0451 (Chapter 2, as main contributors)

2. Lestiani, D.D., Santoso, M., Kurniawati, S., Fachrurony, F., Sari, D.K., Kusmartini, I., Damastuti, E., Atmodjo, D.P.D., Mukhtar, R., 2023. Heavy Metals, Sources, and Potential Risk Assessment of $PM_{2.5}$ in the Vicinity of a Lead Smelter in Indonesia. Aerosol Sci. Eng. 7, 283-293. https://doi.org/10.1007/s41810-023-00179-4 (Chapter 3)

3. Lestiani, D.D., Syahfitri, W.Y.N., Adventini, N., Kurniawati, S., Damastuti, E., Santoso, M., Biswas, B., Mukhtar, R., 2023. Impacts of a lead smelter in East Java, Indonesia: degree of contamination, spatial distribution, ecological risk, and health risk assessment of potentially toxic elements in soils. Environ. Monit. Assess. 195, 1165. https://doi.org/10.1007/s10661-023-11745-1 (Chapter 4)

4. Lestiani, D.D., Kijin, S., Santoso, M., Takagi, I., 2023. Helium and Proton Particle-Induced X-Ray Emission (PIXE) for Characterization of $PM_{2.5}$ from Surabaya, Indonesia. Anal. Lett. 0, 1–14. https://doi.org/10.1080/00032719.2023.2248307 (Chapter 5)

5. Lestiani, D.D., Kijin, S., Santoso, M., Takagi, I., Kurniawati, S.,Syahfitri, W.Y.N., Sutrisno, D.A., Damastuti, E. Revealing the respiratory hazards: toxic elements, sources and health risk assessment of $PM_{2.5}$ in an industrial area of Surabaya, Indonesia (Chapter 6, submitted to Environmental Science and Pollution Research, Springer)

Other related publications as first author and main contributor:

1. Lestiani, D.D., Apryani, R., Lestari, L., Santoso, M., Hadisantoso, E.P., Kurniawati, S., 2018. Characteristics of trace elements in volcanic ash of kelud eruption in East Java, Indonesia. Indones. J. Chem. 18, 457–463. https://doi.org/10.22146/ijc.26876

2. Lestiani, D.D., Santoso, M., Kurniawati, S., Markwitz, A., 2013. Characteristic of airborne particulate matter samples collected from two semi-industrial sites in Bandung, Indonesia. Indones. J. Chem. 13.
3. Lestiani, D.D., Santoso, M., Trompetter, W.J., Barry, B., Davy, P.K., Markwitz, A., 2013. Determination of chemical elements in airborne particulate matter collected at Lembang, Indonesia by particle induced X-ray emission. J. Radioanal. Nucl. Chem. 297. https://doi.org/10.1007/s10967-012-2348-z
4. Lestiani, D.D., Santoso, M., Damastuti, E., Kurniawati, S., Migliori, A., Leani, J.J., Czyzycki, M., Karydas, A.G. and Osan, J., 2021, November. Selected elements characterization of fine particulate matter $PM_{2.5}$ using synchrotron radiation XRF. In AIP Conference Proceedings (Vol. 2381, No. 1). AIP Publishing.
5. Lestiani, D.D., Santoso, M., Kusmartini, I., Atmodjo, D.P.D., Kurniawati, S. and Sari, D.K., 2021. Characterization of Fine Particulate Matters Collected in the Vicinity of Coal-fired Power Plants in Java using ED-XRF. In IOP Conference Series: Materials Science and Engineering (Vol. 1011, No. 1, p. 012056). IOP Publishing.
6. Santoso, M., Hopke, P. K., Damastuti, E., Lestiani, D. D., Kurniawati, S., Kusmartini, I., ... & Riadi, A. 2022. The air quality of Palangka Raya, Central Kalimantan, Indonesia: The impacts of forest fires on visibility. Journal of the Air & Waste Management Association, 72(11), 1191-1200.
7. Santoso, M., Lestiani, D. D., Damastuti, E., Kurniawati, S., Kusmartini, I., Dwi Atmodjo, D. P., Sari, D. K., Muhtarom, T., Permadi, D. A., & Hopke, P. K. 2020. Long term characteristics of atmospheric particulate matter and compositions in Jakarta, Indonesia. Atmospheric Pollution Research, 11(12), 2215–2225. https://doi.org/10.1016/j.apr.2020.09.006
8. Santoso, M., Lestiani, D.D., Damastuti, E., Kurniawati, S., Bennett, J.W., Leani, J.J., Czyzycki, M., Migliori, A., Osán, J. and Karydas, A.G., 2016. Trace elements and As speciation analysis of fly ash samples from an Indonesian coal power plant by means of neutron activation analysis and synchrotron based techniques. Journal of Radioanalytical and Nuclear Chemistry, 309, pp.413-419.
9. Santoso, M., Lestiani, D. D., Mukhtar, R., Hamonangan, E., Syafrul, H., Markwitz, A., & Hopke, P. K. 2011. Preliminary study of the sources of ambient air pollution in Serpong, Indonesia. Atmospheric Pollution Research, 2(2). https://doi.org/10.5094/APR.2011.024
10. Santoso, M., Hopke, P. K., Hidayat, A., & Diah Dwiana, L. 2008. Sources identification of the atmospheric aerosol at urban and suburban sites in Indonesia by positive matrix factorization. Science of the Total Environment, 397(1–3), 229–237. https://doi.org/10.1016/j.scitotenv.2008.01.057

Enlisted below are the working titles for a subset of oral presentations, intended for delivery at conferences, workshops, and seminars. These presentations are actively in development as of the submission of this dissertation:

1. Diah Dwiana Lestiani, Woro Yatu Niken Syahfitri, Natalia Adventini, Syukria Kurniawati, Endah Damastuti, Muhayatun Santoso, Biplab Biswas, Rita Mukhtar

"Heavy metals contamination in soils collected in the vicinity of lead smelter in East Java, Indonesia" at Pre event Second United Nation World Geospatial Information Congress UN WGIC 2022, India (online) May 27, 2022.

2. Diah Dwiana Lestiani, Muhayatun Santoso, Syukria Kurniawati, Fazry Fachrurony, Dyah Kumala Sari, Indah Kusmartini, Endah Damastuti, Djoko Prakoso Dwi Atmodjo, Rita Mukhtar, "Heavy Metal Contamination, Sources and Potential Risk Assessment of $PM_{2.5}$ in the Vicinity of a Lead Smelter Industry in East Java, Indonesia" at International Conference on Health, Environmental, Food and Agricultural 2022 ICHEFA2022, Malaysia (online), June 18-19, 2022.
3. Diah Dwiana Lestiani, Sung Kijin, Muhayatun Santoso, Takagi Ikuji. "Characteristic, Source Identification and Health Risk of $PM_{2.5}$ in an Industrial Area in Surabaya, Indonesia". 2023 International Conference on CMAS-Asia-Pacific, Saitama Japan, 17-21 July 2023.
4. Diah Dwiana Lestiani, Indah Kusmartini, Sung Kijin, Ikuji Takagi, Muhayatun Santoso, "A comparative study of XRF and PIXE analysis on fine particulate matter on polycarbonate and Teflon filters collected in Indonesia". International Conference on Nuclear Science, Technology and Application (ICONSTA) 2023, Tangerang, Indonesia, 5-6 December 2023 (will be presented).

Other related presentations on the air quality research:

1. Diah Dwiana Lestiani, Muhayatun Santoso, Endah Damastuti, Syukria Kurniawati, Janos Osan, Mateusz Czyzycki, Andreas Germanos Karydas and, Alessandro Migliori, "Application of Synchrotron Radiation Based Xray for APM Characterization", World Clean Air Congress 2019, Istanbul, 21-29 September 2019
2. Diah Dwiana Lestiani, Muhayatun Santoso, Endah Damastuti, Syukria Kurniawati, Alessandro Migliori, Juan Jose Leani, Mateusz Czyzycki, Andreas Germanos Karydas, and Janos Osan, "Selected Elements Characterization of Fine Particulate Matter $PM_{2.5}$ using Synchrotron Radiation XRF, International Conference on Nuclear Science, Technology and Application (ICONSTA) 2020, Jakarta, November 23-24, 2020.

ANNEXES

Annexes A Tables

Table A. 1 XRF spectrometer conditions for elemental analysis of APM

No	Targets	Detected elements	Voltage (kV)	Current (mA)	Analysis time (s)
1	CaF2	(Na), Mg, Al, Si, P, S, Cl, K	40	15	600
2	Fe	Ca, Sc, Ti, V, Cr	75	8	400
3	Ge	Mn, Fe, Co, Ni, Cu and Zn	75	8	400
4	Zr	As, Se, Br and Pb	90	6	600
5	CeO2	Sn, Sb and Ba	90	6	400

Table A. 2 Parameters used in health risk assessment [Alias et al., 2020; US EPA, 2011, 1989; Vega et al., 2021]

Parameter	Definition	Units	Adults	Children
IR	Inhalation rate	m^3/day	15.7	10.1
EF	Exposure Frequency	day/year	350	350
ED	Exposure Duration	year	24	6
BW	Body weight	kg	70	18.6
AT_{car}	AT carcinogenic (70×365)	day	25550	25550
AT	AT non carcinogenic (ED×365)	day	8760	2190

Table A. 3 Reference dose (RfD), inhalation unit risk and slope factor values used in health risk assessment [US EPA 2022].

Elements	RfD (mg/kg.day)	IUR (m^3/µg)	SF Children (kg.day/µg)	SF Adults (kg.day/µg)
As	3.01E-04	4.30E-03	7.92E+00	1.92E+01
Co	2.00E-01	7.65E-03	1.41E+01	3.41E+01
Cr	2.86E-05	1.20E-02	2.21E+01	5.35E+01
Cu	4.00E-02	7.65E-03	1.41E+01	3.41E+01
Ni	2.00E-02	2.40E-04	4.42E-01	1.07E+00
Pb	3.52E-03	1.20E-05	2.21E-02	5.35E-02
Zn	3.00E-01			

Annexes A Figures

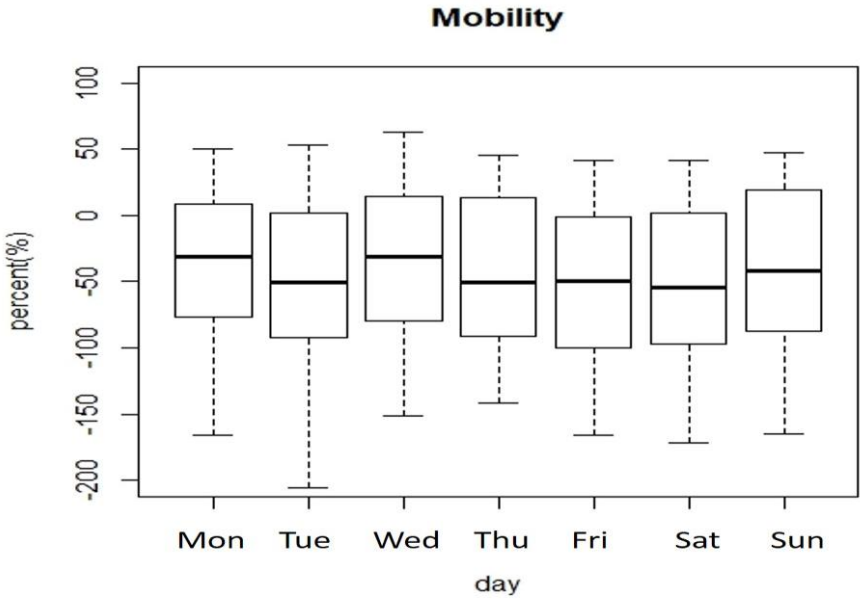

Figure A. 1 Daily mobility patterns throughout a week in 2021